

Winter 2008

Massive Spatiotemporal Watershed Hydrological Storm Event Response Model (MHSERM) with Time-Lapsed NEXRAD Radar Feed

Changqing Song
Old Dominion University

Follow this and additional works at: https://digitalcommons.odu.edu/cee_etds

Part of the [Environmental Engineering Commons](#), [Hydraulic Engineering Commons](#), and the [Hydrology Commons](#)

Recommended Citation

Song, Changqing. "Massive Spatiotemporal Watershed Hydrological Storm Event Response Model (MHSERM) with Time-Lapsed NEXRAD Radar Feed" (2008). Doctor of Philosophy (PhD), dissertation, Civil/Environmental Engineering, Old Dominion University, DOI: 10.25777/0k3b-h287
https://digitalcommons.odu.edu/cee_etds/73

This Dissertation is brought to you for free and open access by the Civil & Environmental Engineering at ODU Digital Commons. It has been accepted for inclusion in Civil & Environmental Engineering Theses & Dissertations by an authorized administrator of ODU Digital Commons. For more information, please contact digitalcommons@odu.edu.

**MASSIVE SPATIOTEMPORAL WATERSHED HYDROLOGICAL
STORM EVENT RESPONSE MODEL (MHSERM) WITH
TIME-LAPSED NEXRAD RADAR FEED**

by

Changqing Song
B.S. July 1995, Beijing University
M.S. August 1998, Institute of Geology, China Earthquake Administration

A Dissertation Submitted to the Faculty of
Old Dominion University in Partial Fulfillment of the
Requirement for the Degree of

DOCTOR OF PHILOSOPHY

ENVIRONMENTAL ENGINEERING

OLD DOMINION UNIVERSITY
December 2008

Approved by:

Jaewon Yoon (Director)

A. Osman Akan (Member)

Resit Unal (Member)

Laura J. Harrell (Member)

ABSTRACT

MASSIVE SPATIOTEMPORAL WATERSHED HYDROLOGICAL STORM EVENT RESPONSE MODEL (MHSERM) WITH TIME-LAPSED NEXRAD RADAR FEED

Changqing Song
Old Dominion University, 2008
Director : Dr. Jaewon Yoon

Correctly and efficiently estimating hydrological responses corresponding to a specific storm event at the streams in a watershed is the main goal of any sound water resource management strategy. Methods for calculating a stream flow hydrograph at the selected streams typically require a great deal of spatial and temporal watershed data such as geomorphological data, soil survey, landcover, precipitation data, and stream network information to name a few. However, extracting and preprocessing such data for estimation and analysis is a hugely time-consuming task, especially for a watershed with hundreds of streams and lakes and complicated landcover and soil characteristics. To deal with the complexity, traditional models have to simplify the watershed and the streams network, use average values for each subcatchment, and then indirectly validate the model by adjusting the parameters through calibration and verification.

To obviate such difficulties, and to better utilize the new, high precision spatial/temporal data, a new massive spatiotemporal watershed hydrological storm event response model (MHSERM) was developed and implemented on ESRI ArcMap platform. Different from other hydrological modeling systems, the MHSERM calculated the rainfall run off at a resolution of finer grids that reflects high precision spatial/temporal data characteristics of the watershed, not at conventional catchment or subcatchment

scales, and that can simulate the variations of terrain, vegetation and soil far more accurately. The MHSERM provides a framework to utilize the USGS DEM and Landcover data, NRCS SSURGO and STATSGO soil data and National Hydrology Dataset (NHD) by handling millions of elements (grids) and thousands of streams in a real watershed and utilizing the Spatiotemporal NEXRAD precipitation data for each grid in pseudo real-time. Specifically, the MHSERM model has the following new functionalities:

1. Grid the watershed on the basis of high precision data like USGS DEM and Landcover data, NRCS SSURGO and STATSGO soil data, e.g., at a 30 meter by 30 meter resolution;
2. Delineate catchments based on the USGS National Digital Elevation Model (DEM) and the stream network data of the National Hydrography Dataset (NHD);
3. Establish the stream network and routing sequence for a watershed with hundreds of streams and lakes extracted from the National Hydrography Dataset (NHD) either in a supervised or unsupervised manner;
4. Utilize the NCDC NEXRAD precipitation data as spatial and temporal input, and extract the precipitation data for each grid;
5. Calculate the overland runoff volume, flow path and slope to the stream for each grid;
6. Dynamically estimates time of concentration to the stream for each interval, and only for the grids with rainfall excess, not for the whole catchment;
7. Deal with different hydrologic conditions (Good, Fair, Poor) for landcover data and different Antecedent Moisture Condition (AMC);

8. Process single or a series of storm events automatically; thus, the MHSERM model is capable of simulating both discrete and continuous storm events;
9. Calculate the temporal flow rate (i.e., hydrograph) for all the streams in the stream network within the watershed, save them to a database for further analysis and evaluation of various what-if scenarios and BMP designs.

In MHSERM model, the SCS Curve number method is used for calculating overland flow runoff volume, and the Muskingum-Cunge method is used for flow routing of the stream network.

ACKNOWLEDGMENTS

There are many people who have contributed to the successful completion of this dissertation. I would first like to thank my supervisor, Dr. Jaewon Yoon, for his support and advice, and his patience and hours of guidance on my research and editing of this manuscript. I also appreciate his efforts to pull together funds from different sources to support my studies and keep the dream alive.

I would also like to thank Professor Ishibashi for his help. He gave me much advice and support after I came to ODU for my PhD studies. I would like to express my appreciation to the committee members of my dissertation research, Professor Akan, Professor Unal and Professor Harrell, for their advice and time on my research. Their classes about hydromechanics, hydraulics and hydrology were also very helpful.

Thanks as well to my fellow students in the Department of Civil and Environmental Engineering, amongst whom Leying Zhang deserves individual recognition for her help after I moved to New Haven, CT.

I would also like to acknowledge the love and encouragement of my wife. Her encouragement kept me going through all the difficulties in this dissertation research.

TABLE OF CONTENTS

Chapter	Page
INTRODUCTION	1
1.1 Watershed Storm Event Hydrological Response Models	1
1.2 Purpose	3
LITERATURE REVIEW	7
2.1 Watershed Hydrological Storm Event Response Models	7
2.2 Geographical Information Systems (GIS) application in the Storm Event Response Models	12
2.3 Public Digital Spatial Datasets Applied In SERM.....	15
2.4 The Next Generation Weather Radar (NEXRAD) Precipitation Data and Its Application in SERM.....	22
STUDAY AREA.....	29
3.1 Study Area: Rivanna River Basin.....	29
3.2 Data Preprocessing.	33
METHODOLOGY.....	39
4.1 Catchment Delineation Based on NHD Data	39
4.2 Parameters' Estimation for Each Cell.....	48
4.3 Establishment of Stream Network Based on NHD Data.....	57
4.4 The Temporal-Spatial Overland Runoff Calculation Based NEXRAD Radar Data.....	62
4.5 Estimation of Base Flow.....	69
4.6 The Lateral Flow Calculation and The Flow Routing in the Stream Network.....	71
RESULTS AND DISCUSSION.....	81
5.1 The Results of Catchments Delineation and Stream Network Routing Sequence.....	82
5.2 The Hydrological Response of Storm Events.....	82
5.3 Conclusion and Discussion.....	127
REFERENCE.....	134
VITA.....	144

LIST OF TABLES

Table	Page
2.1 Summary of Five Storm Event Hydrological Response Models.....	11
2.2 The recent researches on correlationship between Stage III NEXRAD data and co-located rain gage data since 1998	25
3.1 Rivanna River Basin by Hydrologic Unit	31
3.2 Real Time Flow Data from Four Surface Water Gauge Stations, Rivanna Basin, Central Virginia.....	32
3.3 Land Cover Category Lookup Table for NLCD1992 and NLCD2001 Dataset used in the Study	36
4.1 Upstream Search method Procedures to Calculate the Flow Direction.....	44
4.2 Procedures for Delineating Catchments with Flow Direction Raster and Reverse Flow Direction Raster.....	45
4.3 The Availability of NRCS SSURGO Spatial Dataset for Rivanna River Basin till 02/29/2008.....	50
4.4 Procedures for Determining Hydrologic Soil Type for the Cells using SSURGO/STATSGO composite.....	51
4.5 Procedure for Calculating Flow Slope and Flow Distance to the Receiving Streams or Waterbodies.....	56
4.6 Main Parameters for a Flowline Object for Developing the Flow Routing Sequence in a Stream System.....	60
4.7 MHSERM Example Setting File for Rainfall Data.....	63
4.8 Section Information in Chapter IV describing Procedures to Generate Target Parameters from Raster Dataset.....	69

4.9 Steps implemented in the MHSERM for Flow Routing in the Stream Network	80
5.1 The USGS Gage Stations and Their Corresponding Streams.....	86
5.2 Peak Flow Data Extracted from USGS Gauge Stations within the Rivanna River Basin over 2003.09.18-2003.09.19 Storm Event.....	94
5.3 The observed and simulated peak flow and peak time at station 02031000.....	97
5.4 The observed and simulated peak flow and peak time at station 02032640.....	98
5.5 The observed and simulated peak flow and peak time at station 02034000.....	98
5.6 Flow Data Extracted from USGS Gauge Stations within Rivanna River Basin..	118
5.7 Combinations of AMC and landcover condition used in the Simulation for the 2007.8.24-2007.8.27 Storm Events.....	119
5.8 The observed and simulated peak flows for 2007.8.24-2007.8.27 events at station 02031000.....	121
5.9 The observed and simulated peak flows for Event 2 at station 02032250.....	122
5.10 The observed and simulated peak flows for Event 2 at Station 02032640.....	124
5.11 The observed and simulated peak flows for Event 2 at Station 02034000.....	125

LIST OF FIGURES

Figure	Page
3.1 Rivanna River Basin, a Tributary of the James River, Central Virginia.....	30
3.2 Subbasin Delineation and Location of Four Real Time Flow Data Surface Water Gauge Stations (listed in Table 3.2), Rivanna Basin, Central Virginia.....	33
4.1 Massive Watershed Scale Storm Event Hydrological Response Model(MHSERM) Components in form of ArcMap Toolbar.....	39
4.2 Cells of DEM Overlaid with Flowline Raster Cells.....	42
4.3 Gradient-based Determination of the Overland Runoff Flow Direction.....	43
4.4 Encoded Flow Direction Raster in ESRI Grid format for Upstream Search Method.....	46
4.5 Flow Direction Assignment and Aggregation of the Networked Cells through Flowline	47
4.6 886 Catchments Delineated by Automated Procedure, Rivanna river basin, Central Virginia.....	48
4.7 Overlaying of Hydrologic Soil Type Raster Dataset with Land Cover Raster Dataset for CN Estimation.....	52
4.8 CN estimation for different hydrologic conditions (Poor, Fair, Good) of hydrologic soil type raster dataset.....	53
4.9 Manning Roughness Value Assignment to Cells	55
4.10 Flow Distance to stream and Slope to stream Raster.....	56
4.11 Network (HYDRO_NET) for Flowline in NHD dataset, in ESRI Geodatabase Format (NHDinGEO)	58

4.12 Streams Routing Sequence via Upstream Search Method Rank utilizing Rank from the Outlet (=sequence), Downstream Flowline's ID (=connectivity), and Linked Waterbody Object's ID (=identification).....	59
4.13 Elements of a hypothetical trapezoidal waterbody to represent the waterbody in MHSERM.....	61
4.14 NEXRAD Precipitation Intensity Data as a Series of Input Raster Data, Rivanna River Basin, Central Virginia.....	65
4.15 The Example Rainfall Excess Intensity Rasters.....	67
4.16 Daily Discharge Data of USGS gauge station '02034000 RIVANNA RIVER AT PALMYRA'	71
5.1 MHSERM Model Results of 886 Catchments and Stream Networks consisted with 897 Flowlines and 85 Impounded Waterbodies, Rivanna River Basin, Central Virginia	83
5.2 MHSERM Simulation Outcome Datasets for Inflow and Outflow Hydrographs in an Access Database Format	84
5.3 Temporal NEXRAD Radar Image of Storm Event on 2003.09.18-2003.09.19 at 2003.09.18 16:58 UTC.....	87
5.4 Cumulative Rainfall Depth Raster for Storm Event, over 2003.09.18-2003.09.19, Rivanna River Basin, Central Virginia	93
5.5 The comparison between the hydrograph observed at Station 02031000 and the calculated hydrographs of stream 102089	95
5.6 The comparison between the hydrograph observed at Station 02032640 and the calculated hydrographs of stream 86010.....	96
5.7 The comparison between the hydrograph observed at Station 02034000 and the calculated hydrographs of stream 86305.....	96
5.8 Temporal NEXRAD Radar Image of the First Storm Event on 2007.08.24-2007.08.27 at 2007.08.24 20:28.....	101

5.9 Temporal NEXRAD Radar Image of the Second Storm Event on, 2007.08.24-2007.08.27 at 2007.08.25 22:29.....	105
5.10 Temporal NEXRAD Radar Image of the Third Storm Event on 2007.08.24-2007.08.27 at 2007.08.26 21:31.....	111
5.11 Cumulative Rainfall Depth Raster for the First Event of Multiple Storm Events, over 2007.08.24-2007.08.27, Rivanna River Basin, Central Virginia.....	115
5.12 MHSERM Outflow Hydrograph Estimates vs. Observed USGS Gauge Station 02031000, under six SMC-Landcover combinations	120
5.13 MHSERM Outflow Hydrograph Estimates vs. Observed USGS Gauge Station 02032250, under six AMC-Landcover combinations.....	121
5.14 MHSERM Outflow Hydrograph Estimates vs. Observed USGS Gauge Station 02032640, under six AMC-Landcover combinations.....	123
5.15 MHSERM Outflow Hydrograph Estimates vs. Observed USGS Gauge Station 02034000, under six AMC-Landcover combinations	124

CHAPTER I

INTRODUCTION

1.1 Watershed Storm Event Hydrological Response Models

Flooding events are the most devastating weather related hazard in the United States (NRC, 1996) . Moreover, flood damage has increased in the United States in the last century (Pielke *et al.*, 2002). According to the U.S. Army Corps of Engineers (USACE, 2003), flooding causes more damage in the United States than any other severe weather related event--an average of \$5.3 billion a year from 1994 to 2003. Flooding can occur in any of the 50 states or U.S. territories at anytime of the year. Floods happen when the water draining from a watershed, whether from rainfall or melting snow, exceeds the capacity of the river or stream channel to hold it (Association of State Floodplain Managers Inc, 1996). The main causes for a flood to occur include heavy and/or persistent rainfall, or an ice or debris jam that causes a river or stream to overflow and flood the surrounding area.

Watershed level Storm Event Hydrological Response Models are widely used in the areas of water resource planning and management, flow forecasting, flood damage reduction, future urbanization impact study, planning and design of storm-water drainage systems, etc. Since the 1960s, quite a few computer models have been developed by federal and state agencies, universities and consulting companies (Zarriello, 1998; Wurbs, 1997). Among these models, the Hydrologic Modeling System (HEC-HMS) and EPA

The journal model used in this dissertation is based on ASCE (American Society of Civil Engineers) *Journal of Water Resources Planning and Management*.

Storm Water Management Model (SWMM) are the most well-known and routinely applied in water resource planning and management projects. The Hydrologic Modeling System (HEC-HMS) simulates precipitation-runoff and routing processes (US Army Corps of Engineers Hydrologic Engineering Center, 2000a). The EPA Storm Water Management Model (SWMM) is a dynamic rainfall-runoff simulation model used for single event or long-term (continuous) simulation of runoff quantity and quality from primarily urban areas (Rossman, 2007). Besides these two models, there are other well-known models including Hydrologic Simulation Program Fortran (HSPF), CASC2D, CUHP, DR3M, HEC-1, PSRM, TR20, and others (Zarriello, 1998; Wurbs, 1997). These models usually include two parts, overland rainfall-runoff and rivers/channels routing. For the overland rainfall-runoff part, the models usually divide the study watershed into a collection of subcatchment areas that receive precipitation and generate runoff. For the routing part, the models simulate the movement of water flow in rivers/channels, or pipes during a given simulation period. Detailed discussion of these models is provided in Chapter II.

In the last decade, the availability of new geospatial data sources and the use of Geographic Information Systems (GIS) in hydrological modeling has been progressively facilitating modelers with powerful tools to model the watershed and predict possible floods. The new data source includes high resolution USGS National Digital Elevation Model (DEM) data, Landcover raster data, NRCS SSURGO and STATSGO soil data, National Hydrography Dataset (NHD) stream network data and NCDC NEXRAD precipitation data. For most of the models, GIS software is used as a data preprocessor tool to extract the parameters of the watershed studied (Miles and Ho, 1999). A number

of researchers also utilized the data management, analysis and visualization capabilities of the GIS platform such as ESRI ArcView by linking or integrating the hydrologic model with GIS technology (Ye *et al.*, 1996; Ivanov *et al.*, 2004).

1.2 Purpose

Correctly and efficiently estimating hydrological responses corresponding to a specific storm event for the streams or rivers within a watershed is essential for any sound water resource management strategy. However, due to its complexity, hydrologic response within a watershed could vary tremendously. Such variations are in a sense a true system response of the watershed in question, and result from the temporal and spatial distribution of precipitation, topography, soil, land cover and streams' properties, and others within the watershed. Extraction and preprocessing such data for subsequent estimation and analysis is a very time-consuming task, especially for a watershed with hundreds of streams and lakes and complicated landcover and soil characteristics. Moreover, to manage such complexity, traditional models relying on simplification of watershed features and streams networks, logistically use average values for each subcatchment, and validate the model by adjusting the parameters via calibration and verification. Thus, existing difficulties and drawbacks in conventional Hydrological Storm Event Response (SERM) models can be summarized by:

1. Lengthy and difficult assembly requirement of the huge amount of spatiotemporal data per analysis and subsequent design;
2. Time-consuming, additional data processing requirement for interpreting model results;

3. Mostly for design orientation, lacking (real-time) prediction capability;
4. The watershed is often over-simplified, and hundreds (even thousands) of streams and channels must be manually prepared for the model;
5. Processes of calibration and verification are necessary for acquiring reliable results, because model results vary in complexity, functionality, and applicability to a given region or storm type;
6. The new spatial dataset is not fully utilized, and, as a result, the internal variation of the subcatchments is neglected;
7. For different landcover conditions and the Antecedent Moisture Condition typically used for various what-if design scenarios, the models have to repeat all the pre-processing including the parameters' estimation for each subcatchment.

To obviate such difficulties and drawbacks, and to better utilize the new, high precision spatial/temporal data, a fully distributed watershed-scale, Spatiotemporal Massive Hydrological Storm Event Response Model (MHSERM) was developed and implemented in this dissertation research. Unlike other hydrological modeling systems, the MHSERM model can concurrently handle millions of elements (cells or grids) and thousands of streams in a real watershed and utilize the spatiotemporal NEXRAD radar precipitation data for each cell. The MHSERM model utilizes the public digital spatial data including USGS NED DEM, Landcover, SSURGO and STATSGO soil data, NHD Hydrology Dataset, and it automatically estimates parameters from these datasets for overland runoff calculations and stream network flow routing. To deal with hundreds of streams and lakes/reservoir/ponds within the watershed studied, the MHSERM model automatically generates and routes the flow sequence by utilizing NHD dataset. In

addition, users can also manually change/input the parameters of the streams and lakes/reservoir/ponds if localized survey data of better quality are available in hand. For the rainfall data, the MHSERM use the spatiotemporal NCDC NEXRAD radar data for input, moreover, the model fully utilizes the spatial distribution of the rainfall radar data to the grid/cell level.

Specifically, The MHSERM model has the following new functionalities over conventional :

1. Grid the watershed on the basis of high precision data like USGS DEM and Landcover data, NRCS SSURGO and STATSGO soil data, e.g., at a 30 meter by 30 meter resolution;
2. Delineate catchments based on the USGS National Digital Elevation Model (DEM) and the stream network data of the National Hydrography Dataset (NHD);
3. Establish the stream network and routing sequence for a watershed with hundreds of streams and lakes extracted from the National Hydrography Dataset (NHD) either in a supervised or unsupervised manner;
4. Utilize the NCDC NEXRAD precipitation data as spatial and temporal input, and extract the precipitation data for each grids;
5. Calculate the overland runoff volume, flow path and slope to the stream for each grid;
6. Dynamically estimates time of concentration to the stream for each interval, and only for the grids with rainfall excess, not for the whole catchment;
7. Preset manually or estimate automatically the parameters for streams and waterbodies on the streams;

8. Deal with different hydrologic conditions (Good, Fair, Poor) for landcover data and different Antecedent Moisture Condition (AMC);
9. Process single or a series of storm events automatically; thus, the MHSERM model is capable of simulating both discrete and continuous storm events;
10. Calculate the temporal flow rate (i.e., hydrograph) for all the streams in the stream network within the watershed, save them to a database for further analysis and evaluation of various what-if scenarios and BMP designs.

In MHSERM model, the SCS Curve number method is used for calculating overland flow runoff volume, Modified Clark (ModClark) method for transforming water to streams. The ModClark method can account explicitly for variations in travel time to a stream from all the grids in its contributing catchment (Kull and Feldman, 1998). The Muskingum-Cunge method, which is physically based, is used for flow routing of the stream network. The coefficients of the routing method are based on physical data such as cross section and Manning roughness n of the streams; this makes it more favorable for routing in the MHSERM.

CHAPTER II

LITERATURE REVIEW

2.1 Watershed Hydrological Storm Event Response Models

Watershed hydrological Storm Event Response Models (SERM), sometimes called a Rainfall-Runoff model, simulate the natural processes of rainfall loss, overland runoff, flow routing in a river/channel/lake system, and get the spatiotemporal distribution of the flow of water within a watershed or a series of watersheds. Both in research and in professional practice, these models are the primary tool for exploring watershed-scale hydrologic processes and for addressing a wide spectrum of environmental and water resource problems (Singh and Frevert, 2006; Singh, 1995). Simulation of watershed hydrologic processes is difficult at best due to the complexity of the natural elements contributing to a runoff event. Thus, several watershed models were developed with the advances of computer technology in the 1960s. For example, Crawford and Linsley (1966) published the Stanford Watershed Model (SWM). SWM was the first model to simulate the whole hydrologic cycle for a basin (Singh and Frevert, 2005). SWM was further transformed into the U.S. Environmental Protection Agency (EPA) Hydrological Simulation Program - FORTRAN (HSPF), which is also a core part of the EPA's Better Assessment Science Integrating Point and Nonpoint Sources (BASINS) (Donigian and Imhoff, 2002; Donigian and Hubber, 1991).

With the rapid improvement of computer power and subsequent proliferation of the personal computer in the last four decades, many watershed-scale hydrological

models were developed by federal and state agencies, academic researchers and consulting and software companies. Several researchers provided comprehensive reviews for part of the existing models; (Singh and Frevent, 2005; Borah and Bera, 2003, 2004; Singh and Frevent, 2002a, 2002b; Zarriello, 1998; Singh, 1995; WMO, 1992; Donigian and Huber, 1991). In their reviews, several watershed models were identified as SERM or having SERM-equivalent modules. Donigian and Huber (1991) listed thirteen watershed hydrological and nonpoint-source models including the Agricultural NonPoint Source Pollution Model (AGNPS) and Hydrological Simulation Program FORTRAN (HSPF). Zarriello (1998) compared and summarized the results from nine uncalibrated runoff models to observed flows in two small urban watersheds with distinctly different climatic and physiographic settings; Harvard Gulch, a semi-arid watershed near Denver, CO, and Surrey Downs, a coastal watershed in the Pacific Northwest near Seattle, WA. Among the nine models compared, HEC-1 (Hydrologic Engineering Center, 1990), HSPF, SCS TR-20 (Soil Conservation Service, 1983), and SWMM (The EPA Storm Water Management Model) are still widely used. Borah and Bera (2003) reviewed eleven watershed-scale hydrologic and nonpoint-source pollution models including AGNPS, HSPF, ANSWERS, SWAT and MIKE SHE. Additional model comparison studies can be found in a recent summary by Singh and Frevent (2005) that included 24 watershed models. Besides hydrological modeling and flow routing, some models also have capability to deal with pollutants transportation within the models.

There are many watershed storm event response models available to engineers, hydrologists, and planners, with new ones appearing all the time (Akan and Houghtalen, 2003). However, there are a few well-known and widely used general models in the U.S.

and elsewhere (Singh and Frevent, 2005). The models include the U.S. Army Corps of Engineers' Hydrologic Engineering Center Hydrologic Modeling System (HEC-HMS), The Environmental Protection Agency's Storm Water Management Model (EPA-SWMM), The Canadian Distributed Hydrologic Model WATERloo FLOOD system (WATFLOOD), and The Runoff Routing Model (RORB) used in Australia, Europe TOPography-based hydrological MODEL (TOPMODEL) and Systeme Hydrologique Europeen (SHE). Further model descriptions are discussed next.

HEC-HMS is the successor to and replacement for HEC's HEC-1 program and for various specialized versions of HEC-1. HEC-HMS is designed to simulate the precipitation-runoff processes of dendritic watershed system, it improves upon the capabilities of HEC-1 and provides additional capabilities for distributed modeling and continuous simulation (USACE, 2000a, 2000b). The current version (2007) runs in the Windows platform. The EPA-SWMM is a dynamic rainfall-runoff simulation model used for single event or long-term (continuous) simulation of runoff quantity and quality from primarily urban areas (Rossman, 2007). The current version (2007) is available for the Windows platform. SWMM 5 provides an integrated environment for editing study area input data, running hydrologic, hydraulic and water quality simulations, and viewing the results in a variety of formats (Rossman, 2007). WATFLOOD is an integrated set of computer programs to forecast or simulate flood flows in watersheds having response times ranging from one hour to several weeks. WATFLOOD has been under continuous development by University of Waterloo since 1972. The emphasis of the WATFLOOD system is on making optimal use of remotely sensed data by using Grouping Response Units (GRU) (Kouwen, 2007; Kouwen *et al.*, 1993). The WATFLOOD consists of

mostly a set of FORTRAN programs for DOS, or various Unix platforms. The entire WATFLOOD system is bundled with hydrological modeling component of WATFLOOD, and a number of pre and post processors for WATFLOOD's data management system. RORB is a general runoff and stream flow routing program used to calculate flood hydrographs from rainfall and other channel inputs. The first version of RORB was released in 1975; it was a general runoff routing program for rural catchments, and written by Monash University, Australia. The current version (2005) runs in Windows platform. The model can handle spatially distributed catchment data, and applicable to both urban and rural catchments. It makes provision for temporal and spatial variation of rainfall and losses and can model flows at any number of gauging stations (Laurenson *et al.*, 2006). TOPMODEL (1974) is a physically based, distributed watershed model that simulates hydrologic fluxes of water through a watershed on the basis of its distributed predictions on an analysis of watershed topography (Beven *et al.*, 1984, 1995; Beven and Kirkby, 1979). SHE (Systeme Hydrologique Europeen) is a distributed hydrological model using a physics-based representation of the underlying catchment processes (Abbott *et al.*, 1986a, 1986b). SHE model's development was based on Freeze and Harlan's (1969) proposal about the blueprint of physics-based hydrological modeling.

Considering this dissertation research's goal of developing a massive watershed hydrological Storm Event Response Models (MHSERM) that can utilize massive spatial or spatiotemporal digital datasets by tightly integrating with GIS, five watershed models sharing varying degrees of spatiotemporal capabilities were further summarized in Table 2.1.

Table 2.1 Summary of Five Storm Event Hydrological Response Models

Model	Watershed representation	Watershed Parameters Input	Map Display	Rainfall Loss	Runoff on Overland	Routing method or Channel Flow
HEC-HMS	Sub-Basins delineated manually with assumption of Homogeneity; 1-D Dendritic network of channels	Parameters estimated by other program, and manually input by user	Schematic link-node map;	SCS CN; Initial and Constant; Green and Ampt; SMA; And more.....	Clark UH; Snyder UH; SCS CN; ModClark; Kinematic Wave; And more.....	SCS Lag; Muskingum; Modified Puls; Kinematic Wave; Muskingum-Cunge; Straddle-Stagger; And more...
SWMM	Homogenous Subcatchments; 1-D network channels, sewers, pipes etc.	Estimated by other program, and manually input by user	Schematic link-node map;	ET loss Horton	Kinematic Wave; Unit Hydrograph	Kinematic Wave Dynamic Wave
WATFLOOD	The combination of Grouped response units (GRU's) and grids (size 1km –25km);	The data files for catchment, rainfall, parameters prepared before model running	Grids (from support modules)	ET loss; Philip's infiltration equation	Hortonian runoff model	Muskingum-Cunge; Manning Formula
RORB	The watershed divided into Subareas, the actual channel network represented by a network of model storages.	The data files for catchment, rainfall, parameters prepared before model running	N/A (Data files)	(i) Initial loss followed by a runoff coefficient (constant proportional rates of loss and of runoff). (ii) Initial loss followed by a constant (continuing) loss rate.	The rainfall-excess is operated on by a catchment storage model representing the effects of overland flow storage and channel storage to produce the surface runoff hydrograph.	
TOPMODEL	a variable contributing area; Channel networks	The data files for catchment, rainfall, topographic index map prepared before the TOPMODEL running	N/A (Data files)	the exponential Green-Ampt model	the continuity equation, Darcy's Law, the assumption that the saturated hydraulic conductivity decreases exponentially as depth below the land surface increases.	Clark's Time-Area method

Most of the above models are distributed models. Obviously, the real watershed has spatially varying soil characteristics, land covers, terrain, streams' network and rainfall intensity; therefore, distributed hydrological modeling is more suitable and has

more potential to improve estimates of stream flow and water levels both for hydrological simulation and for flood forecasting than non-spatial, conventional lumped-sum parameter models (Smith *et al.*, 2004). Furthermore, the availability of new digital spatial data sources, advancements in remote sensing technology and the application of Geographic Information Systems (GIS) improve watershed-scale modeling and provide powerful tools to accurately model the rainfall-runoff process and corresponding flood prediction.

2.2 Geographical Information Systems (GIS) application in the Storm Event Response Models

A GIS is a computer-based information system that enables capture, modeling, manipulation, retrieval, analysis and presentation of geographically referenced data (Worboys, 1995). It provides a framework for understanding our world and applying geographic knowledge to solve problems and guide human behavior. GIS offers a cognitive spatial representation of complex hydrologic and hydraulic systems and present a more comprehensive view of the target region by incorporating related spatial data into traditional water resources databases (Martin *et al.*, 2005).

For the distributed watershed hydrological response modeling, GIS provides hydrologists a powerful platform to collect, manage, display, analyze and store digital spatial dataset such as Digital Elevation Model (DEM), soil and land cover, stream network, rainfall radar data, etc. GIS is capable of incorporating related spatial data into traditional water resources databases in order to present a more comprehensive view of

the target region (Martin *et al.*, 2005). There have been three approaches to utilize GIS in water resources areas: loose coupling (Linking Interface), tight coupling (Combining Interface) and embedded coupling (Integrating Interface) (Martin *et al.*, 2005; Wesseling *et al.*, 1996). The loose coupling (Linking) method denotes that GIS can only act as a data preprocessor tool, and users have to do data exchange manually between models and GIS (Miles and Ho, 1999), e.g. the Geospatial Hydrologic Modeling Extension (HEC-GeoHMS) for HEC-HMS. GeoHMS uses ArcView GIS and its Spatial Analyst extension to develop a number of hydrologic modeling input, and the results are imported back to HEC-HMS for simulation (USACE, 2003b). In a tight coupling (combining) model, the GIS platform can be the center of model input, management, output and visualization, and the data exchange between models and GIS is symbiotic. The USEPA watershed modeling system BASINS can be classified as a tight coupling (combining) model. It combines the in-stream water quality model QUAL2E with the watershed loading and transport models HSPF and SWAT, and utilizes ArcView GIS as a display and interpretation interface, but each model remains separate and acts as a plug-in module rather than being embedded within GIS (Martin *et al.*, 2005; Whittemore and Beebe, 2000). In the embedded coupling (integrating) method, the model simulation is written in an integrated programming language within GIS, or the GIS module and is then inserted into the model environment. For example, a map-based subsurface and surface hydrologic model was developed entirely within ArcView GIS and applied to simulate surface and subsurface flow on the Niger River Basin in West Africa (Ye, 1996).

Despite the broad application of GIS in watershed modeling, GIS technology was not specifically developed for engineering modeling (Martin *et al.*, 2005). The

hydrological models usually use extensive spatial data to describe the spatial variety of a small area, the flow direction in a stream network, as well as temporal dynamics of precipitation, runoff and channel flow. However, the GIS data model is an efficient spatial relationship database, which doesn't include the temporal dimension. The data model is designed to uniformly process vast quantities of data specific to individual layers of information over a large spatial region (Maidment, 1993).

Environmental Systems Research Institute (ESRI) is a leading GIS software company, and a number of models have been coupled with ESRI GIS platform in last 20 years. ESRI had a major upgrade of their desktop GIS software from ArcView to ArcGIS since 2000. One of the most important upgrades is that the new ArcGIS platform is now composed of ArcObjects. ArcObjects is an embeddable and programmable toolbox extension of ESRI GIS, and with ArcObjects, users can embed GIS maps/functionality in other applications, build and deploy custom desktop applications, configure/customize ArcGIS applications, and extend the ArcGIS architecture and data model (Burke, 2003). The new ArcGIS software is designed to facilitate the development of custom applications that are compatible with other Windows-based programs (Whiteaker et al., 2004). Geodatabases is the default data structures for the ArcGIS, which is more robust than the older yet popular ArcView system database. Geodatabases provide a well-structured, intuitive framework for storing spatial data, tabular data, and relationships amongst data (Johnson et al., 2005). Thus, with many new features available in the GIS platform, various model functionalities can be easily integrated into GIS platform by using general programming language like Visual C++ or Visual Basic. In addition, the new data model of the geodatabase structure is better suited for hydrological modeling. In

collaboration with several prominent universities (Consortium of Universities for the Advancement of Hydrologic Sciences) and ESRI, Maidment (2003) introduced Arc Hydro, a geospatial and temporal data model for water resource application that operates within ArcGIS. Arc Hydro describes natural surface water systems including hydro networks, drainage systems, river channels, hydrography, and time-series data. Therefore, Arc Hydro is a data structure or a data model that supports hydrologic simulation models, but it is not itself a simulation model.

2.3 Public Digital Spatial Datasets Applied In SERM

The accurate representation of the watershed topography, soil and vegetation properties, and streams network requires a huge amount of different spatial datasets. There are plenty of spatial datasets maintained by government agencies and made publicly accessible on-line including Digital Elevation Model (DEM), landcover data, soil data, and hydrology dataset. Distributed watershed hydrological Storm Event Response Models (SERM) rely on these spatial datasets to describe and characterize a watershed's topographic surface, soil and vegetation properties, stream network and waterbodies.

2.3.1 Digital Elevation Model (DEM)

The Digital Elevation Model (DEM) is generally used to represent the surface of watershed in SERM. Computer programs are used to process the raw DEM data to extract topographic attributes including the boundary of watershed and subwatersheds, the overland flow slope and path, the delineation of streams etc. The National Map Seamless Server of the US Geological Survey (USGS) provides national DEM data

download at no cost with ESRI ArcGRID format and various spatial resolution such as 1 arc second/30m/7.5 minute unit, or 1/3 arc second and/or 1/9 arc second (<http://seamless.usgs.gov>). Topographic representation through DEMs has increased our capability of modeling the surface and subsurface hydrologic processes that govern the rainfall-runoff conversion (Vivoni and Sheehan, 2000).

There are two major data structures designed to represent the Earth's surface in GIS: Grid and TIN (Triangulated Irregular Network) (Bernhardsen, 1999). The grid in GIS is an array of fixed-size square cells arranged in rows and columns. The numeric value is stored with these cells to represent the elevation of the grid space. Each grid cell is referenced by its x,y coordinate location. Obviously, the smaller the size of a grid cell, the higher the level of accuracy in describing the terrain of interest. In contrast to grids, TIN is made up of irregularly distributed nodes and lines with three-dimensional coordinates resulting from trilateration that are arranged in a network of non-overlapping triangles. In the TIN models, the x-y-z coordinates of all points, as well as the triangle attributes of inclination and direction are stored. The area with little variation are described with fewer data than the similar area with greater variation, so compared to the grid model, the TIN model is cumbersome to establish but more efficient to store (Vivoni *et al.*, 2004; Bernhardsen, 1999).

The terrain analysis based on DEM data is widely used to delineate watersheds or catchments, derive the stream network, and calculate the slope and the distance from each cell to the outlet (Ivanov *et al.*, 2004a and 2004b; Tarboton, 2003; Tarboton and Ames, 2001; Wilson and Gallant, 2000; Tarboton *et al.*, 1991; Fairfield and Leymarie, 1991;

Band, 1986). Tarboton (2003) provides an ArcMap toolbar, TauDEM (Terrain Analysis Using Digital Elevation Models), a set of tools for the analysis of terrain using digital elevation models. The analysis includes the functions of channel network delineation, as well as delineation of watersheds and subwatersheds draining. Ivanov *et al.* (2004a, 2004b) introduced a TIN hydrologic model. However, the watershed boundary and the stream network are derived from DEM raster data, that are used as lines for the generation of TIN (Vivoni *et al.*, 2004).

2.3.2 Landcover Raster Dataset and Soil Data

In a hydrological Storm Event Response Models (SERM) model, land use properties, with soil properties are used extensively to determine the partitioning of incident rainfall into infiltration and runoff (Vivoni and Sheehan, 2000). For physical infiltration models, the soil hydraulic parameters are estimated by the surface soil texture. For example, for Green and Ampt (1911) model, the porosity and the suction head can be estimated by the percentage of sand and clay (Rawls and Brakensiek, 1985; Rawls *et al.*, 1983, 1989). For the Horton method (Horton, 1940) and Modified Horton method (Akan, 1993, 1992), the initial infiltration capacity, final infiltration capacity and exponential decay constant can be estimated by soil type (Akan and Houghtalen, 2003; Terstriep and Stall, 1974). For the Soil conservation Service Curve Number (SCS CN, now called the Natural Resources Conservation Services, NRCS), an empirical combined loss model, landcover and soil data is used to determine the CN number, which can be used to calculate the initial loss and rainfall excess based on the SCS empirical runoff equation (SCS, 1986).

For the spatially distributed land cover/land use data set, the National Land Cover Dataset (NLCD) is available from the National Map Seamless Server of the USGS (<http://seamless.usgs.gov/>). There are two types of land cover dataset: NLCD1992 and NLCD2001. NLCD1992 is based primarily on the unsupervised classification of LANDSAT TM (Thematic Mapper) 1992 imagery. It has 21-category land cover classification derived at the approximate Anderson *et al.*, (1976) Level II thematic detail, is provided as raster data with a spatial resolution of 30 meters (1 arc-second) (Vogelmann *et al.*, 2001). The raster files are available in GeoTIFF, ArcGrid, or BIL format. The extent of land cover coverage is expressed in geographic coordinates (latitude/longitude) and referenced to the North American Datum of 1983 (NAD83). NLCD 2001 was produced more recently in 2001, and is a compilation of across all 50 states and Puerto Rico as a cooperative mapping effort of the MRLC 2001 Consortium based on nation-wide LANDSAT 5 and 7 imagery (Homer *et al.*, 2004). NLCD 2001's raster data files are also available in GeoTIFF, ArcGrid, or BIL format with a spatial resolution of 30 meters (1 arc-second) and referenced to the NAD83 datum. NLCD2001 has 29 classes of land cover data such as 'Evergreen Forest', 'Cultivated Crops', 'Woody Wetlands' etc.

The Natural Resources Conservation Service (NRCS) of United States Department of Agriculture (USDA) has archived and distributed two types of soil spatial dataset: State Soil Geographic Database (STATSGO) and The Soil Survey Geographic Database (SSURGO). Both the soil map data can be publicly downloaded from NRCS soil data mart (<http://soildatamart.nrcs.usda.gov/>) in an ESRI shape file format based on the NAD1983 datum. STATSGO was renamed to the U.S. General Soil Map

(STATSGO). The source map for STATSGO was 1:250,000 USGS topographic quadrangles, and the approximate minimum area delineated per STATSGO coverage was 625 hectares (=1,544 acres). The STATSGO covers multi-county, river basin, state, multi-state and regional areas and are designed for regional planning and management uses; however, it is not as detailed enough for sub-county level due to the low resolution. Every STATSGO polygon is linked to the Soil Interpretations Record (SIR) attribute data base, which includes over 25 physical and chemical soil properties such as available water capacity, soil reaction, period of flooding, depth to seasonal water table, and depth to bedrock, as well as interpretations of soil properties for engineering uses, and for cropland, woodland, rangeland, pastureland, wildlife, and recreation development – the similar information available in the USGS County Soil Survey (Watermeier, 2004). SSURGO map data are derived from detailed soil survey maps at scales between 1:12,000 and 1:63,360. Information from soil survey sheets is recompiled onto a 3.75-minute digital orthophoto quarter quadrangle (DOQQ), a 7.5 minute digital orthophoto quadrangle (DOQ) or other planimetrically accurate base maps, and in turn, producing georeferenced data compatible with and readily usable in GIS programs. The soil map units are linked to attributes in the Map Unit Interpretations Record (MUIR) relational database, which includes over 25 physical and chemical soil properties and interpretations for use, as in STATSGO (Watermeier, 2004; NRCS, 1995).

2.3.3 The National Hydrography Dataset (NHD)

The National Hydrography Dataset (NHD, 2000) is a newly combined dataset that provides hydrographic data for the United States. It was developed by the U.S. Environmental Protection Agency (USEPA) and the U.S. Geological Survey (USGS).

The hydrographic data can be defined as the surface water features such as lakes, ponds, streams, rivers, springs and wells. Within the NHD, surface water features are combined in order to form "reaches," that provide the framework for linking water-related data to the NHD surface water drainage network. These linkages enable the analysis and display of water-related data in networked, sequential upstream-to-downstream order. This surface water hydrography feature was compiled from a combination of topographic maps and additional sources. The NHD is available nationwide at a medium resolution at 1:100,000-scale and in much of the Country at a higher resolution of 1:24,000-scale or better (1:12,000-scale). Various formats of the NHD are available in ESRI geodatabase format (NHDinGEO), in ESRI Arc/INFO coverage format (NHDGEOinARC), and in ESRI shape file format (NHDGEOinShape). Organization and cataloging of NHD is based on the traditional USGS 8-digit hydrologic cataloging units (HUCs), that whole catalog can be accessible from USGS NHD website (<http://nhd.usgs.gov/data.html>). For regional-level catalogs of HUC is also accessible from USGS pre-staged personal geodatabases website (<ftp://nhdftp.usgs.gov/SubRegions>). The Characteristics of the NHD are summarized as below (USGS, 1999):

1. It is a feature-based dataset that interconnects and uniquely identifies the stream segments or "reaches" that make up the Nation's surface water drainage system;
2. Unique reach codes (originally developed by the USEPA) are provided for networked features and isolated water bodies;
3. The reach code structure is designed to accommodate higher resolution data;
4. Common identifiers uniquely identify every occurrence of a feature;
5. It is based on the content of the USGS 1:100,000-scale or 1:24,000 data, giving it accuracy consistent with those data;

6. Data are in decimal degrees on the North American Datum of 1983;
7. Names with GNIS identification numbers are included for lakes, other water bodies, and many stream courses;
8. It provides flow direction and centerline representations through surface water bodies.

With the stated features and its public availability, NHD is a very important data source for establishing stream network, delineating watersheds, tracing upstream pollutants, and studying flood plains with the help of GIS in the last several years. The NHD data, along with DEM, was recently added to the EPA's Better Assessment Science Integrating Point and Nonpoint Sources (BASINS) version 3.1. EPA's BASINS is a multipurpose environmental analysis system designed for regulatory modeling by regional, state, and local agencies performing watershed and water quality-based studies (Duda *et al.*, 2005). Furthermore, NHD is frequently used to create stream network for flood analysis (Judi *et al.*, 2007), and upstream tracing of pollutants (Samuels *et al.*, 2003). For the study of watershed and streams delineation in the areas with the problem of map scale and lack of adequate DEM vertical resolution, Di Luzio *et al.* (2004, 2002) integrated the NHD layer into the DEM in order to correct the certain hydrologic features of a watershed that may become obscured or oversimplified during the digital delineation process by "stream burning" in the ArcView-SWAT (AVSWAT). The algorithm used in the research simply adds 500 m to all off-stream DEM cells in addition to the DEM values, and assigns all stream grid cells with the elevation values from the original DEM. AVSWAT is an ArcView GIS extension written in AVENUE programming language

and a GIS based hydrological system linking the Soil and Water Assessment Tool (SWAT) water quality model and ArcView GIS.

2.4 The Next Generation Weather Radar (NEXRAD) Precipitation Data and Its Application in SERM

For the Storm Event Response Models (SERM), time series precipitation data is the key input. Rain gauge data have been used as the primary source for the precipitation data input. For rain gauge data, interpolation may be necessary due to the sparse rain gauge distribution within the watershed, which would not be ideal for capturing the spatial variability associated with precipitation, especially for scattered storms. It is also very difficult for the rain gauge stations to provide real-time data, which is necessary for real-time or near real-time flood prediction. To obviate such difficulties, more and more researchers use the Next Generation Weather Radar (NEXRAD) radar data as the rainfall input in hydrological models. The NEXRAD radar data of the National Weather Service (NWS) became available in 1990's.

2.4.1 The NEXRAD Data

The Next Generation Weather Radar (NEXRAD) program of the National Weather Service (NWS) has deployed a network of approximately 160 weather radars throughout the United States and at selected overseas sites since 1988. This system is a joint effort of the United States Departments of Commerce (DOC), Defense (DOD), and Transportation (DOT). The controlling agencies are the National Weather Service (NWS), Air Force Weather Agency (AFWA) and Federal Aviation Administration (FAA),

respectively. The weather radar is formally known as the Weather Surveillance Radar-1988 Doppler (WSR-88D), which provides highly sensitive, fine-resolution measurements of reflectivity, mean radial velocity, and spectrum width data and generate up to 39 categories of analysis products derived from the basedata every five to ten minutes. WSR-88D systems have been modified and enhanced during their operational life to meet changing requirements, technology advances, and improved understanding of the application of these systems to real-time weather operations. (Klazura and Imy, 1993).

Real-time and Historical NEXRAD data can be accessible from the website of National Climatic Data Center (NCDC) of National Oceanic and Atmospheric Administration (NOAA) of U.S. Department of Commerce (<http://www.ncdc.noaa.gov/>). There are two kinds of NEXRAD data: Level-II data and Level-III data. Level II data are the three meteorological base data quantities: reflectivity, mean radial velocity, and spectrum width. From these quantities, further computer processing generates numerous meteorological analysis products known as Level III data. The archive data is autocumulative, and available data range is from 1991 to 1-day minus from today. Real-Time Level-III images and data are also available from the National Weather Service, and this Real-Time Level-III data is a critical data source for real-time or near real-time flood prediction in SERM. NCDC also provides a Java NEXRAD Viewer which visualizes WSR-88D Level-II and Level-III NEXRAD Radar data from the NCDC Archive and a Java NEXRAD Data Exporter that allows the export of NEXRAD data to common scientific formats such as Shapefile, Arc/Info ASCII Grid and more (<http://www.ncdc.noaa.gov/oa/radar/radardata.html>).

2.4.2 The Comparison of The Rain Gauge Data and NEXRAD Data

Although the NEXRAD can provide real-time rainfall data with better spatial and temporal resolutions than the current rain gauge networks, the accuracy of radar-based rainfall estimates is still under evaluation due to the complex nature of the radar-rainfall measurement process and the errors due to incorrect hardware calibration and ground clutter contamination (Over *et al.*, 2007; Jayakrishnan *et al.*, 2004). It should be noted that the rain gauge becomes the only reference available to check the validity and accuracy of NEXRAD data, but the gauge data itself has random, systematic, and representative or sampling errors, especially for time scales less than 10-15 minutes (Xie *et al.*, 2006; Habib *et al.*, 2001).

There are several comparative studies on correlation between Stage III NEXRAD data and co-located rain gage data since 1998 as shown in Table 2-2. Because of the modifications to the Stage III algorithms during 1996, including removal of bi-scan maximization during image mosaicking (Over *et al.*, 2007; Young *et al.*, 2000), studies with the Stage III data after 1996 would be more meaningful.

Table 2-2 The Recent Researches on Correlation between Stage III NEXRAD Data and Co-located Rain Gage Data Since 1998

Researchers	Area	Data	Result
Pereira Fo et al. (1998)	The Lake Altus area in southwest Oklahoma	185 NEXRAD Stage III hourly maps of precipitation accumulation and Rainfall measurements from the Oklahoma Mesonet network. From June 1995 to July 1996	The stage III analysis has a 40 percent underestimate of accumulative rainfall.
Johnson et al. (1999)	Eight basins in the southern plains region of the United States	Over 4,000 pairs of Mean areal precipitation values (MAPX) derived from NEXRAD stage III data and Mean areal precipitation (MAP) values derived (by Thiessen polygon weighting) from a precipitation gauge network over a 3-year time period.	Over the long term, mean areal estimates derived from NEXRAD generally are 5–10% below gauge-derived estimates. For storm events, a slight tendency for NEXRAD to measure fewer yet more intense intervals of precipitation is identified.
Wang et al. (2000)	Eight basins in the region near the Oklahoma-Arkansas-Missouri state boundaries	Mean areal precipitation (MAPX, 1 hr) derived from The NEXRAD Stage III data, River Forecast Centers (RFC)'s operational rain gage data (MAPO, 6hr) and NCDC's historic rain gage data (MAPH, 1hr) from June 1, 1993 to December 31, 1997	The radar-based MAPX are in good agreement with the gauged MAPO for most of the basins, and The remainder of the basins have MAPX values being lower than MAPO values at a range of 3–6%.
Stellman et al., (2001)	The Flint River basin, specifically the Culloden basin located in central Georgia south of Atlanta	NEXRAD stage III mean areal precipitation (MAPX) and rain gauge-derived mean areal precipitation (MAP). Jun 1996–Jul 1998.	Results show that the radar (MAPX) underestimates gauge-derived rainfall (MAP) by 38% at the end of the 2-yr period. This underestimate is most pronounced during the winter months of November–April when MAPX underestimates MAP by 50%. Comparisons during the summer (May–Oct) indicate that MAPX is similar to MAP.
Jayakrishnan et al. (2004)	the Texas-Gulf basin	NEXRAD Stage III and 24-h accumulations from 545 raingages for the period 1995-99	Overall under-estimation over the period from 1995-99 but over-estimation during 1998-99
Xie et al. 2006	the Sevilleta National Wildlife Refuge (NWR), located in central New Mexico	NEXRAD Stage III product and a network of gauge (10 stations) precipitation estimates during 1995 to 2001	NEXRAD underestimates rainfall accumulation in the nonmonsoon season, and overestimates rainfall accumulation in the monsoon season.
Westcott and Knapp, 2006	In the vicinity of the Fox River in northeastern Illinois	NEXRAD Multi-sensor precipitation estimates (MPE) compared to point measurements of daily precipitation from precipitation gages in the vicinity of the Fox River for the period February 2002–September 2004	In comparison to the daily gage data, however, the multi-sensor precipitation estimates were on average 25 percent lower throughout the year.
Over et al. 2007	DuPage County, Illinois	The NEXRAD data used in this comparison consist of Stage III (1997-2001) and Multisensor Precipitation Estimate (MPE) (2002-2005) gridded hourly products. The rain-gage data used in this study are from a network of 27 radio-telemetered tipping-bucket rain gages for the period from July 1997 through September 2005 was carried out at the daily time scale.	(1) July 1997 through September 1999; On average NEXRAD underestimated the rain-gage rainfall by about 25% (2) October 1999 through October 2001; Over-estimated the gage rainfall by about 9% (3) February, 2002 through September 2005. Under-estimated the gage rainfall by about 3%.

Clearly, NEXRAD kept improving its data processing over the history of the technology based on the above studies. Moon *et al.* (2004) used both NEXRAD stage III data and rain gauge data to simulate stream flow by SWAT in the Trinity River Basin, Texas. The accuracy of the model results suggests that NEXRAD is a good alternative to rain gauge data. Jayakrishnan's (2004, 2001) study also suggested that NEXRAD was more accurate when compared to rain gauge data based on improved data processing algorithms and on-going developments after 1998. Jayakrishnan compared NEXRAD and rain gauge data in the Texas-Gulf basin, and the study stated that rain gauges with more than 20% underestimation dropped from 75% in 1995 to 6% in 1999. From Young *et al.* (2000), the NEXRAD Stage III underestimates the gauge rainfall because the Stage III data has fewer precipitation hours in the case of light precipitation. Also, the Stage III data works well in warmer or monsoon seasons (Xie *et al.*, 2006; Seo and Breidenbach, 2002; NWS, 2002). Statistical comparisons of the rain gauge and NEXRAD data shows that the NEXRAD radar data have a good agreement with recent rain gauge data (Over *et al.*, 2007) and can be represented as the observed rainfall as rain gauge data. NEXRRAD data provides the better real-time, spatially and temporally distributed rainfall estimates available with the current technologies (Moon *et al.*, 2004).

2.4.3 The Application of NEXRAD Data in the SERMs

For SERMs, the spatial-temporal rainfall, as the driving force behind all hydrologic processes, may be the most critical input data. The rain gauge data is used as the primary source for SERMs, and users used to have to do mathematical interpolation due to the generally sparse rain gauge network especially for large watersheds. Compared

to rainfall data derived from rain gauge measurements, rainfall estimates from NEXRAD capture the spatial as well as temporal variability associated with rainfall, and do so in a near real-time fashion (Moon *et al.*, 2004).

Based on the advantages listed above, researchers recently began to utilize NEXRAD rainfall estimates for flood modeling, near real-time flood prediction, and water resource management. Knebl *et al.* (2005) presents a regional scale flood modeling study for the San Antonio River Basin (about 4000 square miles) incorporating Summer 2002 storm events with a new framework that integrates NEXRAD Level III rainfall, GIS, and a hydrological model (HEC-HMS/RAS). In the study, Stream network and 12 subbasins were delineated by HEC-GeoHMS with DEM. For the rainfall-runoff part, the 4×4 km grid, a resolution consistent with the resolution of NEXRAD data, was used by HEC-HMS. Hydrographs extracted from the rainfall-runoff model were saved as time series data and inputted directly into the hydraulic model. Similar research was also done with similar framework for small basins like the Salado Basin (222 square miles) and the Rosillo Creek Basin (29 square miles) (Whiteaker *et al.*, 2006; Robayo *et al.*, 2004). Giannoni *et al.* (2003) simulate extreme floods (the 27 June 1995 Rapidan River flood, VA) by combining radar rainfall estimates and a distributed hydrologic model. Rainfall estimates at the 1 km horizontal scale and 5 min time scale are used to reconstruct flood response to the Rapidan storm at basin scales ranging from 1 to 295 km². The Rapidan storm was a multi-cell thunderstorm with a characteristic horizontal scale of approximately 8–10 km. A radar-based flood warning system for Houston, TX utilizes the real-time NEXRAD rainfall (resolution is up to 1Km × 1Km) coupled with the real-time lumped model (RTHEC-1) and a distribute model to achieve more accurate, greater

lead time and timely flood forecast estimates (Fang *et al.*, 2006; Vieux *et al.*, 2005; Bedient *et al.*, 2003). Besides flood modeling, NEXRAD data is also utilized for a continuously hydrologic simulation. Zhang *et al.* (2004) compared six years of continuously simulated hydrographs from an eight-subbasin model to those from a single-basin (or lumped) model of the Blue River basin (1,232 km²) in Oklahoma. Subdividing the basin into eight subbasins captures spatially variable rainfall reflected in NEXRAD and produces improved results without greatly increasing the computational and data requirements. NEXRAD is also integrated with SWAT model for long-term daily simulation (Jayakrishnan *et al.*, 2005; Moon *et al.*, 2004). Daily NEXRAD rainfall data consist of NEXRAD hourly data at 4Km × 4 Km grid cell was used for these studies.

CHAPTER III

STUDY AREA

3.1 Study Area: Rivanna River Basin

The following criteria was used to identify the case study watershed for this dissertation research:

- Size of the watershed would be about 500-1000 square miles, so that the watershed is easier to handle, at the same time, would provide sufficient spatial variability and complexity to test the capability of MHSERM;
- The watershed should contain USGS gauge stations both on branches and mainstream, and measured data should be available from gauge stations;
- The watershed would locate in the State of Virginia;
- Regardless of how complex the stream network might be, the overall shape of the stream network would be dendritic because the Muskingum-Cunge routing method can't handle multiple downstream branches;
- The watershed would have very high peak flood flows with usually abundant rainfall, and would have a limited surface water reservoirs storage capacity. The local government usually controls the outflow of reservoirs during a big storm event, thus it can't be simulated by the routing method only.

After examining numerous watersheds in Virginia, the Rivanna River Basin was selected for the case study area by satisfying the above criteria.

The Rivanna River is a tributary of the James River located in the mountains and foothills of Central Virginia as shown in Figure 3.1. The Rivanna river basin spans the Blue Ridge Mountains in the west to the James River in the east (The Rivanna River Basin Roundtable, 1998). In the National Hydrography Dataset (NHD, 2000) hierarchical levels, the Rivanna Subbasin is at the fourth level and has 8-digit Hydrologic Unit Code (HUC), 02080204. From the first level to the third level, the Rivanna Subbasin belongs to

the Mid-Atlantic Region (HUC: 02), the Lower Chesapeake Subregion (0208), and the James River Basin (020802). The James River Basin occupies the central portion of Virginia and covers 10,206 square miles or approximately 25 percent of the Commonwealth's total land area. The Rivanna River Basin is a 761 square mile (486,900 acre, 1,971 square km) fan-shaped sub-basin representing approximately 2% of Virginia's total land area and 7.5% of the drainage of the James River watershed. The Basin is bordered by the Rapidan River basin to the north, the South Anna River basin to the east, the South Fork Shenandoah River basin to the west, and the Rockfish and Hardware River basins to the south. The Virginia Department of Conservation and Recreation (VADCR) has divided the Rivanna River Basin into ten hydrologic units (HU). The Rivanna River and its tributaries drain major portions of Albemarle and Fluvanna Counties, relatively small portions of Greene and Orange Counties, the City of Charlottesville, the town of Columbia, the village of Palmyra, and a tiny fraction of Nelson County (The Rivanna River Basin Roundtable, 1998).

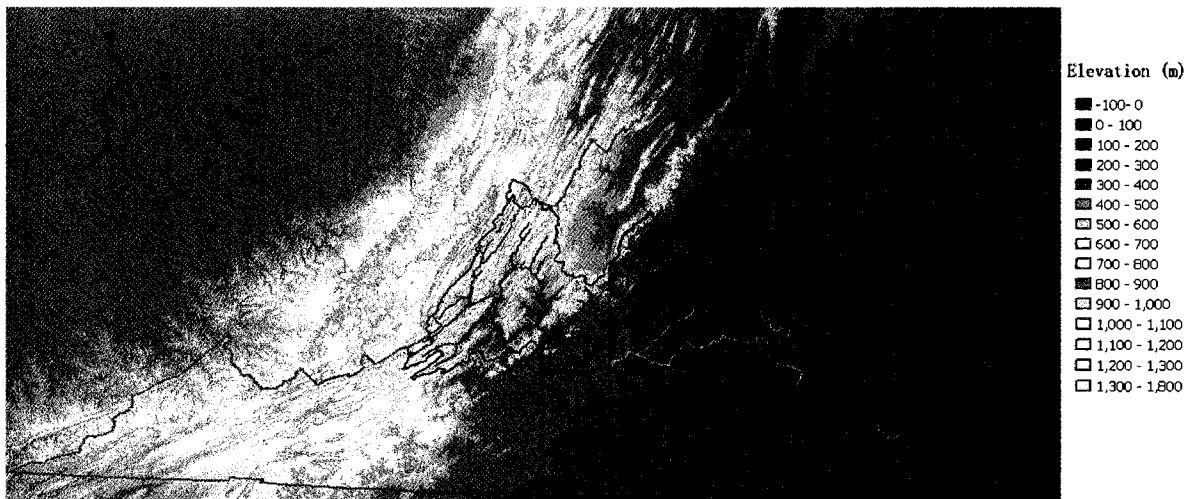


Figure 3.1 Rivanna River Basin, a Tributary of the James River, Central Virginia

Table 3.1 Rivanna River Basin by Hydrologic Unit (Rivanna River Basin Roundtable, 1998)

HU Name	Area (km²)	Major communities, Subdivisions, and Landmarks
Mechums River	257	Crozet, Batesville
Moormans River	201	Doylesville, Brown's Cove
Buck Mountain Creek	93	Free Union, Boonesville
S. Fork Rivanna/Ivy Creek	141	Along 29 north from Northfields to Forest Lakes subdivisions, South Fork Reservoir, and Ivy
N. Fork Rivanna/Swift Run/Preddy Creek	437	Advance Mills, Dyke, Stanardsville
Upper Rivanna River	153	Charlottesville and Ragged Mountain Reservoir
Middle Rivanna River/Buck Island Creek	184	Shadwell
Mechunk Creek	160	Cismont, Cobham, Cash Corner
Lower Rivanna River/Ballinger Creek	243	Lake Monticello, Palmyra, Carysbrook
Cunningham Creek	94	Fluvanna Ruritan Lake

The Rivanna Basin is subject to very high peak flood flows with usually abundant rainfall and has a limited surface water reservoirs/lakes storage capacity. USGS reports stated that the mean annual runoff of lands in the Rivanna Basin is about 16 inches, most of this runoff water cannot be stored, and flows directly into the James River. Three types of weather events including the summer super-cell rainstorm, a hurricane event, and a winter rain-snowmelt event can generate unusual floods in the basin on an annual basis. With continuing urbanization, and concomitant creation of impervious areas, the flood potential will increase. USGS has four surface water gauge stations in the basin to provide real time flow data as listed in Table 3.2 and Figure 3.2. Automated measurements are commonly recorded at 5-60 minute intervals and transmitted to the USGS National Water Information System (NWIS) database every 1-4 hour. There is

only one long-term gauging station measuring precipitation in the basin. It is located at the University of Virginia's McCormick Observatory on Observatory Hill, near the Basin's geographic center. The State Climatology Office provided precipitation data of this station, which is located at the University of Virginia's Clark Hall. The data were used to represent the entire basin (Rivanna River Basin Roundtable, 1998).

Table 3.2 Real Time Flow Data from Four Surface Water Gauge Stations, Rivanna Basin, Central Virginia

Site Number	Site Name	Decimal Latitude	Decimal Altitude	Datum
02031000	MECHUMS RIVER NEAR WHITE HALL	38.10263608	-78.59279350	NAD83
02032250	MOORMANS RIVER NEAR FREE UNION	38.14069020	-78.5558478	NAD83
02032640	N F RIVANNA RIVER NEAR EARLYSVILLE	38.16346740	-78.42473230	NAD83
02034000	RIVANNA RIVER AT PALMYRA	37.85791920	-78.26583730	NAD83

From the Rivanna River Basin Roundtable (1998), most of the region is now covered by the forest classification (approximately 64%). The second largest land cover classification is grazed pasture land (approximately 20%). 5+ acre residences in woodlands and one-acre residences are the third largest land cover classifications at approximately 4%. The mowed lawns/ moderately grazed pasture/golf courses and the ungrazed grass/shrubland each comprise approximately 2% of the land cover in the basin. Other classifications of interest include croplands at approximately 1% and ½-acre residences, 1/3- acre residences, and ¼-acre residences collectively comprising approximately 2%. Water surface occupies the remaining 7%.

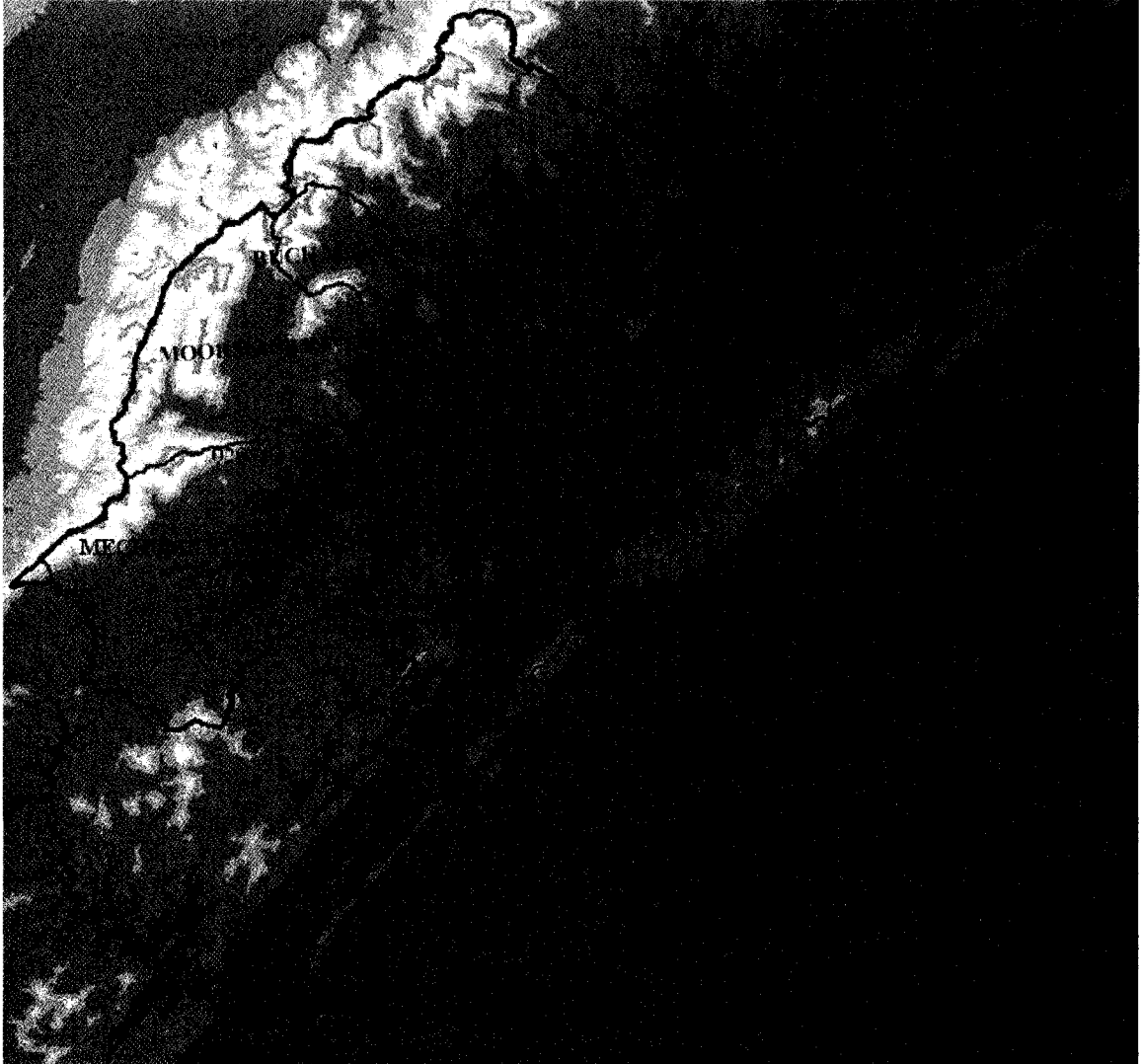


Figure 3.2 Subbasin Delineation and Location of Four Real Time Flow Data Surface Water Gauge Stations (listed in Table 3.2), Rivanna Basin, Central Virginia

3.2 Data Preprocessing

3.2.1. Synchronization of Projected Coordinate System

The spatial datasets used in the MHSERM that cover the Rivanna river basin were obtained from the data servers of different government agency such as USGS, NRCS and NOAA. These datasets were further clipped and transferred to the same projected coordinate systems of UTM, State Plane, or other customized projected coordinate

system. For this dissertation study, a customized projected coordinate system named Virginia_Lambert_Conformal_Conic is defined as below:

Projection: Lambert_Conformal_Conic
Datum: NAD1983
Linear Unit: meter
False Easting: 0
False Northing: 0
Central_Meridian: -79.5°
Standard Parallel 1: 37.0°
Standard Parallel 2: 39.8°
Latitude of Origin: 36°

All the spatial datasets are transformed to this coordinate system for this case study.

3.2.2. USGS DEM

The Digital Elevation Model data (DEM) was obtained from the National Map Seamless Server of the USGS in ESRI ArcGRID format with 1 arc second (30m/7.5 minute unit) resolution. The DEM data comes with NAD 83 (Geodetic North American Datum 83) Geographic coordinate system, and cell size was at a 00.00028 degree scale. It was then transformed to the Virginia_Lambert_Conformal_Conic projected coordinate system, and the cell size was re-sampled to 30 meters by the ESRI Project Raster tool. Transformed and preprocessed data was subsequently clipped to the area slightly larger than the study area to ensure complete coverage over the study area, Rivanna River Basin by using the ESRI Raster Clip tool.

3.2.3. NLCD Landcover Data

Similar to USGS DEM data, The National Land Cover Datasets (NLCD), NLCD1992 and NLCD2001 were obtained from the National Map Seamless Server of the USGS. They were in the following format:

Output Format: GeoTIFF

USA Contiguous Albers Equal Area Conic USGS version

X cell Size: 30.00 Meters

Y cell Size: 30.00 Meters

They were also transformed to the Virginia_Lambert_Conformal_Conic projected coordinate system. The datasets are clipped to cover the study area. The relationship of the value of the cells and the land cover category was established for both NLCD1992 and NLCD2001 as illustrated in Table 3.3.

3.2.4. NRCS SSURGO STATSGO

The NRCS (Natural Resources Conservation Service) has archived and distributed two types of soil spatial dataset: State Soil Geographic Database (STATSGO) and The Soil Survey Geographic Database (SSURGO). For the Rivanna River Basin, SSURGO soil map data obtained from NRCS Soil Data Mart in an ESRI shape file format with Projected Coordinate System - UTM_Zone_18N. The same manner, STATSGO soil map was also obtained in an ESRI shape files format and with Geographic Coordinate System - GCS_North_American_1983.

Table 3.3 Land Cover Category Lookup Table for NLCD1992 and NLCD2001 Dataset used in the Study

NLCD 1992		NLCD 2001	
VALUE	Category	VALUE	Category
11	Open Water	11	Open Water
12	Perennial Ice/Snow	12	Perennial Ice/Snow
21	Developed, Low Intensity Residential	21	Developed, Open Space
22	Developed, High Intensity Residential	22	Developed, Low Intensity
23	Developed, Commercial/Industrial/Transportation	23	Developed, Medium Intensity
31	Barren Land (Rock/Sand/Clay)	24	Developed, High Intensity
32	Quarries/Strip Mines/Gravel Pits	31	Barren Land (Rock/Sand/Clay)
33	Transitional	32	Unconsolidated Shore
41	Deciduous Forest	41	Deciduous Forest
42	Evergreen Forest	42	Evergreen Forest
43	Mixed Forest	43	Mixed Forest
51	Shrubland	51	Dwarf Scrub
61	Orchards/Vineyards/Other	52	Shrub/Scrub
71	Grassland/Herbaceous	71	Grassland/Herbaceous
81	Pasture/Hay	72	Sedge/Herbaceous
82	Row Crops	73	Lichens
83	Small Grains	74	Moss
84	Fallow	81	Pasture/Hay
85	Urban/Recreational Grasses	82	Cultivated Crops
91	Woody Wetlands	90	Woody Wetlands
92	Emergent Herbaceous Wetlands	91	Palustrine Forested Wetland
		92	Palustrine Scrub/Shrub Wetland
		93	Estuarine Forested Wetland
		94	Estuarine Scrub/Shrub Wetland
		95	Emergent Herbaceous Wetlands
		96	Palustrine Emergent Wetland (Persistent)
		97	Estuarine Emergent Wetland
		98	Palustrine Aquatic Bed
		99	Estuarine Aquatic Bed

The table is based on The NLCD 1992 21 Land Cover Classifications definition at: <http://landcover.usgs.gov/classes.php> and The NLCD 2001 Land Cover Classifications definitions at: http://www.mrlc.gov/nlcd_definitions.asp

The SSURGO soil data for the Rivanna River Basin is composed of several counties' SSURGO soil survey map, i.e. Albemarle, Fluvanna, Greene, Louisa, Nelson, and Orange. The SSURGO maps from these counties were merged into one big file, and

then transformed into the same projected coordinate system as DEM data for further data overlay. The merged shape file is transformed to the Virginia_Lambert_Conformal_Conic and then clipped to the size of the study. The clipped shape file was then converted to an ESRI Raster format (set the MUKEY field as the cell value) with cell size as 30m by using ESRI Feature to Raster tool. Here, MUKEY field stand for a unique numerical code, by which each soil type defined in the attributes table. The STATSGO soil map was transformed to an ESRI Raster format with similar steps as SSURGO.

3.2.5. National Hydrography Dataset (NHD)

The NHD data used in this study were originally available in pre-staged personal geodatabases by subregion. Applicable pre-staged personal geodatabases was obtained from the USGS NHD ftp server in an ESRI geodatabase format (NHDinGEO) with medium resolution and with the Geographic Coordinate System (GCS_North_American_1983). The NHD dataset was clipped to the study area using steps listed below:

1. Delete the Hydro_Net network in the GeoDatabase;
2. Delete all the features outside of research area – Rivanna River Basin;
3. Make sure there is no loops in the flowline network;
4. Delete all the features that don't belong to the network;
5. Create new dataset in the geodatabase with x/y domain that can cover the research area;
6. Transform all the Feature classes to the Virginia_Lambert_Conformal_Conic projected coordinate system, and save them into the new dataset;
7. Re-establish the network for the geodatabase.

3.2.6. NCDC NEXRAD

Historical or archived NEXRAD data was obtained from the NCDC (National Climatic Data Center) website of NOAA. The SERM model developed in this dissertation, MHSERM was using the Level-III 1 hour precipitation data of station STERLING, which is located at Sterling, VA (ICAO ID: KLWX; Latitude: 38°58'31.008"N, Longitude: 77°28'41.016"W). After the data files covering a storm event or a series of events were obtained, a Java NEXRAD Viewer provided by NCDC was used to export the data files to the ESRI shape files. Then the shape files were further transformed to the raster files for MHSERM using following procedure:

1. Choose the files whose recording time are close to each time steps, these time steps will be used in the MHSERM as the intervals, e.g. 10 minutes, or 15 minutes;
2. The Shape files are transformed to the shape files with the Virginia_Lambert_Conformal_Conic projected coordinate system;
3. The Shape files are burned to Raster data by setting the cell's value as rainfall intensity;
4. The rainfall intensity raster datasets are clipped to the size that covers the study area.

CHAPTER IV

METHODOLOGY

In this chapter, the methodology for developing a framework of a massive watershed scale storm event hydrological response model (MHSERM) is described. The MHSERM, integrated closely in an ArcGIS platform, is a fully distributed hydrological model. The model incorporates 5 modeling process-oriented components: (1) catchment delineation, (2) parameters extraction of Grid cells, (3) stream network establishment, (4) NEXRAD rainfall processing, and (5) overland runoff and flow routing.

The MHSERM was closely integrated with the ArcGIS platform by programming with ESRI ArcObjects. ArcObjects are a set of computer objects specifically designed for programming with ArcGIS desktop applications (Burke, 2003; Zeiler 2001), which provides us a powerful tool to integrate external models. The functions of the MHSERM model are provided as an ArcMap toolbar as illustrated in Figure 4.1.



Figure 4.1 Massive Watershed Scale Storm Event Hydrological Response Model(MHSERM) Components in form of ArcMap Toolbar

4.1 Catchment Delineation Based on NHD Data

The terrain analysis based on DEM data is widely used to delineate watersheds or catchments, derive the stream network and calculate the slope and the distance from each

cell to the outlet (Ivanov *et al.*, 2004a and 2004b; Tarboton, 2003; Tarboton and Ames, 2001; Wilson and Gallant, 2000; Tarboton *et al.*, 1991; Fairfield and Leymarie, 1991; Band, 1986). To delineate catchments or subwatersheds, most traditional methods rely only on flow direction dataset and another “starter” dataset (Jenson and Domingue, 1988). The flow direction dataset is calculated based on the elevation gradient estimated from DEM, and the starter dataset is used to mark the outlets of the catchments. However, in physical actuality, rainfall runoff goes to the rivers/streams as lateral flow before it goes to the outlet of the catchment. Also, logistically and computationally it can be very time-consuming to calculate flow directions for the whole watershed based solely on algorithms of computing flow directions using a watershed-scale, high-resolution DEM data set. In this dissertation, a new method was developed to delineate the catchments. This method utilizes NHD river/stream flowlines as the end of rainfall overland runoff, and the catchments are defined as the DEM grids whose rainfall runoff will go to the same river Reach of the NHD. This is more realistic in the natural system because the rainfall runoff usually goes to the streams or ponds, not to the outlet directly.

4.1.1 Remove Pits and NoData Cells in a DEM

DEMs almost always contain depressions (pits) that hinder flow routing (Jenson and Domingue, 1988), as well as some “NoData” grids that do not contain any value. The first step is to fill the depressions and the NoData grids in the DEM. The NoData grids are assigned with an approximate interpolated from the surrounding grids’ value. The pits are removed using ESRI filling pits methods within the RasterHydrologyOp class. The method is to create an adjusted “depressionless” DEM in which the cells contained in

depressions are raised to the lowest elevation value on the rim of the depressions (Jenson and Domingue, 1988).

4.1.2 Flowline Raster Dataset

To delineate catchments, NHD Flowline data are used to get the streams information. The flowline data is converted to Raster format by the ArcGIS 'Feature to Raster' tool. This process is usually called 'burn.' During the 'burn,' the cell size is set to the same with the cell size of DEM data, e.g. 30m. In this process, OBJECTID, a key value for each stream object in the NHD flowline dataset, was selected as the value of 'burned' flowline cells. The cells of DEM that are overlaid with flowline raster cells are marked with the OBJECTID as shown in Figure 4.2.

4.1.3 Flow Direction Calculation Based on the Steepest Path to the Streams

With the depressionless DEM prepared with ESRI filling sinks methods and with the flowline raster, flow direction was estimated and built for each cell. It can be emphasized enough that correct estimation of flow direction from a cell or within a catchment in a collective sense is the most critical step toward the correct and accurate estimation of runoff triggered by single or series of storm events.

To mark the flow directions in a DEM grid, a standard method of assigning its flow to one of its eight neighboring directions was used (Martz and Garbreche, 1992; Jenson, 1991; Jenson and Domingue, 1988; Tarboton *et al.*, 1988; Band, 1986; O'Callaghan and Mark, 1984). For example, flow direction of a cell is divided by 8 directions from the center of the cell, marked with the value of 2^x (x is from 0 to 7, from

East to Northeast), and is encoded to correspond to the orientation of one of the eight neighbor cells (Jenson and Domingue, 1988) as shown below in Figure 4.3.

Determination of the flow direction is based on the assumption that overland runoff will flow along the steepest path. The slope is calculated by dividing the elevation difference with the distance. Here, the distance is the cell's size for the non-corner cell, or multiple 1.414 ($2^{1/2}$) for the corner cell.

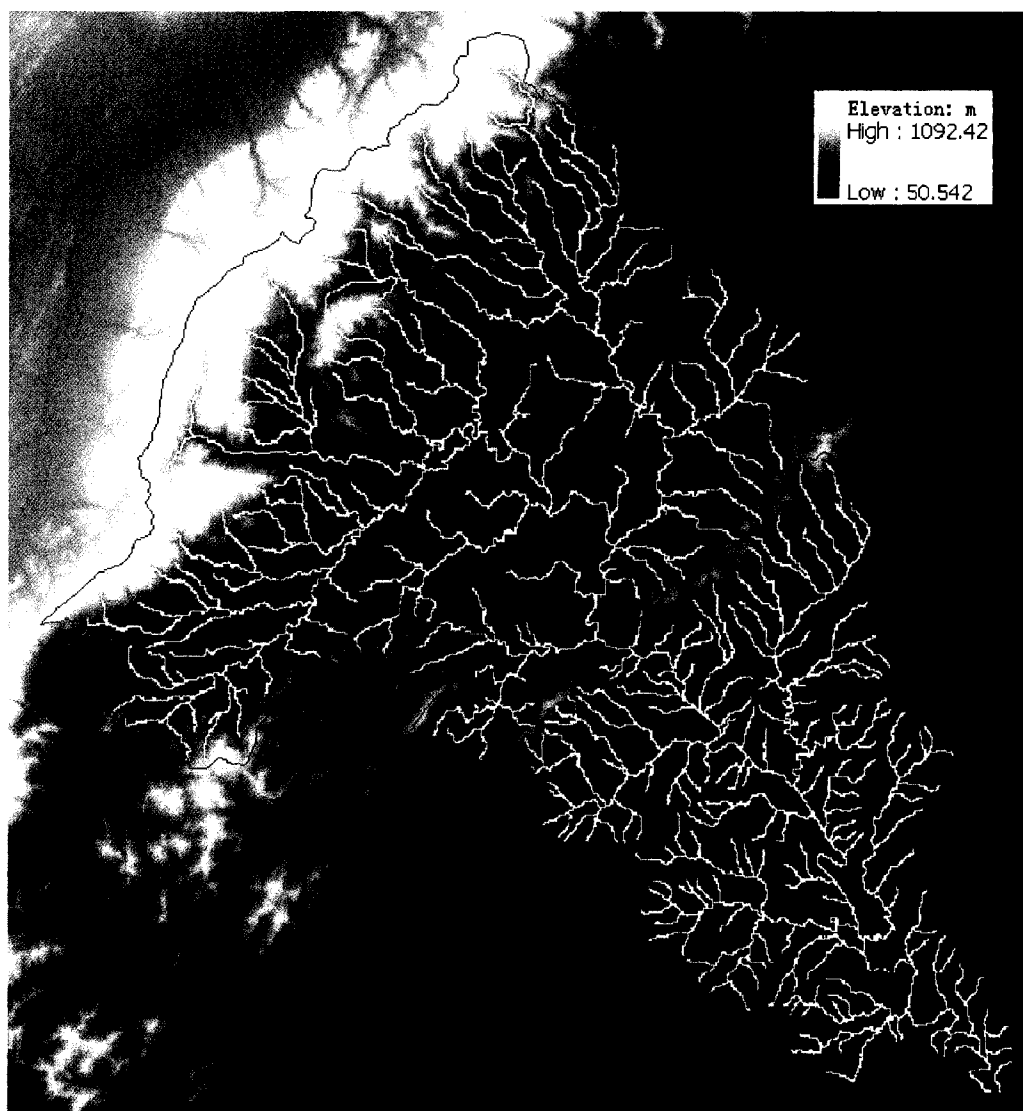


Figure 4.2 Cells of DEM Overlaid with Flowline Raster Cells

32 (2^5)	64 (2^6)	128 (2^7)
16 (2^4)	Cell	1 (2^0)
8 (2^3)	4 (2^2)	2 (2^1)

Figure 4.3 Gradient-based Determination of the Overland Runoff Flow Direction

The traditional algorithm to calculate the flow direction from DEM data is a Forward Search method to find the steepest path from a starting grid to the side of the DEM data (Jenson and Domingue, 1988). With this method, the slopes to each of one grid's eight directions are computed, and the flow direction is assigned to a neighbor cell that has the largest slope, but if the largest slope occurs at more than one neighbor, the method has to mark the grid and repeat the steps until it can determine the downstream grid. Since the method needs to search the path to the edge of the DEM data, the calculation is very time-consuming even for an average-sized DEM data, especially for a flat terrain area with a minimum elevation gradient presents.

In this dissertation research, an Upstream Search method is introduced to calculate the flow directions and the catchments. This method utilizes the NHD flowline

dataset as another input data source besides the DEM data for estimating flow directions, and calculates the flow path from the downstream end, i.e. streams, waterbodies or DEM data edges toward upstream in a reverse direction. Table 4.1 describes the Upstream Search method procedures to calculate the flow direction using DEM and NHD flowline data concurrently. The cells in the flow direction raster are encoded with the following values: 0, 1, 2, 4, 8, 16, 32, 64, 128 and >1000 (specifically for stream cells). The resulting flow direction raster is generated in ESRI Grid format as shown in Figure 4.4.

Table 4.1 Upstream Search method Procedures to Calculate the Flow Direction

Step	Procedures		
1	Mark all the grids on the DEM edge, Streams and Waterbodies as starting grids;		
2	Mark the flow distance as 0 for starting grids, and other grids are -999 as N/A;		
3	Calculate all grids' 8 direction slopes;		
4	Compare the slope values of the neighbor grids of the starting grids, the result will be one of the below two situation:		
	<table border="1"> <tr> <td>the largest slope occurs at the starting grids: 1) If the largest slope occurs only at one starting grid, assign the flow direction to that grid, and mark the flow distance from the current grid to the flowline grids, or waterbodies grids, or edge grids; 2) If the largest slope occurs at more than one starting grids, the program compares the distances from current grid to the starting grids, assign the flow direction to the grid with the shortest distance, and then mark the flow distance to the flowline grids, or waterbodies grids, or edge grids;</td> <td>The largest slope occurs at the other grids, not the starting grids 1) The program does nothing, the grid is still marked as 'To be determined' with value -999;</td> </tr> </table>	the largest slope occurs at the starting grids: 1) If the largest slope occurs only at one starting grid, assign the flow direction to that grid, and mark the flow distance from the current grid to the flowline grids, or waterbodies grids, or edge grids; 2) If the largest slope occurs at more than one starting grids, the program compares the distances from current grid to the starting grids, assign the flow direction to the grid with the shortest distance, and then mark the flow distance to the flowline grids, or waterbodies grids, or edge grids;	The largest slope occurs at the other grids, not the starting grids 1) The program does nothing, the grid is still marked as 'To be determined' with value -999;
the largest slope occurs at the starting grids: 1) If the largest slope occurs only at one starting grid, assign the flow direction to that grid, and mark the flow distance from the current grid to the flowline grids, or waterbodies grids, or edge grids; 2) If the largest slope occurs at more than one starting grids, the program compares the distances from current grid to the starting grids, assign the flow direction to the grid with the shortest distance, and then mark the flow distance to the flowline grids, or waterbodies grids, or edge grids;	The largest slope occurs at the other grids, not the starting grids 1) The program does nothing, the grid is still marked as 'To be determined' with value -999;		
5	Now, the grids with known flow direction from step 4 are also considered as starting grids with flow distance value;		
6	For the grids still encoded as -999, repeat the step 4 until all grids has flow direction assigned.		

4.1.4 Catchments Delineation

With the flow direction raster and reverse flow direction raster that records the upstream grid, overland accumulation area to the stream is obtained by tracing the flow path to stream cells, and as a result, catchments are delineated successfully. The procedures for delineating catchments are listed in Table 4.2.

Table 4.2 Procedures for Delineating Catchments with Flow Direction Raster and Reverse Flow Direction Raster

Step	Procedure
1	Extract the cell's value of the flow direction raster and reverse flow direction raster;
2	If the cell's flow direction code is 0 or >1000 (stream cells), set the value to the cell of catchment raster dataset;
3	If the cell's flow direction code is 1,2,4,8,16,32,64,128,
4	Trace the flow path down to any stream cells, and set the code of the stream cell to this cell.

The cells within a contributing area to a NHD flowline (stream) are coded with the flowline's OBJECTID flag. Aggregation of the networked cells through flowline is then defined as a catchment. Application of the automated delineation procedure produced 886 catchments for the entire study area of the Rivanna river basin resulting catchment delineations are shown in Figure 4.6.

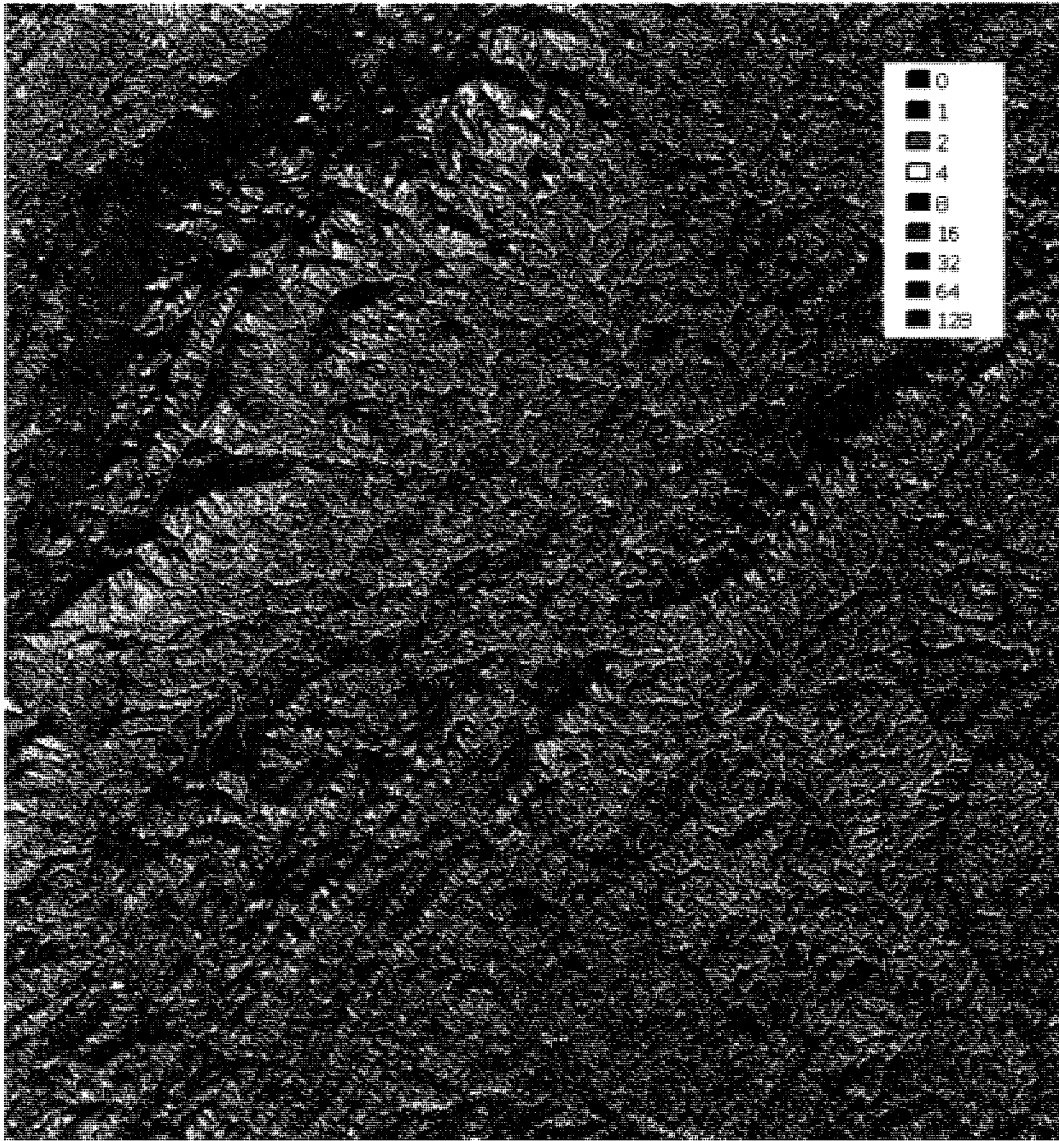


Figure 4.4 Encoded Flow Direction Raster in ESRI Grid format for Upstream Search Method

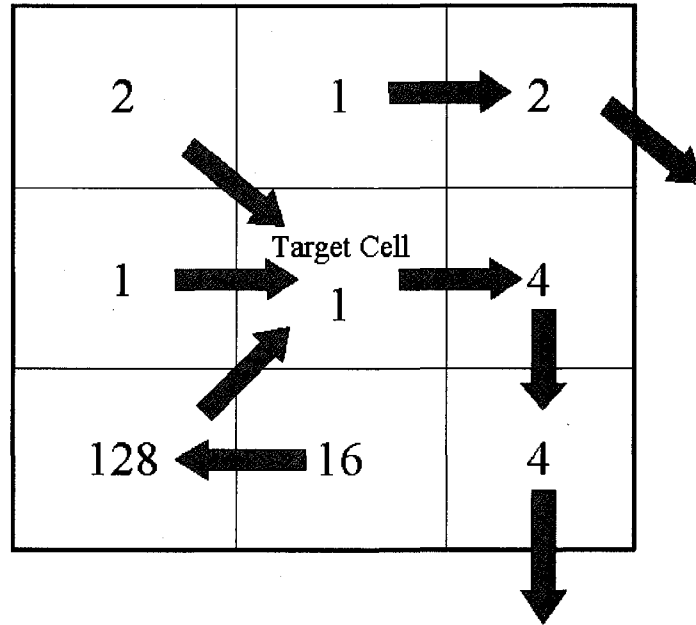


Figure 4.5 Flow Direction Assignment and Aggregation of the Networked Cells through Flowline



Figure 4.6 886 Catchments Delineated by Automated Procedure, Rivanna river basin, Central Virginia

4.2 Parameters Estimation for Each Cell

The massive watershed scale storm event hydrological response model (MHSERM) conceptualized, developed and implemented in this dissertation research is designed to estimate the parameters for millions of cells automatically. Cell parameters

are for estimating runoff from a single or a series of storm events, and include NRCS runoff curve number (CN), Manning's roughness coefficient, the true flow distance to streams or waterbodies, and the downstream slope. NRCS CN method is an empirical procedure presented by NRCS (formerly known as SCS, the Soil Conservation Service) (SCS, 1986). It is a combined loss model to calculate rainfall excess resulting from a given rainfall, which accounted for interception, depression storage, evaporation and infiltration together for loss calculations (Akan and Houghtalen, 2003). The CN number is determined by combining the hydrologic soil groups, land cover type and its hydrologic condition. In the study, the entire study area was divided into millions cells as the same resolution of DEM (e.g. 30m by 30m), and each cell's CNs for Good, Fair and Poor land cover conditions were estimated.

Because MHSERM can simulate a watershed at various resolutions of DEM desired, millions of cells representative of a selected DEM resolution also need their respective CN values assigned to reflect spatial variability within the watershed. The task of manually assigning CN values to these millions of cells, respectively, is simply not logistically sound, even if it is attainable. To solve this core problem, a method was developed in this dissertation to estimate and assign the CNs for millions of cells automatically.

4.2.1 Determine Hydrologic Soil Groups Automatically Based on SSURGO and STATSGO Soil Dataset

To estimate one cell's CN, the hydrologic soil group of the cell must be determined first. The SCS (1986) classifies soils into four groups (A, B, C and D)

according to their minimum infiltration rate. With respect to soil textures, group A includes sand, loamy sand, and sandy loam; group B includes silt loam and loam; group C includes sandy clay loam; group D includes clay loam, silty clay loam, sandy clay, silty clay and clay (Akan and Houghtalen, 2003). To determine the hydrologic soil type for millions of cells, a method was developed to use the NRCS soil spatial dataset, State Soil Geographic Database (STATSGO) and The Soil Survey Geographic Database (SSURGO) dataset in the ArcGIS platform. Although SSURGO spatial dataset has a higher resolution and more detailed information than STATSGO, the study area may not be completely covered by SSURGO dataset as summarized in Table4.3. To obviate partial deficiency in applicable SSURGO dataset, alternative STATSGO dataset was used as a supplement dataset. The detailed steps for determining hydrologic soil type for the cells using SSURGO/STATSGO composite are listed in Table4.4.

Table 4.3 The Availability of NRCS SSURGO Spatial Dataset for Rivanna River Basin till 02/29/2008

Counties	NRCS County Code	SSURGO Available?
Albemarle	VA003	Yes
Fluvanna	VA065	Yes
Greene	VA079	Yes
Louisa	VA109	Yes
Nelson	VA125	Yes
Orange	VA137	Yes
Charlottesville City	VA540	No

Table 4.4 Procedures for Determining Hydrologic Soil Type for the Cells using SSURGO/STATSGO composite

Step	Procedure
1	Merge the SSURGO Spatial datasets of the corresponding counties, and Clip the datasets to a little bigger than the study area;
2	Transfer the projection to the same one with other dataset;
3	Transfer the SSURGO Spatial dataset to ESRI Raster (use the MUKEY value);
4	Set up a look up table to link the MUKEY with Hydrologic Soil Type;
5	If the available SSURGO dataset can't cover the whole study area, STATSGO dataset will be used to extract the soil information of the area (Figure 4.7);
6	Determine the hydrologic soil type for all the cells (Figure 4.7).

4.2.2 Estimate NRCS CN Number

NRCS (SCS) CN number for each cell was estimated by overlaying the landcover raster dataset over hydrologic soil type raster dataset estimated in the previous step. SCS (1986) provides the runoff CN tables for urban areas, cultivated agricultural lands, other agricultural lands, arid and semiarid rangelands. A look up table (LUT) was established based on SCS tables and USGS landcover classification. Combining the cell's hydrologic soil type and land cover class, the MHSERM estimates a cell's CN number by matching conditions in the look up table. Since land cover type can have different hydrologic conditions (Poor, Fair, Good), the MHSERM generates three different CN raster datasets that can be used effectively without re-estimation when the hydrologic condition for the cell changes or when various what-if scenarios reflecting a different BMPs are evaluated. Figure 4.7 illustrates overlaying of hydrologic soil type raster dataset with landcover raster dataset for CN estimation. Figure 4.8 illustrates CN estimation for different hydrologic conditions (Poor, Fair, Good) of hydrologic soil type raster dataset.

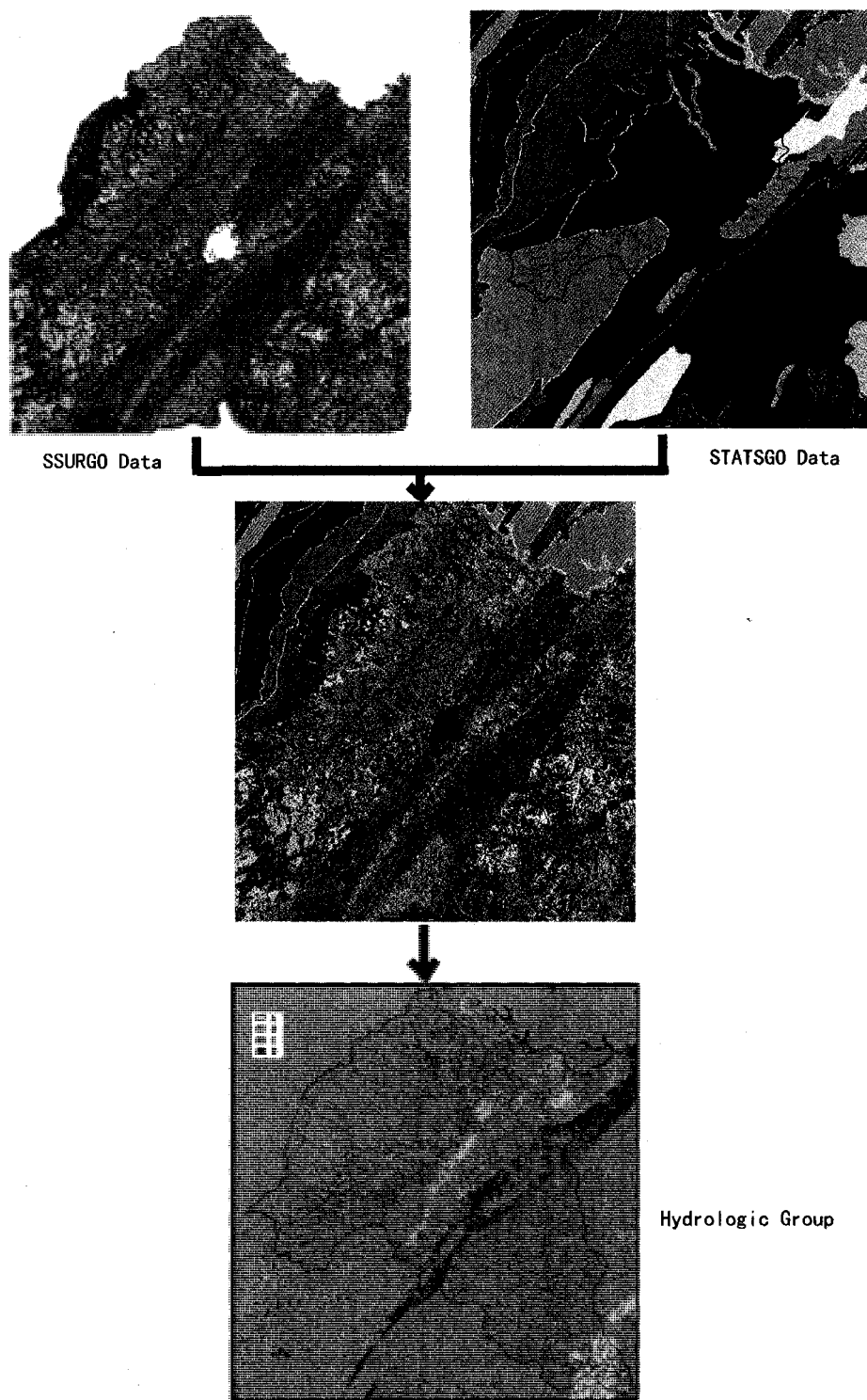


Figure 4.7 Overlaying of Hydrologic Soil Type Raster Dataset with Land Cover Raster Dataset for CN Estimation.

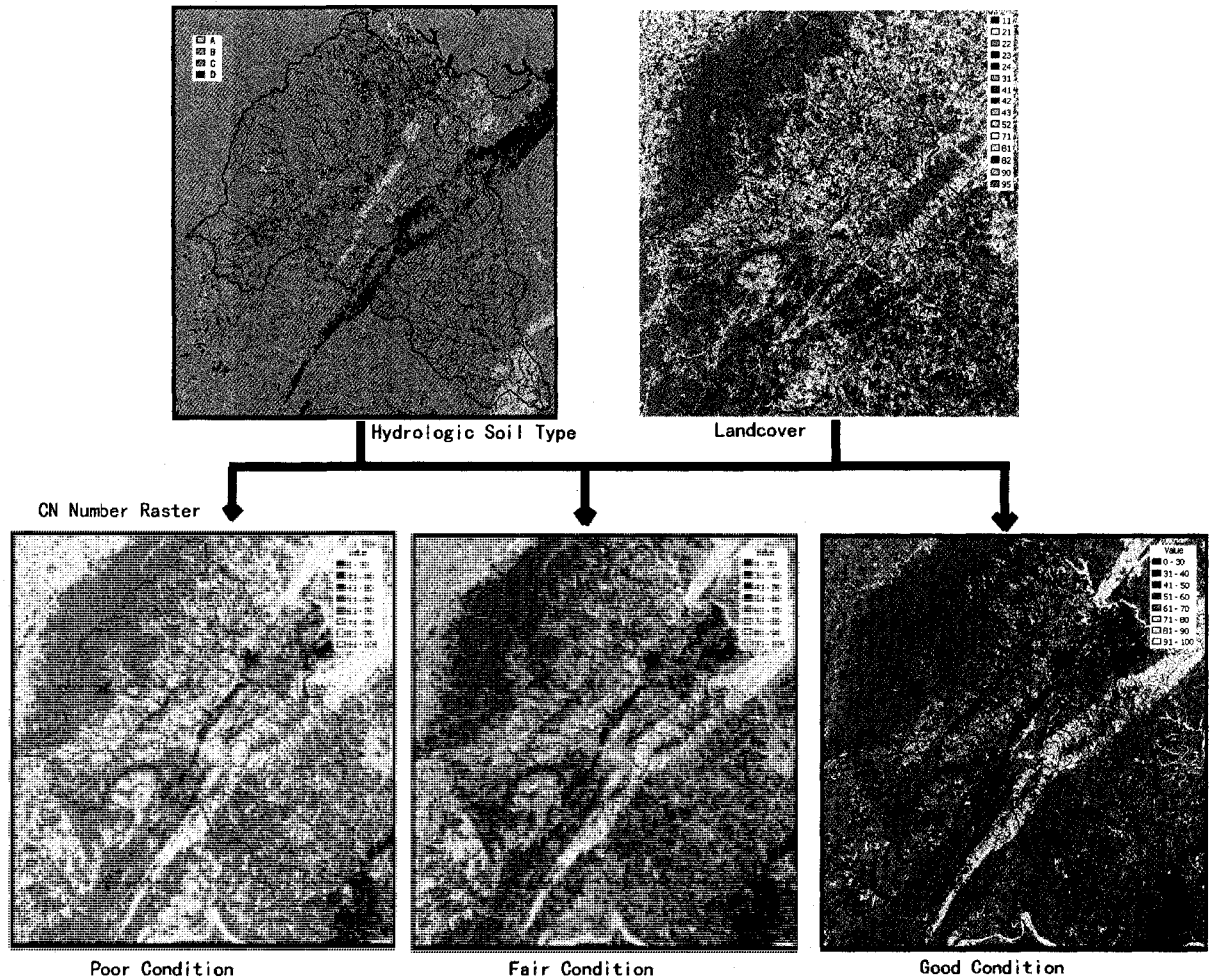


Figure 4.8 CN estimation for different hydrologic conditions (Poor, Fair, Good) of hydrologic soil type raster dataset

4.2.3 Estimate Manning Roughness Value for Cells

Overland flow is a special type of open-channel flow with a very shallow depth (Akan and Houghtalen, 2003). For describing such overland flow, Manning's roughness factor (n) is an effective roughness coefficient that includes the effect of raindrop impact; drag over the plane surface; obstacles such as litter, crop ridges, and rocks; and erosion

and transportation of sediment (SCS, 1986). SCS (1986) also gives a table of Manning's n values for sheet flow for various surface conditions. MHSERM was designed to estimate overland Manning roughness value 'n' for each cell automatically by its landcover value and SCS table. The resulting Manning roughness value assignment to cells is shown in Figure 4.9.

4.2.4 Calculate the Downstream Flow Slope and Distance to the Streams or Waterbodies for Cells

The flow slope and flow distance to the receiving streams or waterbodies in a cell are calculated based on the DEM dataset and flow direction dataset prepared in previous steps, as well as with NHD flowline dataset and the NHD waterbody dataset. Procedures are described in Table 4.5, that calculate the flow slope and distance to the streams/waterbodies of cells for one catchment. MHSERM then goes through all catchments and repeats the procedures. Calculated results are stored in an ESRI Grid raster format as shown in Figure 4.10.

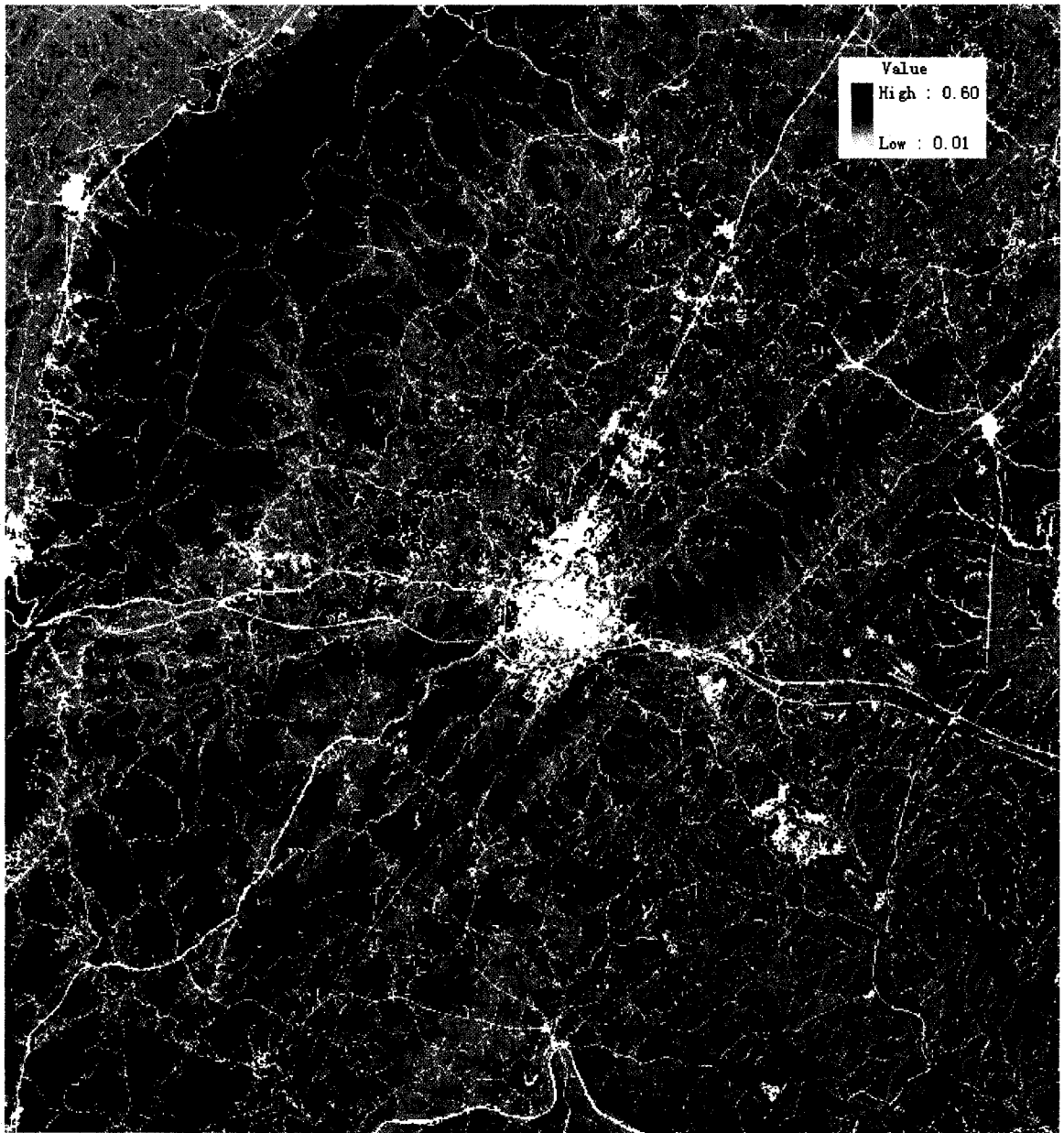


Figure 4.9 Manning Roughness Value Assignment to Cells

Table 4.5 Procedure for Calculating Flow Slope and Flow Distance to the Receiving Streams or Waterbodies

Step	Procedures
1	Extract the boundary of the catchment from the catchment raster dataset;
2	Locate one start cell within the catchment;
3	Record the elevation of the start cell from DEM data, set the distance =0;
4	Get the downstream cell on the basis of Flow direction dataset;
5	If the downstream cell is a stream cell or waterbody cell, extract the cell's elevation from DEM dataset, sum the flow distance between these two neighbor cells, calculate the elevation drop between the start cell and this cell, then calculate the slope by divide the elevation drop with distance;
6	If the downstream cell is not a stream cell or waterbody cell, sum the distance by adding the flow distance between these two neighbor cells, then go to step 4 to get the next downstream cell;
7	Loop all the cells within the catchment;
8	Set 1 for the slope and distance of stream/waterbody cells, and -1 for the slope and distance of the cells outside of the study watershed;
9	Loop all the catchments in the catchment raster dataset.

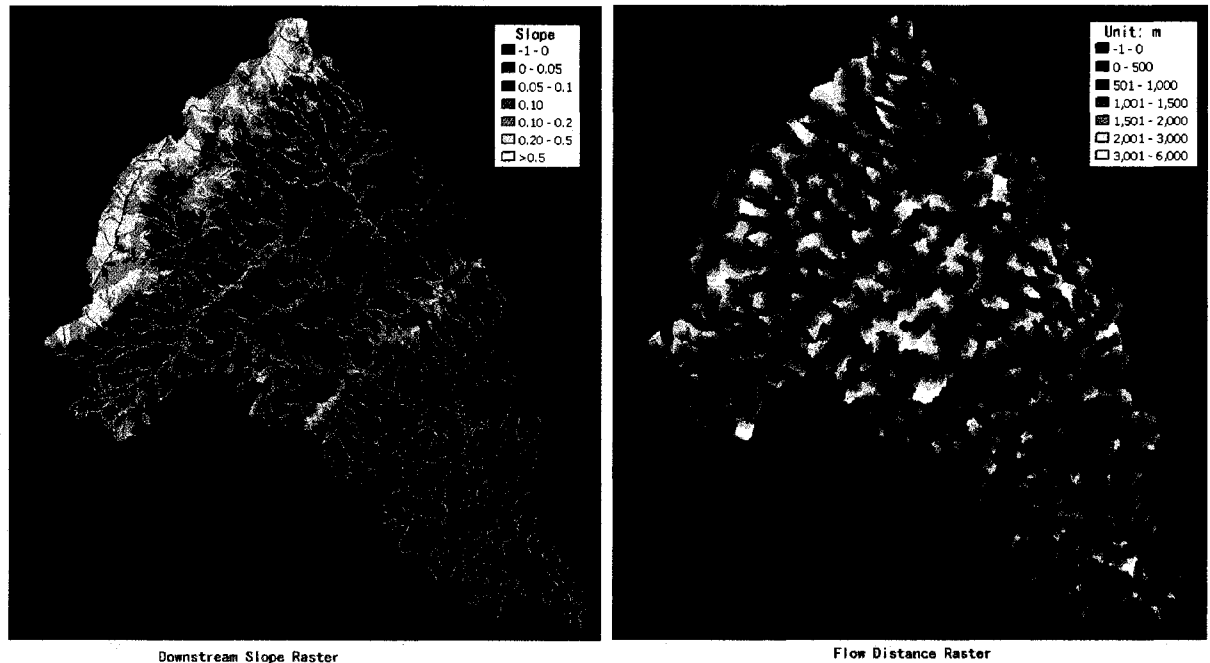


Figure 4.10 Flow Distance to stream and Slope to stream Raster

4.3 Establishment of Stream Network Based on NHD Data

The NHD dataset in ESRI geodatabase format (NHDinGEO) has built-in network (HYDRO_NET) for its flowline data that provides the flow direction as shown in Figure 4.11. ESRI ArcGIS was used to trace the flowline by using its Network Analyst utility. However, a hydrological model cannot route flow by only using traced flowline information. Further routing sequence and the stream's geometric parameter are still required for correct flow routing. MHSERM was implemented with a method to establish the stream routing sequence and set the stream's parameters, as well as link the lake/reservoirs with the stream network.

4.3.1 Establish the Flow Routing Sequence for the Stream Network

MHSERM estimates the stream's routing sequence by extracting the flow direction information stored in the NHD HYDRO_NET. The resulting stream's routing sequence is stored in a Microsoft Access database first. For recording the routing location of a flowline/stream object, three attributes are essential. These three attributes are its rank from the outlet (=sequence), the downstream flowline's ID (=connectivity), and the linked waterbody object's ID (=identification). The waterbodies are then linked with the flowline objects by recording their ObjectID with the related flowline's data to complete the flow routing sequence.

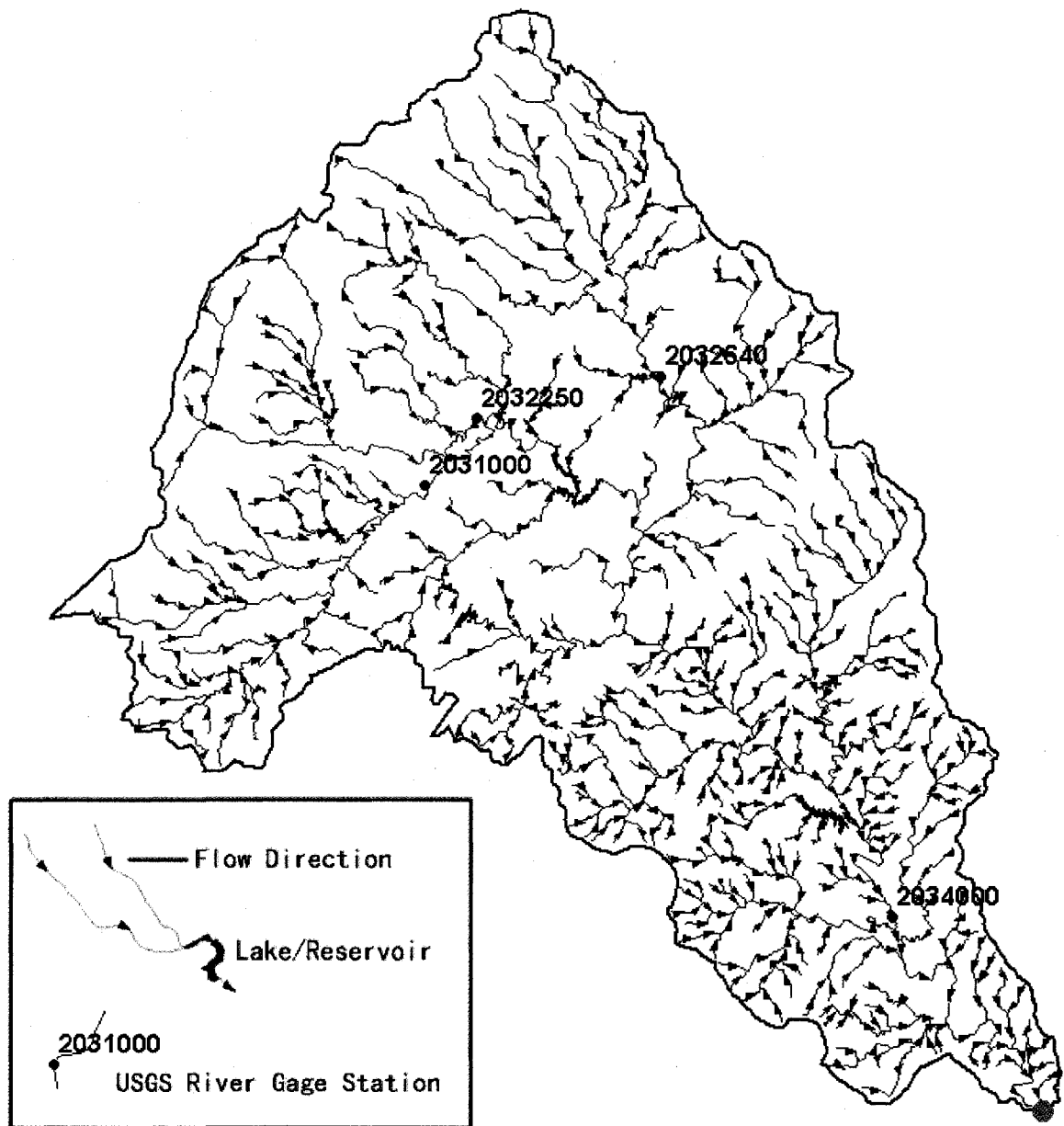


Figure 4.11 Network (HYDRO_NET) for Flowline in NHD dataset, in ESRI Geodatabase Format (NHDinGEO)

For example, the initial starting rank is set at the outlet, and the first upstream flowline object is recorded as 1000, and the second one is 1001, and so on as illustrated

in Figure 4.12. As the example map shown in Figure 4.12, the flowline 95879 is ranked 1000, and its two upstream flowlines, 94780 and 101625 are ranked 1001. The two upstream flowlines also have an attribute to record the downstream flowlines objected, i.e. 95879 in this example. The waterbody with ObjectID 69 is then linked with flowline 90997. Since a flowline does not have an upstream flowlines, it is marked as “leaf.”

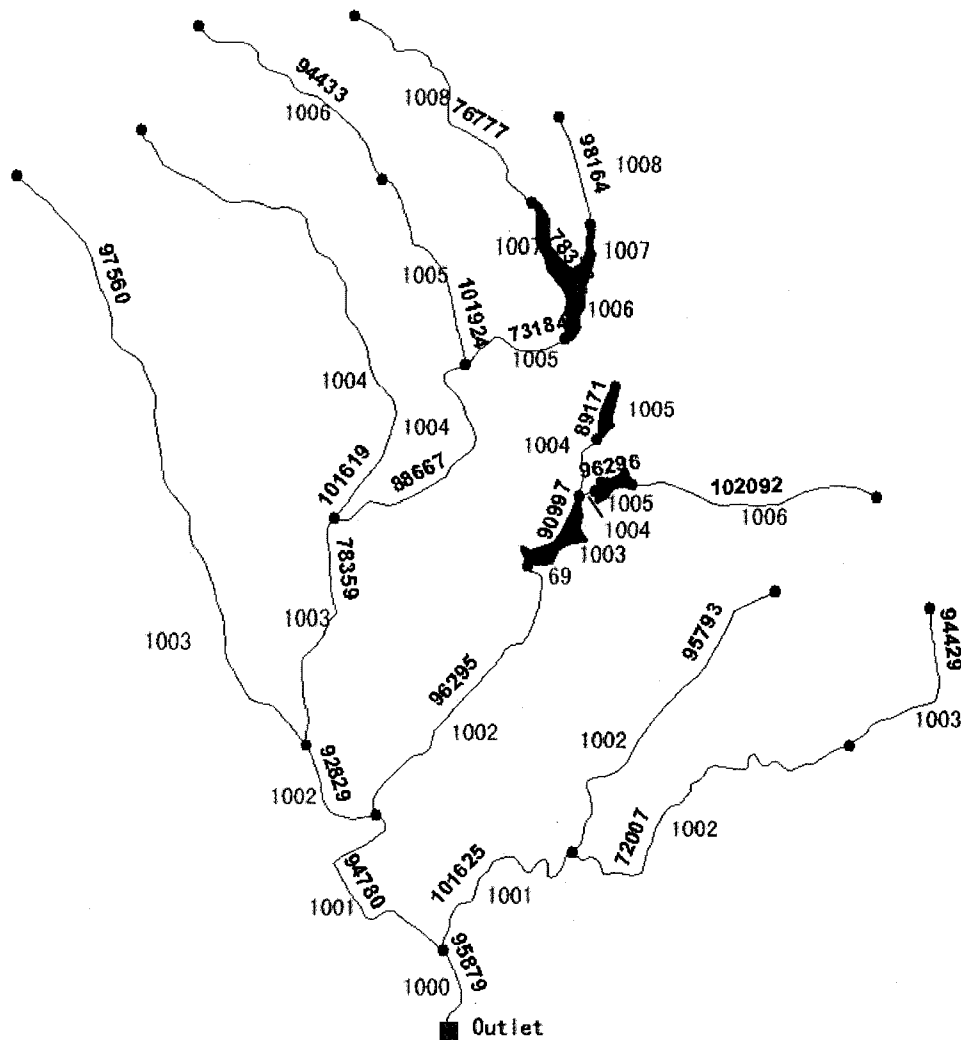


Figure 4.12 Streams Routing Sequence via Upstream Search Method Rank utilizing Rank from the Outlet (=sequence), Downstream Flowline’s ID (=connectivity), and Linked Waterbody Object’s ID (=identification)

4.3.2 Extract Streams' Parameters

Basic geometric and physical parameters representative of flowlines and waterbodies are critical components for developing the flow routing sequence in a stream system. Two types of parameters are utilized by the MHSERM, one of which can be extracted from the available public dataset like the stream's slope and length, and the other is which can be heuristically assumed like the cross section profile. Because the cross section profiles of the streams are very difficult to obtain, MHSERM assumed and generalized that the stream cross section would be a triangular shape, but different values can be set by users, if necessary, for slope H and V for any flowline objects in the database. At the same time, MHSERM can calculate the overland accumulation area for each flowline object, and its total upstream area. The main parameters for a flowline object are listed in Table 4.6.

Table 4.6 Main Parameters for a Flowline Object for Developing the Flow Routing Sequence in a Stream System

Parameter	Methods
Length	The length of a flowline object is extracted from the flowline object's property automatically.
Slope	The slope of a flowline object is calculated by dividing the elevation drop with its length; the elevation drop of the flowline is calculated from DEM data automatically.
Overland Accumulation Area	The Overland Accumulation Area of a flowline object is calculated on the basis of the catchment raster data .
Upstream Contribution Area	The Upstream Contribution Area of a flowline object is calculated with the overland accumulation area and the NHD stream network data.
Manning's Roughness Coefficient n	User can set n value for each flowline object. The estimation of n can be found in the table of Manning's Roughness Coefficient n (Henderson, 1966).
Cross Section	The cross section of a flowline object is assumed as a triangular shape, and the side slope H:V can be set by users.

4.3.3 Extract Waterbodies' Parameters

Waterbody data is included in the NHD dataset and represents various impounded waterbodies such as lakes, reservoirs, ponds, etc. Besides some waterbodies isolated from the stream network, most of the waterbodies are within the stream network. For flow routing purposes in the stream network, MHSERM considers only waterbodies within the stream network since the Stage-Area or Stage-Storage data for those non-stream network waterbodies is not available. MHSERM assumes the trapezoidal body for all the waterbodies, and a rectangular weir control at the bottom of its outlet as illustrated in Figure 4.13. For a waterbody, the surface area is extracted from NHD Waterbody data set by MHSERM, and users can set its width and length based on the surface area and shape, as well as the side slope. Also, users can set the length and the coefficient of the hypothetical weir control. The waterbodies are added to the flow routing network by writing its ObjectID into the corresponding flowline's record.

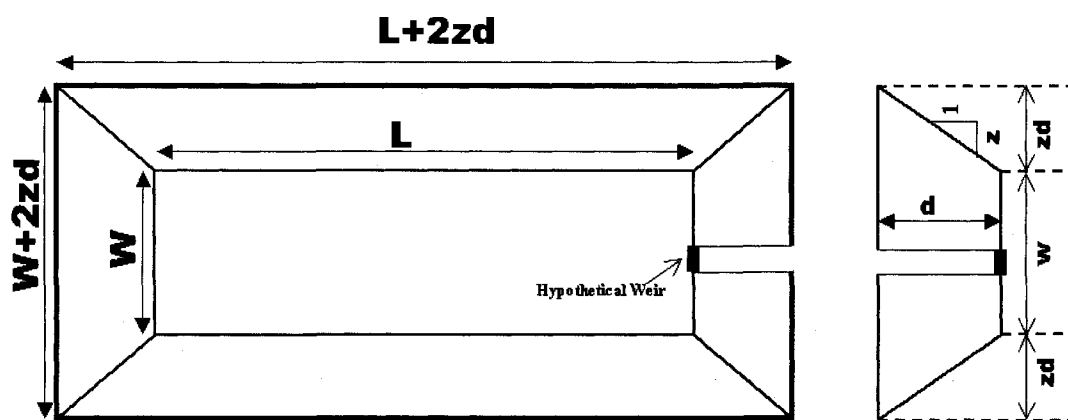


Figure 4.13 Elements of a hypothetical trapezoidal waterbody to represent the waterbody in MHSERM (the figure is from Akan and Houghtalen, 2003 and slightly modified). W and L are the width and length of a regular rectangular base, z is a side slope, d is the flow depth.

4.4 The Temporal-Spatial Overland Runoff Calculation Based NEXRAD Radar Data

Compared to rainfall data derived from physical rain gauge measurements, rainfall estimates from NEXRAD radar capture the spatial as well as temporal variability associated with rainfall to the watershed, and do so in a near real-time fashion (Moon *et al.*, 2004). MHSERM takes advantage of NEXRAD precipitation radar data as the temporal-spatial rainfall input. As a full-scale distributed model, MHSERM thus provides a GIS framework to best utilize the spatial variability of NEXRAD data on very detailed spatial terrain, landcover and soil data. Also, MHSERM can utilize the shortest possible interval of the NEXRAD data (less than 10 minutes), which provides a new paradigm for near real-time flood prediction.

4.4.1 Rainfall Excess Calculation for a Storm Event or a Series of Storm Events

Rainfall Excess calculation uses the rainfall intensity raster data extracted from NEXRAD data as its input data. The rainfall intensity raster was first clipped to the study area, and then further transformed to the same projection with DEM data for subsequent overlay. MHSERM utilizes ArcGIS to display the intensity data as a series of raster as shown in Figure 4.14. In the figure, four samples of the NEXRAD precipitation intensity raster of the Rivanna River basin show us the spatiotemporal variability of a scattered storm event. The storm moves from the north to the south of the basin.

MHSERM utilizes a setting file to configure how the model to manage the rainfall data. The setting file defines the number of intervals for a single or a series of storm events, start and end time, storm event numbers, AMC condition for these events, start

interval and end interval number for each event, etc. as listed in Table 4.7. With configuration in this setting file, the cumulative rainfall raster series are firstly calculated. MHSERM calculates the cumulative rainfall depth of each cell for each event. For this purpose, the cell size of the cumulative rainfall raster is set the same size of the cell for DEM raster, or Curve Number (CN) raster, thus the rainfall excess for each cell can be calculated by MHSERM.

Table 4.7 MHSERM Example Setting File for Rainfall Data.

Row Number	Contents	Definition
1	Rasters count:	
2	215	The total interval number for the simulation.
3	Start:	
4	20070824 19:59	The start time of the storms
5	end:	
6	20070827 02:10	The end time of the storms
7	Interval:	
8	15 minutes	The interval time of the NEXRAD data used
9	Storm Event Number:	
10	3	The number of the storm events
11	the start, end interval and AMC condition (1,2, or 3) for these storm events:	For the AMC condition, 1 means drier, 2 is normal, and 3 means wetter.
12	0	The start interval number for the first event
13	15	The end interval number for the first event
14	1	The AMC-I for the first event
15	88	The start interval number for the second event
16	0	Consider the event as the same event with the last one? 0 means yes, and 1 is not.
17	133	The end interval number for the second event
18	2	The AMC-II condition for the second event
19	196	The start interval number for the third event
20	0	Consider the event is the same with its foregoing event, 0 means yes, and 1 is not.
21	214	The end interval number for the third event
22	3	The AMC-III condition for the third event
23	1	Consider the event as the same event with the last one? 0 means yes, and 1 is not.

Table 4.7 (Continued)

24	-----	
25	0	The interval number
.	0824 20:00	The time for this interval
.	0824_1959	The NEXRAD raster name
.	1	
.	0824 20:15	
.	0824_2016	
	...	
67	15	
68	0824 23:45	
69	0824 2345	The last NEXRAD raster of event 1.
70	16	'n/a' means no precipitation between events
71	0825 00:00	
72	n/a	
...	...	
286	88	The first NEXRAD raster of Event 2.
287	0825 18:00	
288	0825_1759	
...	...	

MHSERM calculates the rainfall excess for each cell using the NRCS (SCS) runoff curve number method with cumulative rainfall raster. With three hydrologic conditions and three AMC conditions, MHSERM can have nine different rainfall excess intensity raster series for a storm event. Rainfall excess is calculated with the SCS runoff equation shown below (Akan and Houghtalen, 2003):

$$R = \frac{(P - I_a)^2}{(P - I_a) + S_D} \quad (4.1)$$

$$R = \frac{(P - 0.2S_D)^2}{P + 0.8S_D} \quad (4.2)$$

(If $P > I_a$ Or $P > 0.2 S_D$; otherwise $R=0$.)

where

R=rainfall excess (unit: inches),

P=cumulative rainfall (unit: inches),

I_a = initial abstraction (unit: inches), and

S_D = soil moisture storage deficit at the time runoff begins (unit: inches).

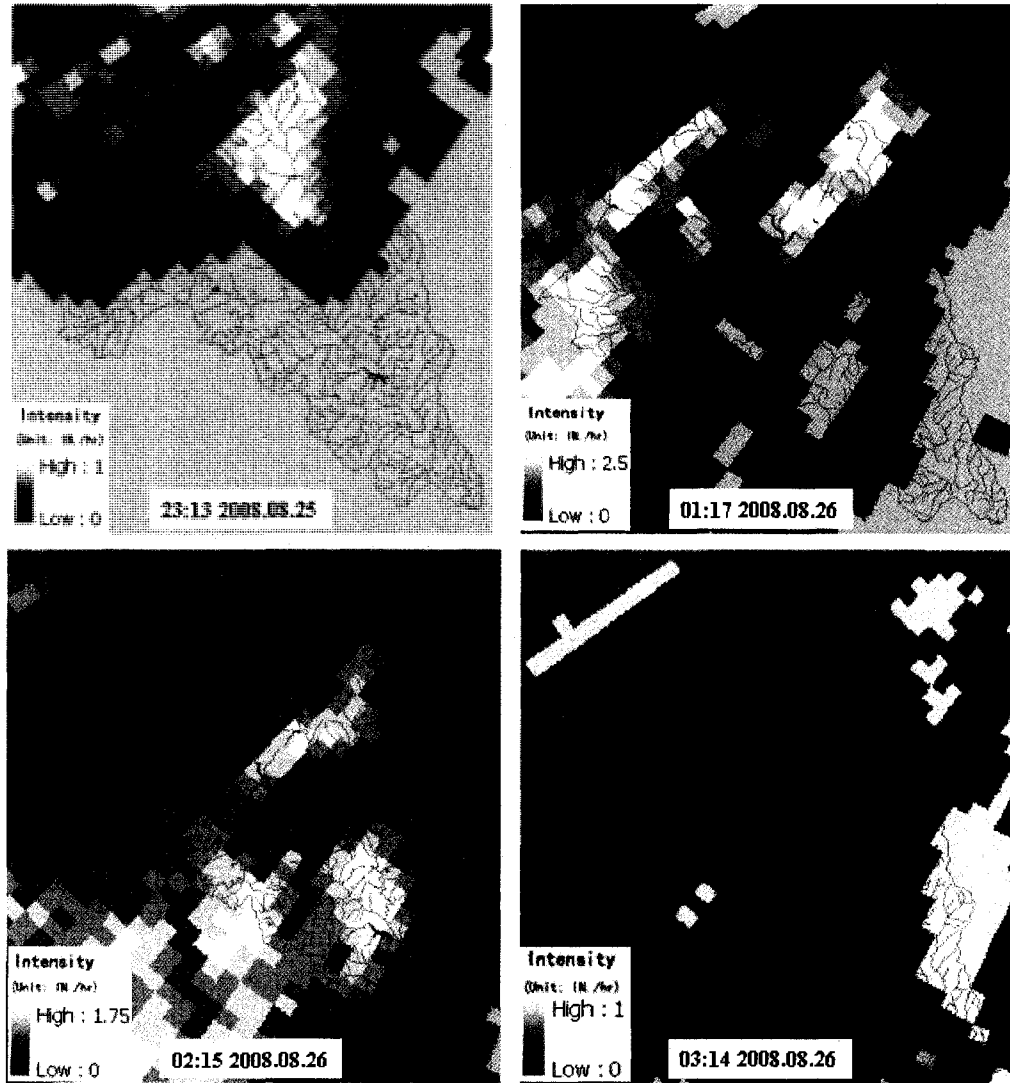


Figure 4.14 NEXRAD Precipitation Intensity Data as a Series of Input Raster Data, Rivanna River Basin, Central Virginia

If P , R , and S_D are in inches, then the SCS runoff equation is expressed as

$$S_D = \frac{1000 - 10CN}{CN} \quad (4.3)$$

$$I_a = 0.2S_D \quad (4.4)$$

The initial CN for each cell is extracted from one of Good, Fair or Poor CN rasters based on the user-defined hydrologic condition. Then, the CN is adjusted with the AMC condition. CN numbers corresponding to AMC-I and AMC-II conditions are computed by using the below equations (Chow *et al.*, 1988).

$$CN_I = \frac{4.2CN_{II}}{10 - 0.058CN_{II}} \quad (4.5)$$

$$CN_{III} = \frac{23CN_{II}}{10 + 0.13CN_{II}} \quad (4.6)$$

Where CN_{II} is the curve numbers extracted from the CN raster for a cell, which is corresponding to AMC-II condition, and CN_I and CN_{III} are curve numbers for AMC-I and AMC-III, respectively.

With the rainfall excess for each cell at every interval, MHSERM calculates the rainfall excess intensity for each cell at every interval by the following relationship:

$$i_e = \frac{R_i - R_{i-1}}{\Delta t} \quad (4.7)$$

where i_e is the rainfall excess intensity at i th interval, the unit is in/hr; R_i is the rainfall excess at i th interval; R_{i-1} is the rainfall excess at $i-1$ interval; Δt is the length of an interval in hours.

The rainfall excess intensity for the study area is also saved as a series of raster with the same resolution of DEM data shown in Figure 4.15.

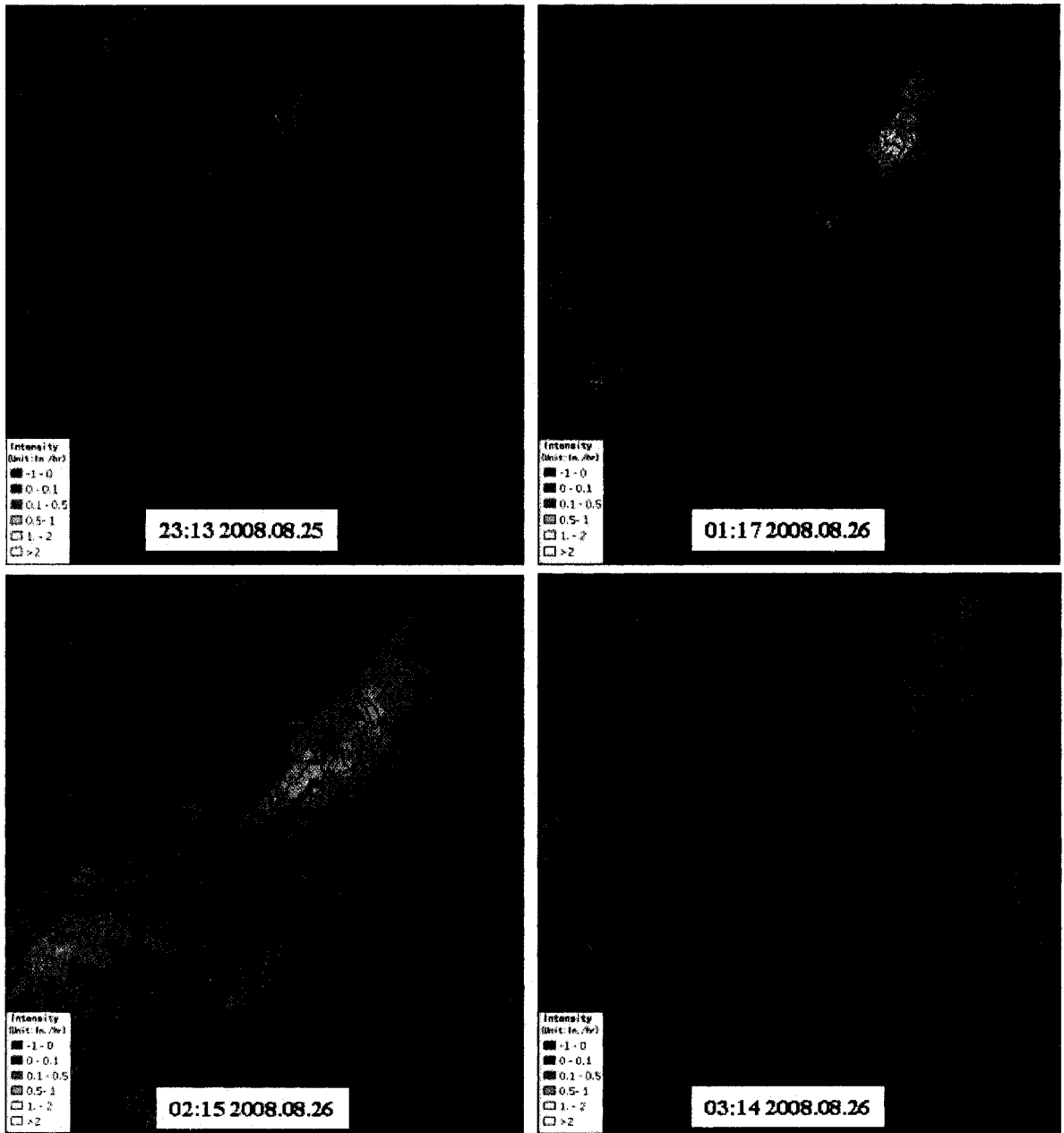


Figure 4.15 The Example Rainfall Excess Intensity Rasters

4.4.2 Estimation of the Variable Time of Concentration of Catchments for Each Interval

The rainfall runoff is considered as lateral flow for streams in the MHSERM, so the time of concentration of a catchment is the time of the excess rainfall runoff from the farthest cell that has excess rainfall flowing to a stream. Due to the temporal and spatial variability of a storm event, the far most cell of a catchment with non-zero rainfall excess could vary for every interval. Furthermore the rainfall excess intensity is not constant for the whole event. MHSERM was designed to calculate the rainfall excess at each cell level, it can reflect and capture the temporal and spatial variability of a storm event to estimate the variable time of concentration for each catchment.

MHSERM estimates the time of concentration by using the kinematic Time-of-Concentration formulas (Morgali and Linsley, 1965). From Akan and Houghtalen (2003), the time of concentration for overland flow in a rectangular catchment can be calculated as:

$$T_c = \frac{(Ln)^{0.6}}{k^{0.6} S^{0.3} i^{0.4}} \quad (4.8)$$

where

T_c = time of concentration

L = flow length

n = Manning roughness factor

$k = 1.0 \text{ m}^{1/3} / \text{s} = 1.49 \text{ ft}^{1/3} / \text{s}$

S = average slope of the catchment in the flow direction, and

i = rate of rainfall excess (assumed constant)

The equation then becomes:

$$T_c = \frac{0.94L^{0.6}n^{0.6}}{i^{0.4}S^{0.3}} \quad (4.9)$$

where T_c is in minutes, L is in feet, and i is in inches per hour.

In the MHSERM, the L (flow length) is the length of the flow path of the farthest cell with rain excess to stream; n (Manning roughness factor) is the average Manning roughness of the flow path; i (rate of rainfall excess) is the average rainfall excess intensity of the cells that have greater than 0.1 in/hr excess of a catchment at given interval; S is the slope of the flow path. The parameters can be extracted from the raster generated in the steps described early in this chapter. Table 4.8 summarizes information in this Chapter, describing procedures to generate target parameters from raster dataset. MHSERM saves resulting parameter estimates into a data file for every catchment for further calculation.

Table 4.8 Section Information in Chapter IV describing Procedures to Generate Target Parameters from Raster Dataset

Parameter	Raster Dataset	Section describing procedures to generate the target parameter
L	The Distance of the flow path to the Streams	4.2.4
n	Manning	4.2.3
i	Rainfall Excess Intensity	4.4.1
S	The Slope of the flow path to the streams	4.2.2

4.5 Estimation of Base Flow

4.5.1 Estimation of the Reference Flow for Each Stream at Time Step 0

The reference flow for each stream at time step 0 is also considered as a base flow in the MHSERM. The estimation is based on a simple assumption that the base flow

of a stream is linearly related to its upstream accumulation area. Compared to the flow incurred by storm events, the base flow is assumed proportionally very small. For example, stream flows of the Rivanna river basin, which can be relied upon ninety percent of the time, are relatively small because the river basin is not a large watershed with poor ground water storage and in a hilly terrain (The Rivanna River Basin Roundtable, 1998). From the daily discharge data of USGS gauge station '02034000 RIVANNA RIVER AT PALMYRA' listed in Table 3.2, the stream flows observed between storm events are usually less than 200 cfs, but the flows of the storm events can increase very quickly to 10000 cfs as shown in Figure 4.16.

MHSERM calculates the upstream accumulating area for all the streams in the catchments, then estimates the base flow or the reference flow at time step 0 based on the linear equation in Equation 4.10 with the observed flow at the downstream gage station at time step 0.

$$Q_{i0} = Q_{gage0} \frac{A_i}{A_{gage}} \quad (4.10)$$

where

- Q_{i0} = the base flow or reference flow at time step 0 of a stream;
- Q_{gage0} = the observed flow at the USGS gage station at time step 0;
- A_i = the upstream accumulation area of the stream;
- A_{gage} = the upstream accumulation area of the stream where the USGS gage station located.

Calculated base flow data for each stream is recorded into the stream's database and MHSERM was designed to also facilitate user flexibility for setting the base flow manually based on her/his own judgment or with other methods.

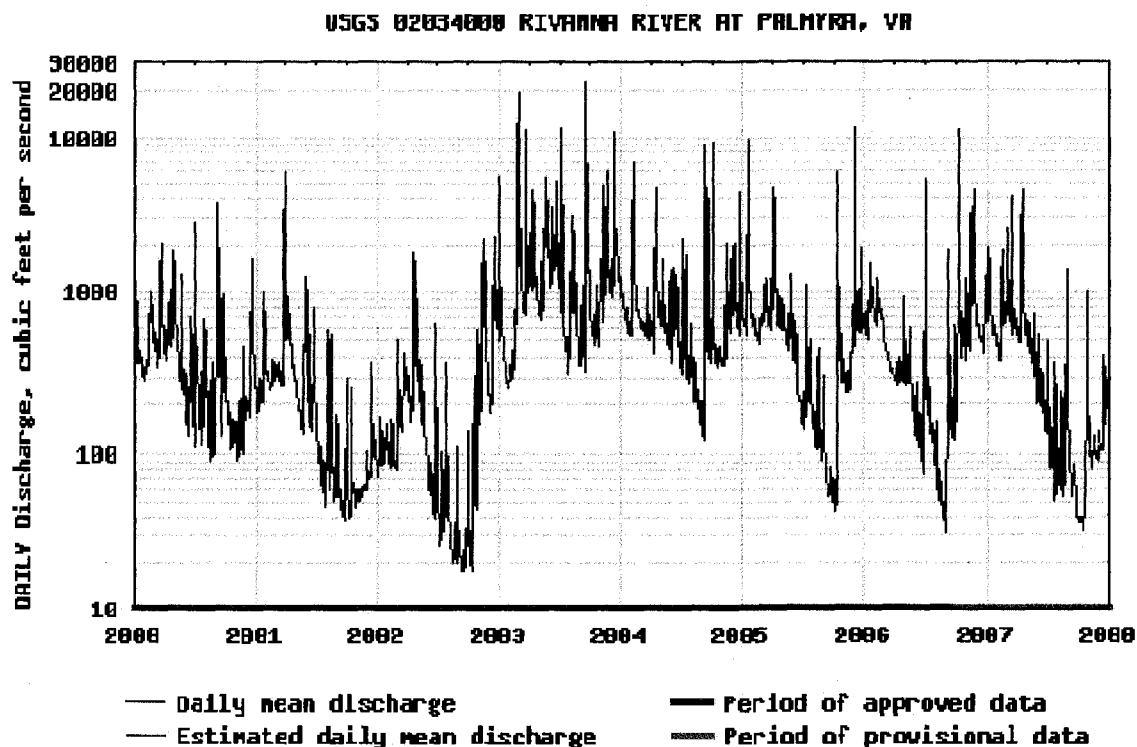


Figure 4.16 Daily Discharge Data of USGS gauge station '02034000 RIVANNA RIVER AT PALMYRA'

4.6 The Lateral Flow Calculation and The Flow Routing in the Stream Network

MHSERM delineates the catchments on the basis of the NHD flowline data and DEM data; it also considers the rainfall excess runoff as the lateral flow to the stream system. Then MHSERM establishes routing sequences for the stream networks based on the NHD Hydro_Net data. With the overland flow runoff and the stream network data,

MHSERM calculates the hydrographs of all the streams at their upstream and downstream ends, which can be used for flood prediction purpose.

4.6.1 The Lateral Flow Volume Calculation

MHSERM is a completely distributed model that can capture the temporal and spatial variability of a storm event in the catchments. To capture spatiotemporal variability of a storm event, the modified Clark (ModClark) method was used in MHSERM to calculate the lateral runoff of the streams. The ModClark in HEC-HMS (U.S. Army Corps of Engineers, 2000a) is a distributed parameter method to calculate the direct runoff.

The ModClark method includes two parts, translation and storage. Translation component was accounted by using a grid-based travel-time model from MHSERM. With the ModClark method, a grid is superimposed on the watershed. For each cell of the grid representation of the watershed, the distance to the watershed outlet is specified in HEC-HMS. However, it is the distance to the stream or waterbodies in the MHSERM instead of the distance to the watershed outlet. The translation time to the streams or waterbodies for every cell is computed as:

$$t_{cell} = t_c \frac{d_{cell}}{d_{max}} \quad (4.10)$$

where

t_{cell} = time of travel to the streams or waterbodies for a cell (hours);

t_c = time of concentration for the catchment at the current interval (hours);

d_{cell} = travel distance from a cell to the streams or waterbodies (feet)

d_{\max} = travel distance for the cell with rainfall excess that is most distant from the outlet at the current interval (feet).

The storage component in the ModClark method is accounted for by the linear reservoir model. The linear reservoir represents the effects of the short-term storage of water throughout a catchment, which plays an important role in the transformation of precipitation excess to runoff. From the HEC-HMS's Technical Reference Manual, the linear reservoir model begins with the continuity equation:

$$\frac{dS}{dt} = I_t - O_t \quad (4.11)$$

Where dS/dt = time rate of change of water in storage at time t (hours); I_t = average inflow to storage (cfs) at time t ; and O_t = outflow (cfs) from storage at time t .

And with the linear reservoir model, storage at time t is related to outflow as:

$$S_t = RO_t \quad (4.12)$$

where R = a constant linear reservoir parameter. A simple finite difference approximation for the continuity equation is:

$$O_t = C_A I_t + C_B O_{t-1} \quad (4.13)$$

where C_A, C_B = routing coefficients. Then, The coefficients are calculated from:

$$C_A = \frac{\Delta t}{R + 0.5\Delta t} \quad (4.14)$$

$$C_B = 1 - C_A \quad (4.15)$$

The unknown parameter for a catchment in the MHSERM is R (a constant linear reservoir parameter), which can be set by user input in the model. The parameter can be

estimated by calibrating gauged precipitation and stream flow data. For example, R can be computed as the flow at the inflection point on the falling limb of the hydrograph divided by the time derivative of flow (Clark, 1945). In the MHSERM, users can set the R for each catchment and save the value into the related stream database.

With the ModClark method, the rainfall excess runoff moves from its origin cell throughout the catchment to the streams or waterbodies, and is routed to the streams or waterbodies with a linear reservoir that represents the aggregated impacts of the surface storage of the catchment. This flow is considered as lateral flow for the later stream routing calculation.

4.6.2 The Flow Routing in the Stream Network

The flow routing method in the MHSERM is based on the Muskingum-Cunge method for flowlines. If there is a Waterbody object such lakes, reservoirs or ponds linked with the flowline, MHSERM assumes the Waterbody as a trapezoidal body with a rectangular contracted weir control at the bottom of its outlet as described in Section 4.3.3 and Figure 4.13. The MHSERM calculates the Stage-Outflow relationship of the Waterbody using equation shown below (Akan and Houghtalen, 2003):

$$Q = K_w L \sqrt{2g} (h)^{3/2} \quad (4.16)$$

Where

K_w = dimensionless weir discharge coefficient,

L = effective crest length (feet), and

h = water depth above the crest (feet)

The Muskingum-Cunge Method

The Muskingum method (Akan and Houghtalen, 2003) is used to calculate the outflow hydrograph at the downstream end of a channel reach given the inflow hydrograph at the upstream end. With the assumption of a linear equation for upstream inflow rate, storage of the channel, and downstream outflow rate, Muskingum method solves hydrologic storage equation for a channel reach in Equation (4.17) (Akan and Houghtalen, 2003):

$$\frac{dS}{dt} = I - Q \quad (4.17)$$

Where

S = volume of water in storage in the channel reach;
 I = Upstream inflow rate;
 Q = Downstream outflow rate;
 t = time.

The linear equation of Equation 4.17 is then

$$S = K[XI + (1 - X)Q] \quad (4.18)$$

Where

K = travel time constant;
 X = weighting factor between 0 and 1.0.

The K and X by themselves in the Muskingum method are weighting factors describing the relationship between inflow and outflow, and do not directly represent physical characteristics of the channel. However, Cunge (1969) expressed K and X in terms of various physical channel characteristics as

$$K = \frac{L}{mV_0} \quad (4.19)$$

$$X = 0.5 \left(1 - \frac{Q_0 / T_0}{S_0 m V_0 L} \right) \quad (4.20)$$

Where

Q_0 = a reference discharge;

T_0 = top width corresponding to the reference discharge;

V_0 = cross sectional average velocity corresponding the reference discharge;

S_0 = longitudinal slope of the channel;

L = Length of the channel reach;

m = exponent of the flow area A of the Open-Channel Rating Curve Equation

$Q = eA^m$, $m=4/3$ for a triangular channel section.

For solving the Muskingum-Cunge Method, K and X need to be calculated repeatedly during routing process due to the variable reference discharge for each step.

The reference discharge is updated at every time step as:

$$Q_0 = \frac{I_1 + I_2 + Q_1}{3} \quad (4.21)$$

In case of routing without any lateral flow, Muskingum-Cunge routing equation becomes:

$$Q_2 = C_0 I_2 + C_1 I_1 + C_2 Q_1 \quad (4.22)$$

where

$$C_0 = \frac{(\Delta t / K) - 2X}{2(1 - X) + (\Delta t / K)} \quad (4.23)$$

$$C_1 = \frac{(\Delta t / K) + 2X}{2(1 - X) + (\Delta t / K)} \quad (4.24)$$

$$C_2 = \frac{2(1 - X) - (\Delta t / K)}{2(1 - X) + (\Delta t / K)} \quad (4.25)$$

$$C_0 + C_1 + C_2 = 1 \quad (4.26)$$

For the channel routing with lateral flow, Akan (1993) proposed below equation:

$$Q_2 = C_0 I_2 + C_1 I_1 + C_2 Q + C_3 (Q_{L1} + Q_{L2}) \quad (4.27)$$

where

$$Q_{L1} = (L)q_{L1};$$

$$Q_{L2} = (L)q_{L2};$$

q_{L1} = lateral inflow rate per unit length of channel at time t_1 ;

q_{L2} = lateral inflow rate per unit length of channel at time t_2 ;

L = length of the channel reach;

$$C_3 = \frac{\Delta t / K}{2(1 - X) + (\Delta t / K)} \quad (4.28)$$

Ponce and Theurer (1982) and Akan and Houghtalen (2003) indicated that the interval Δt should be smaller than one-fifth of the time from the beginning to the peak of the inflow hydrograph to obtain accurate result, and also the length of channel reach should be limited to:

$$L \leq 0.5(mV_0 \Delta t + \frac{Q_0 / T_0}{mV_0 S_0}) \quad (4.29)$$

The reference discharge Q_0 in equation (4.29) is estimated by the equation (4.10) at time step 0.

The Waterbody's Stage-Storage-Discharge Relationship

MHSERM assumes a trapezoidal body for all the waterbodies, and a weir control at the bottom of its outlet as illustrated in Figure 4.13 and in Section 4.3.3. The relationship between the storage (S) and the flow depth (Akan and Houghtalen, 2003) becomes:

$$S = LWd + (L + W)zd^2 + \frac{4}{3}z^2d \quad (4.30)$$

Stage-Discharge relationship for a waterbody with a single weir outlet (Akan and Houghtalen, 2003) can be then expressed with equation 4.16.

The Parameters of Streams and Waterbodies

To simulate the flow routing in the complicated stream system, MHSERM uses parameters to describe the shape and physical properties of the streams and waterbodies. These parameters include the length and the longitudinal slope of the streams; the area of the waterbodies are extracted from the NHD dataset and DEM data by MHSERM. Additional parameters can be estimated and set by users. These parameters include cross section shape and the manning roughness of the streams and the shape (the length, the width and the slope of boundary), the outlet length, the synthetic weir coefficient of the waterbodies. Estimated parameters are then saved in a Microsoft Access database for each stream and waterbody in the stream network.

The Flow Routing in the Stream Network

For flow routing in the stream network by the Muskingum-Cunge method with lateral flow (Equation 4.26), MHSERM first extracts all the overland runoff information for all the catchments over a duration with a given time step (interval) based on landcover condition, and all the stream's parameters and waterbodies parameters from the stream database created in preprocessing steps. With the stream's data, initial K and X are calculated by using Equations 4.18 and 4.19. Streams are then subsequently divided into a number of sections based on Equation 4.28. Whole routing process is consist of three nested loops: (1) a loop for all the time steps/ duration of the simulation, (2) a loop for all

the streams or waterbodies, and (2) a loop for sections of a stream. Muskingum-Cunge K and X value are constantly updated for each step based on variable reference flow and stream flow parameters outlined in Equations 4.18, 4.19 and 4.20. Resulting inflow and outflow for each stream over the duration of the simulation are saved into an Access database file, which can be easily transferred later to a spreadsheet program and graphed. Steps implemented in the MHSERM for flow routing in the stream network are summarized in Table 4.9.

Table 4.9 Steps implemented in the MHSERM for Flow Routing in the Stream Network

Steps	Procedures		
1	Reading all the overland runoff information for all the catchments at all the time steps (intervals) based on landcover condition;		
2	Reading all the streams' parameters and waterbodies parameters;		
3	Calculating the reference flow for streams and waterbodies at time step 0;		
4	Calculate the initial parameters for streams like K_0 , X_0 (Equation 4.17, 4.18) ;		
5	Calculate the split's number with the initial parameters if a stream is longer than the length (Equation 4.28);		
6	Loop from time step 0 to the specified last time step (interval);		
	6.1	Loop from the streams with highest rank (the far most stream) to the outlet based on the flow sequence data;	
	6.2	If the stream is linked with a Waterbody.	
		No	
		Yes	
	6.3	Loop for the stream sections from the upstream to the downstream;	Calculate Q_2 based on the stage-storage-discharge relationship established on the basis of equation 4.29, 4.36.
	6.3.1	Calculate K and X for the section	
	6.3.2	Calculate the Q_2 based on equation 4.26 till the last section	
	6.3.3	Set the Q_2 of the last section of the stream as the stream's Q_2	
	6.4	Add Q_1 , Q_2 to the downstream stream's I_1 , I_2 and set Q_2 as the current stream's Q_1	Set Q_1 , Q_2 as the downstream stream's I_1 , I_2 and set Q_2 as the current stream's Q_1
	6.5	Go to the stream ranked next	
7	Save the results to an Access database (Fig 4.17) for each stream with inflow and outflow at all the time steps.		

CHAPTER V

RESULTS AND DISCUSSION

The methodology and procedures implemented in the MHSERM model, described in Chapter IV, were applied to a study area of the Rivanna River Basin in central Virginia. Detailed discussion of the Rivanna River Basin and its spatial and temporal data characteristic, procedures for preprocessing the raw data, and preparing dataset for MHSERM model simulation can be found in the Chapter III. Base stream flows or observed stream flows of the Rivanna River Basin were obtained from USGS Virginia Water Science Center, and used in comparisons with MHSERM model results.

The MHSERM model results are discussed on four parts: (1) catchments delineation, (2) stream network routing sequence, (3) direct runoff and (4) flow routing for storm events. The first two resulted from terrain analysis and network analysis, which include generation and estimation of parameter rasters such as SCS CN number and Manning value for each grid representing the study watershed. These first two model outcomes needed to be generated and estimated only once for a watershed due to their static nature. On the contrary, the third and fourth model outcomes, direct runoff and flow routing are specific for each storm event and needed to be simulated and estimated corresponding to the specific storm event series over time.

5.1 The Results of Catchments Delineation and Stream Network Routing Sequence

The delineation of the runoff catching area for streams, i.e., catchments and network analysis were described in Chapter IV. The Rivanna River Basin was divided into 886 catchments that catch rainfall runoff for their stream networks. The average size of a catchment was about 550 acres (0.86 Mile² or 2.2 km²). After a catchment's partitioning, a routing sequence was established for stream networks, that include 897 flowlines and 85 impounded waterbodies as the result from MHSERM model is shown in Figure 5.1. By using the flowline's object ID, MHSERM model linked each catchment with its corresponding flowline, and the rainfall runoff calculated was considered as the lateral flow of the flowline and was then routed into the stream network system.

5.2 The Hydrological Response of Storm Events

Direct rainfall runoff and flow routing estimated by MHSERM were compared with two storm events occurred in the Rivanna River Basin, where almost 900 streams and 100 waterbodies are situated within its 2,000 km² area. Some of physical parameter of the streams and waterbodies that cannot be extracted from the NHD dataset and DEM data, e.g. the cross section of streams and the shape waterbodies, and Manning roughness for the streams, were separately estimated by using general assumption or based on published general data as described in Chapter IV.

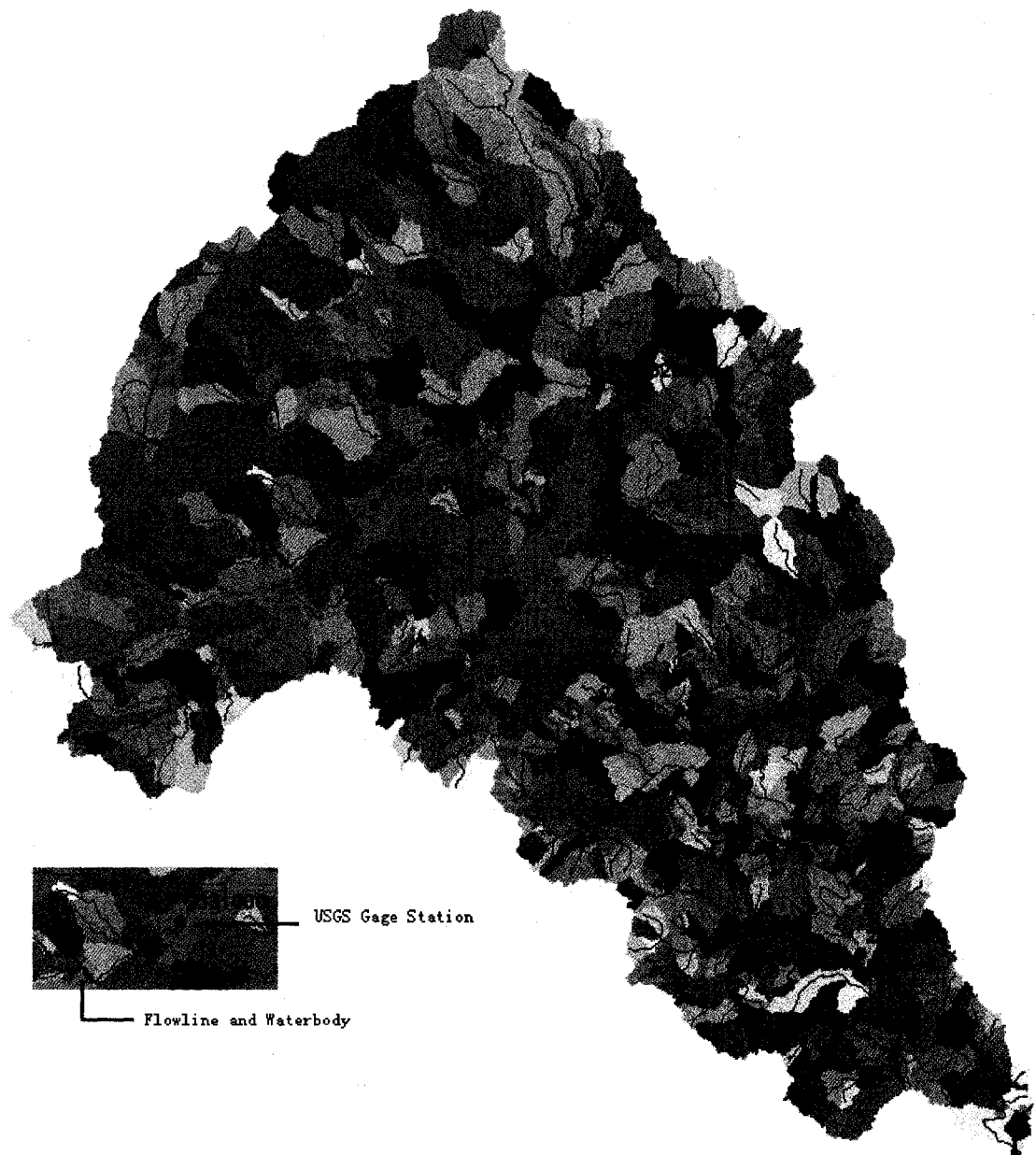


Fig. 5.1 MHSERM Model Results of 886 Catchments and Stream Networks consisted with 897 Flowlines and 85 Impounded Waterbodies, Rivanna River Basin, Central Virginia

The MHSERM was used to estimate inflow and outflow hydrographs of the storm series for all streams within the Rivanna River Basin. The simulation outcome for all streams was resulted in a very large dataset. To manage such a large dataset and for easier

handling of data, simulation outcome datasets were stored in an Access database in a number of data tables, with a data table for a corresponding stream. In these tables, calculated surface flows at each time step over the duration of a simulated storm event were recorded for the corresponding stream as shown in Figure 5.2.

Object ID	Object ID	Object ID	Object ID
84924	86027	87484	88668
85478	86028	87485	88669
85479	86029	87486	88670
85480	86030	87487	88852
85481	86031	87488	88853
85482	86032	87489	88854
85483	86033	87490	88855
85484	86235	87762	88856
85485	86236	87763	88857
85486	86237	87764	88858
85487	86238	87765	88859
85488	86304	87766	88860
86007	86305	87767	88861
86008	86306	87768	88862
86009	86333	87769	88863
86010	86334	87770	88864
86011	86335	87771	88865
86012	86336	88502	88866
86013	86337	88503	88867
86014	86338	88504	89169
86015	87080	88505	89170
86016	87081	88506	89171
86017	87082	88507	89172
86018	87083	88508	89173
86019	87084	88509	89174
86020	87085	88510	89175
86021	87086	88511	89176
86022	87087	88512	89177
86023	87088	88664	89178
86024	87089	88665	89470
86025	87482	88666	89471
86026	87483	88667	89472

Figure 5.2 MHSERM Simulation Outcome Datasets for Inflow and Outflow Hydrographs in an Access Database Format

INTERVAL	I1	I2	BASEQ	R1	R2	Q1	Q2	K
21	73.54687984376	75.58777402959	3.955223098214	418	547	62.65209439147	62.65764965560	
22	75.58777402959	79.23236710285	3.955223098214	547	648	62.65764965560	63.21114735597	
23	79.23236710285	82.87251336540	3.955223098214	648	951	63.21114735597	64.40043026180	
24	82.87251336540	88.17832125182	3.955223098214	951	1357	64.40043026180	65.9627233166	
25	88.17832125182	95.26508175907	3.955223098214	1357	1923	65.9627233166	67.59203477480	
26	95.26508175907	104.2535092630	3.955223098214	1923	2818	67.59203477480	69.20378147912	
27	104.2535092630	116.4325028466	3.955223098214	2818	3892	69.20378147912	70.97229324053	
28	116.4325028466	130.7603251033	3.955223098214	3892	5477	70.97229324053	73.20798951795	
29	130.7603251033	149.0292457234	3.955223098214	5477	8789	73.20798951795	76.28154148826	
30	149.0292457234	171.4581166084	3.955223098214	6789	8415	76.28154148826	80.11375029818	
31	171.4581166084	201.4857538067	3.955223098214	8415	9883	80.11375029818	84.42906425060	
32	201.4857538067	240.9320894616	3.955223098214	9883	11055	84.42906425060	89.47734006747	
33	240.9320894616	289.8410310964	3.955223098214	11055	12016	89.47734006747	96.03206369827	
34	289.8410310964	342.3665860681	3.955223098214	12016	12614	96.03206369827	104.8741597532	
35	342.3665860681	399.6327710756	3.955223098214	12614	13071	104.8741597532	117.0010077694	
36	399.6327710756	470.2369833765	3.955223098214	13071	13295	117.0010077694	133.8563518782	
37	470.2369833765	548.8972271862	3.955223098214	13295	13635	133.8563518782	157.0849862430	
38	548.8972271862	628.2490396444	3.955223098214	13635	14569	157.0849862430	189.3090191178	
39	628.2490396444	715.3273174275	3.955223098214	14569	17397	189.3090191178	234.4011522647	
40	715.3273174275	808.9732282713	3.955223098214	17397	19926	234.4011522647	295.8428294266	
41	808.9732282713	898.3185845277	3.955223098214	19926	21716	295.8428294266	373.1496228283	
42	898.3185845277	985.1736821311	3.955223098214	21716	24049	373.1496228283	461.7035820971	
43	985.1736821311	1070.982904794	3.955223098214	24049	26100	461.7035820971	558.7703130334	
44	1070.982904794	1155.387232836	3.955223098214	26100	28036	558.7703130334	664.5771458419	
45	1155.387232836	1240.584232700	3.955223098214	28036	32454	664.5771458419	775.682579781	
46	1240.584232700	1328.788577559	3.955223098214	32454	37956	775.682579781	886.5331546663	
47	1328.788577559	1425.027624696	3.955223098214	37956	44250	886.5331546663	994.9875092539	
48	1425.027624696	1537.059160683	3.955223098214	44250	52817	994.9875092539	1099.98535865	
49	1537.059160683	1664.812939464	3.955223098214	52817	60798	1099.98535865	1202.288900437	
50	1664.812939464	1821.026159609	3.955223098214	60798	73701	1202.288900437	1306.851105822	
51	1821.026159609	2016.495524117	3.955223098214	73701	92746	1306.851105822	1420.13229024	
52	2016.495524117	2256.632477526	3.955223098214	92746	117825	1420.13229024	1547.797567751	
53	2256.632477526	2532.059198177	3.955223098214	117825	144519	1547.797567751	1699.350492683	
54	2532.059198177	2844.488605959	3.955223098214	144519	177077	1699.350492683	1884.516374985	
55	2844.488605959	3201.361522785	3.955223098214	177077	209234	1884.516374985	2113.120417273	
56	3201.361522785	3628.071270510	3.955223098214	209234	239260	2113.120417273	2393.1781444	
57	3628.071270510	4108.869843288	3.955223098214	239260	255547	2393.1781444	2728.442211950	
58	4108.869843288	4633.25998958	3.955223098214	255547	271000	2728.442211950	3114.328002268	
59	4633.25998958	5195.691496494	3.955223098214	271000	289346	3114.328002268	3553.054099063	
60	5195.691496494	5740.879388994	3.955223098214	289346	311001	3553.054099063	4057.109416032	
61	5740.879388994	6268.112155321	3.955223098214	311001	335798	4057.109416032	4629.294900982	
62	6268.112155321	6757.889162680	3.955223098214	335798	354616	4629.294900982	5248.466118861	
63	6757.889162680	7162.014639846	3.955223098214	354616	370104	5248.466118861	5874.780780480	
64	7162.014639846	7474.658345519	3.955223098214	370104	389975	5874.780780480	6470.890455989	
65	7474.658345519	7897.375221638	3.955223098214	389975	362542	6470.890455989	7004.715572247	
66	7897.375221638	7785.701594602	3.955223098214	362542	353639	7004.715572247	7451.586080629	
67	7785.701594602	7823.638558428	3.955223098214	353639	343902	7451.586080629	7792.905284180	

Record: 1 of 267

Figure 5.2 (Continued)

To compare the simulation results with the observed values at USGS gauge stations, the corresponding stream's inflow data or outflow data was extracted first from the database. Depending on the location of the four USGS gauge stations, closest streams within the Rivanna River Basin were used for MHSERM simulation. If a gauge station is located closer to the downstream end of a stream, the outflow of this stream was used; if it is closer to the stream's upstream end, the inflow was used. Selected streams and an

upstream/downstream part of the stream use in the simulation are summarized in Table 5.1.

Table 5.1 The USGS Gage Stations and Their Corresponding Streams

Site No. and Name	Stream ID	Site is Close to Upstream or Downstream End?
02034000 RIVANNA RIVER AT PALMYRA, VA	86305	Downstream
02031000 MECHUMS RIVER NEAR WHITE HALL, VA	102089	Upstream
02032640 N F RIVANNA RIVER NEAR EARLYSVILLE, VA	86010	Downstream
02032250 MOORMANS RIVER NEAR FREE UNION, VA	93605	Downstream

5.2.1 The Hydrological Response of Storm Event on 2003.09.18-2003.09.19

5.2.1.1 The Introduction of Storm Event on 2003.09.18-2003.09.19

The storm event occurred when Hurricane Isabel passed through the Rivanna River Basin in 2003 after it made a landfall near Drum Inlet, North Carolina on 1700 UTC (=Coordinated Universal Time) September 18th as a Category 2 hurricane. The hurricane weakened to a tropical storm over southern Virginia, then lost its tropical characteristics as moved across western Pennsylvania on September 19th (Beaven and Cobb, 2003). On the basis of NEXRAD radar data used in the MHSERM simulation, the storm event began from the noon of September 18th with scattered light rainfall at about 0.1-0.2 inch/hr. Then it intensified after 23:00 because of the influence of Hurricane Isabel; the most intense period was from 2:30 to 4:00 on September 19th with the rainfall intensity ranges at 0.8-1.5 inches/hr for most of the Rivanna River Basin. The rainfall

weakened quickly after 4:00 and moved out of the Basin from the north as illustrated in a series of temporal NEXRAD radar images in Figures 5.3(a) through (f).

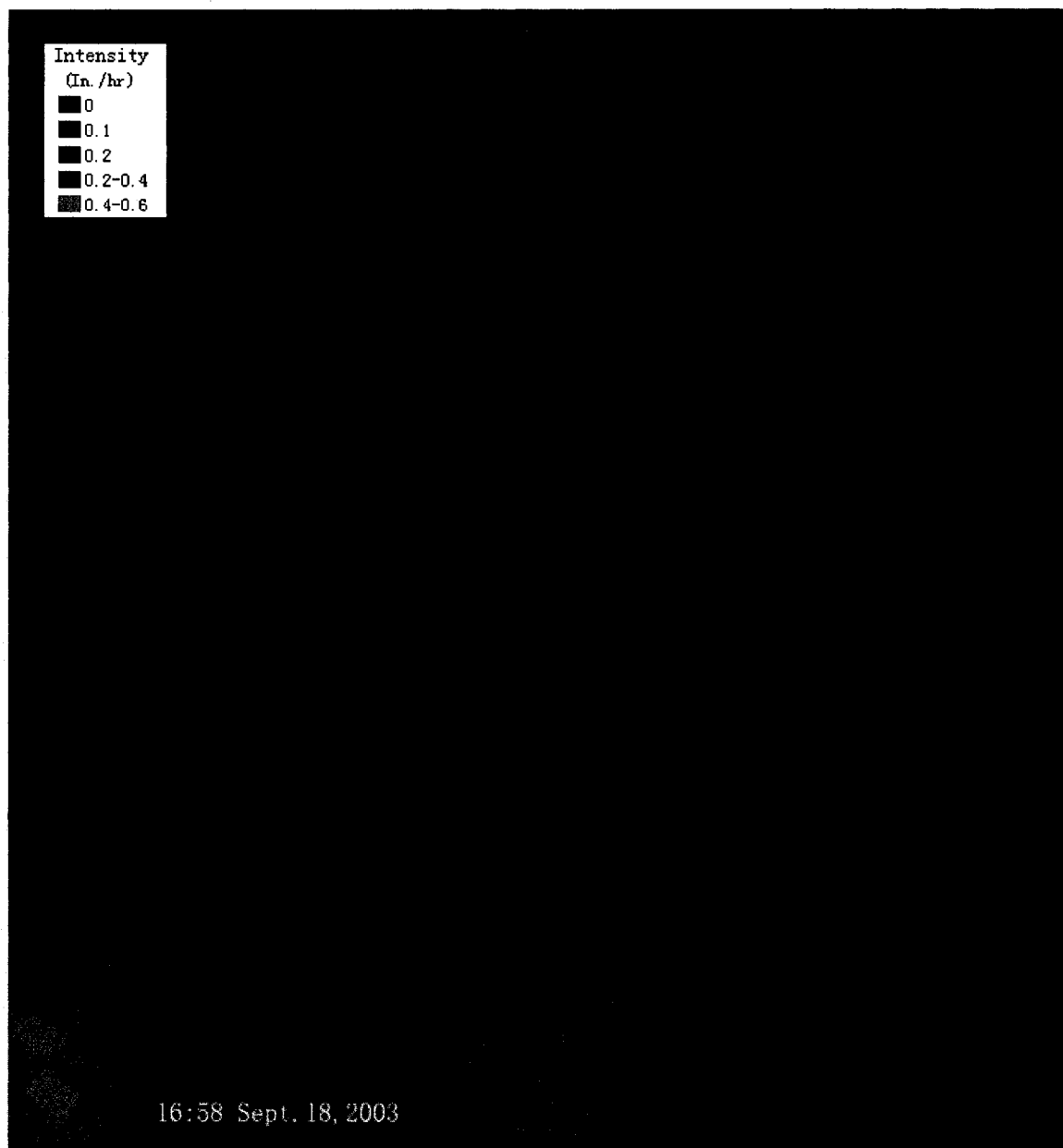


Figure 5.3(a) Temporal NEXRAD Radar Image of Storm Event on 2003.09.18-2003.09.19 at 2003.09.18 16:58 UTC.

There is only light rainfall (0.2-0.4 In./hr) in the southeastern part of this area.

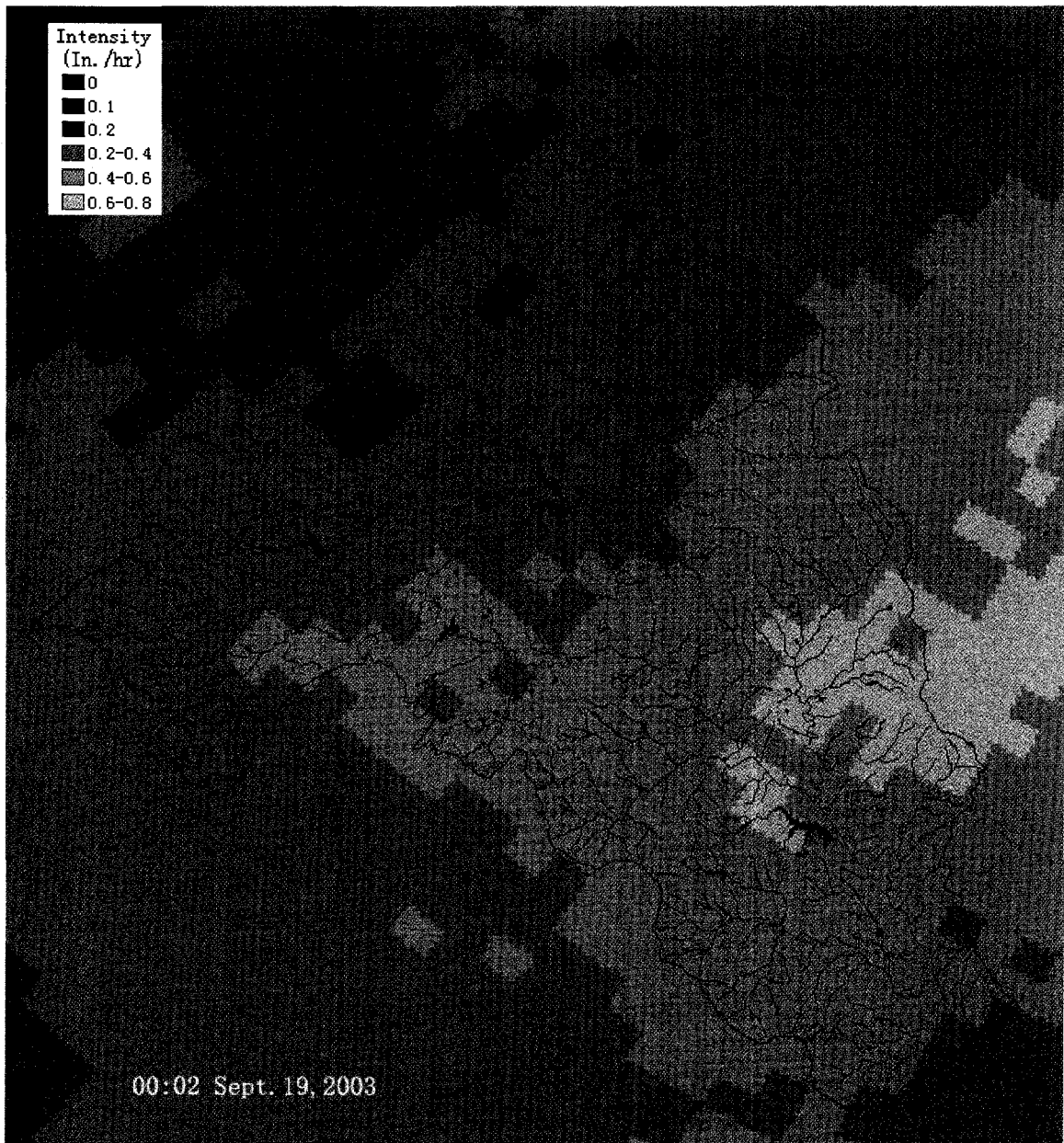


Figure 5.3(b) Temporal NEXRAD Radar Image of Storm Event on 2003.09.18-2003.09.19 at 2003.09.19 00:02 UTC.

The rainfall was getting intensified as the Isabella reached this area from the southeast.

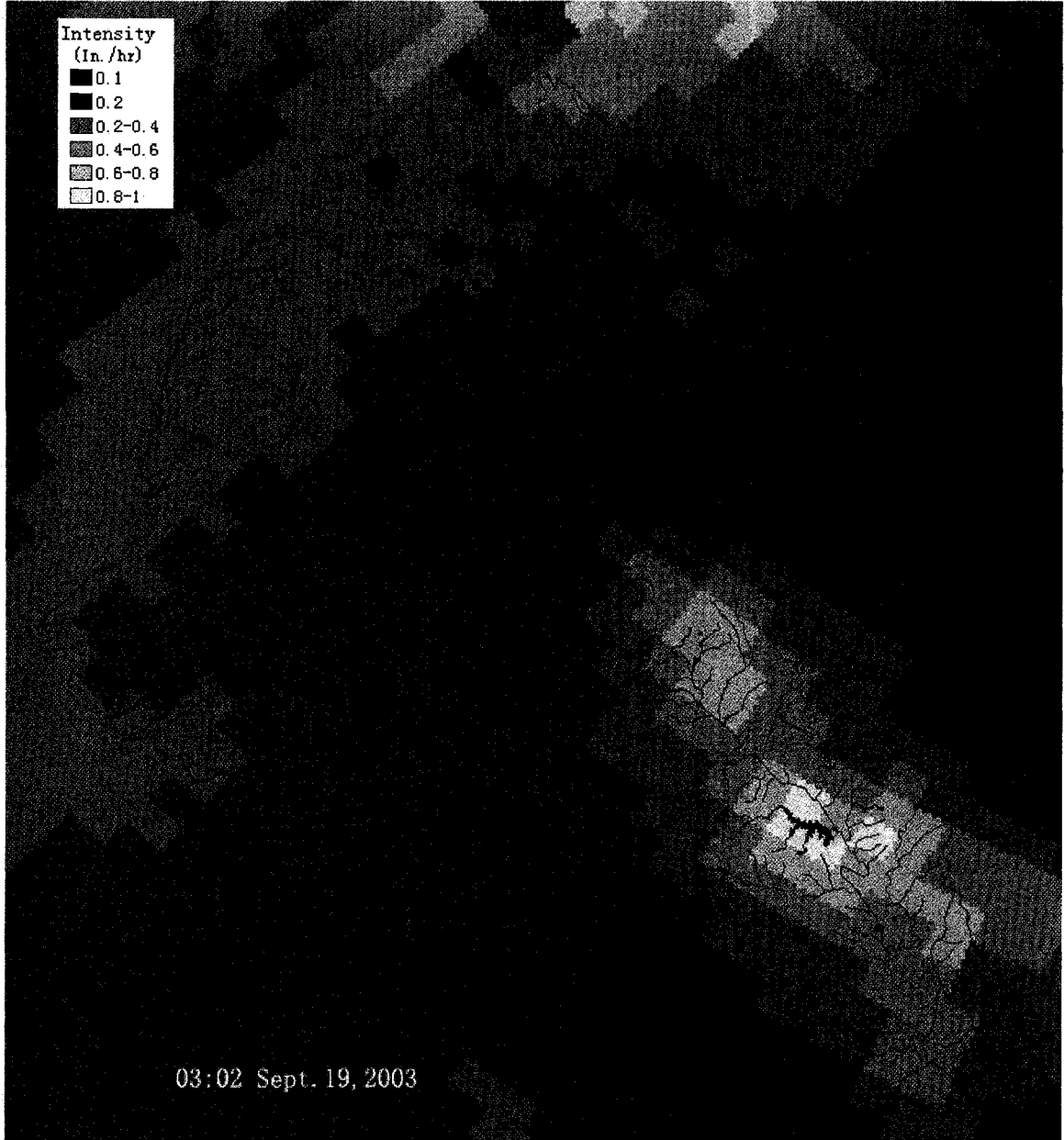


Figure 5.3(c) Temporal NEXRAD Radar Image of Storm Event on 2003.09.18-2003.09.19 at 2003.09.19 03:02 UTC.

From 3am to 4am 9/19/2003, the rainfall was the most intensified and concentrated, its intensity was about 0.8-1 in./hr in the southeastern part of this area.



Figure 5.3(d) Temporal NEXRAD Radar Image of Storm Event on 2003.09.18-2003.09.19 at 2003.09.19 03:32 UTC.

The rainfall center of this event moved quickly to the northwestern part of the area, its intensity was about 1.0-1.5 in./hr.

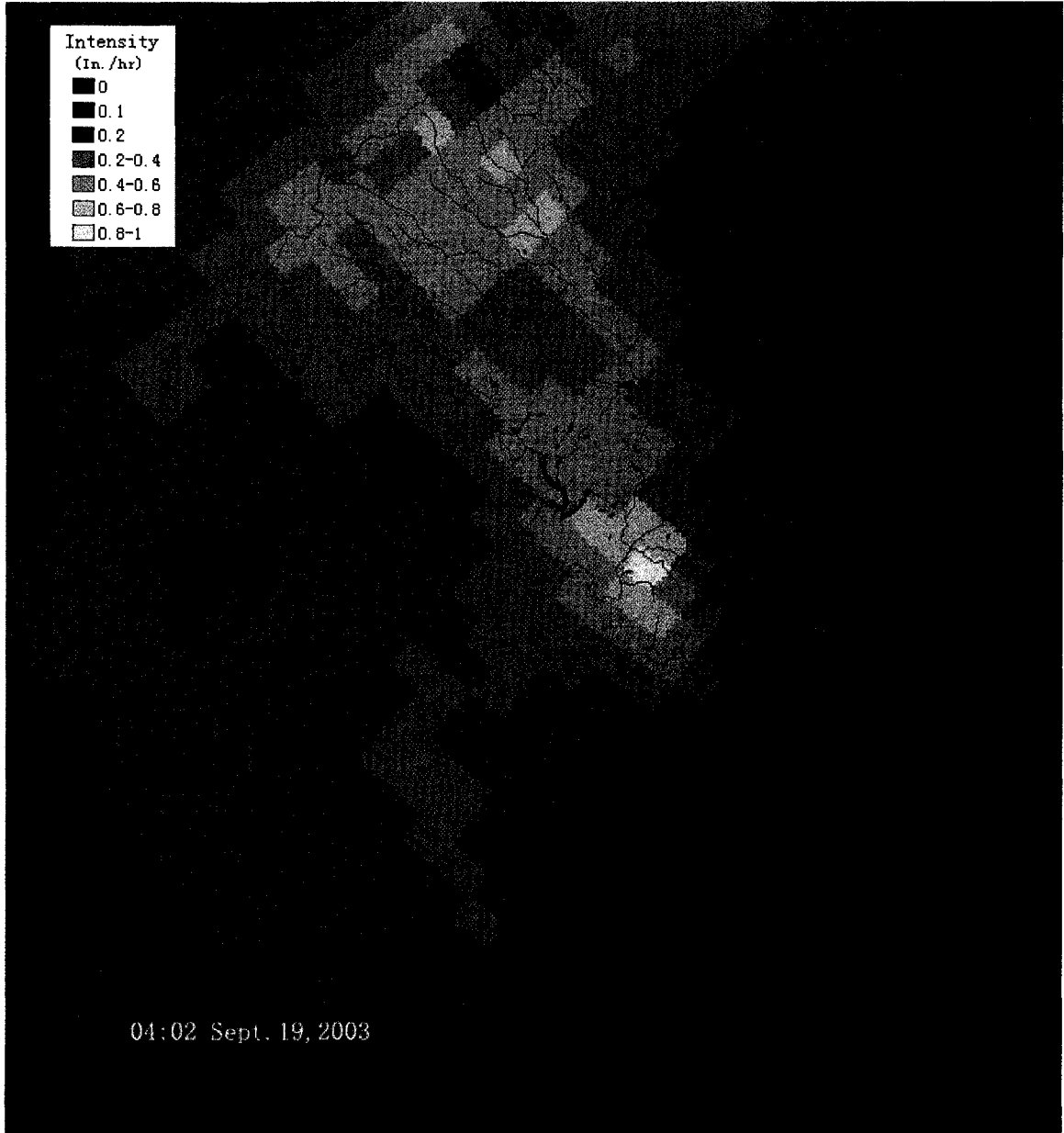


Figure 5.3(e) Temporal NEXRAD Radar Image of Storm Event on 2003.09.18-2003.09.19 at 2003.09.19 04:02 UTC.

The rainfall center of this event was moved to the center and northern part of the area, its intensity was about 0.6-1.0 in./hr.

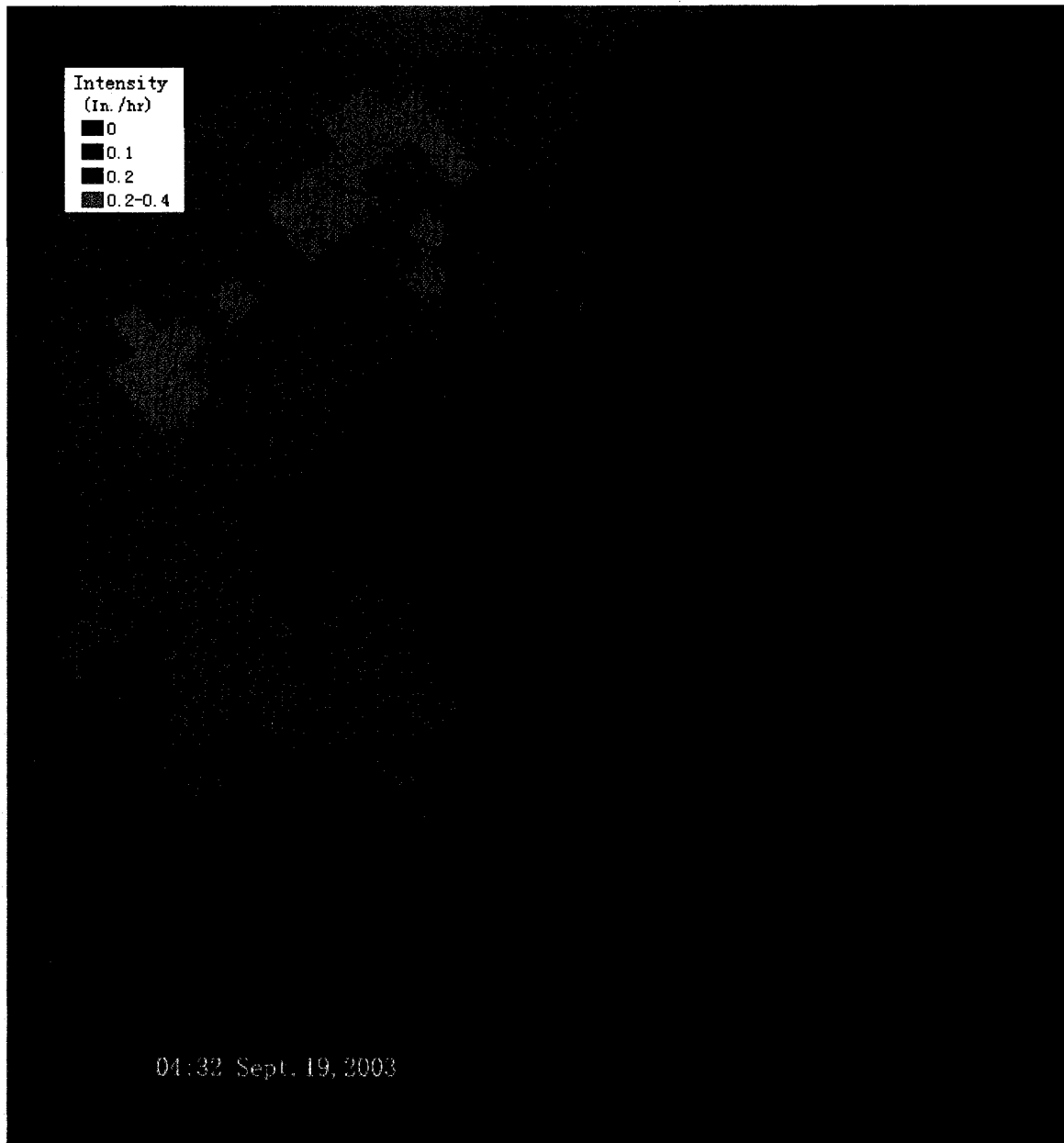


Figure 5.3(f) Temporal NEXRAD Radar Image of Storm Event on 2003.09.18-2003.09.19 at 2003.09.19 04:32 UTC.

The rainfall center of this event was moved out of the area, its intensity was decreased to about 0.2-0.4 in./hr.

The storm event brought about 2-4 inches of rainfall for Rivanna River Basin in a relative short time period over 2003.09.18-2003.09.19. From the cumulative rainfall depth raster

of this storm event shown in Figure 5.4, where most of the area had >2 inches rainfall, and the central and southern part even had >3 inches of the rainfall depth. The intense rainfall resulted in high surface flow in the stream system. As summarized in Table 5.2, the flow data at three USGS gauge stations indicated that the peak flow can be sharply increased to 150 times that of the base flow before the storm event. For example, at the downstream station, 02034000, the peak flow had reached 30000 cfs from its base flow of 622 cfs.

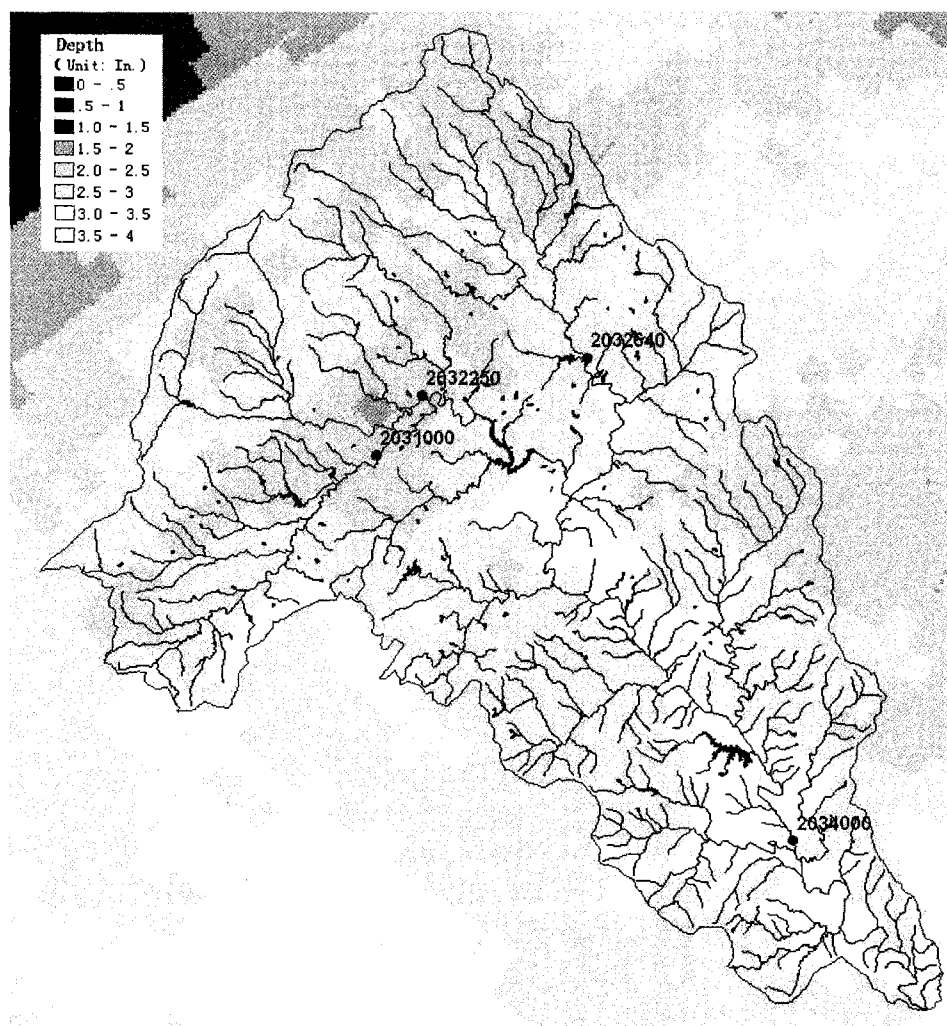


Figure 5.4 Cumulative Rainfall Depth Raster for Storm Event, over 2003.09.18-2003.09.19, Rivanna River Basin, Central Virginia

Table 5.2 Peak Flow Data Extracted from USGS Gauge Stations within the Rivanna River Basin over 2003.09.18-2003.09.19 Storm Event

Site No. and Name	Peak Time	Peak Flow (cfs)	Stream Flow before the storm event (cfs)
02034000 RIVANNA RIVER AT PALMYRA, VA	0:45am, 9/20/2003	30000	622
02031000 MECHUMS RIVER NEAR WHITE HALL, VA	7:00 am, 9/19/2003	9620	63
02032640 N F RIVANNA RIVER NEAR EARLYSVILLE, VA	5:30am, 9/19/2003	8340	54
02032250 MOORMANS RIVER NEAR FREE UNION, VA	N/A	N/A	N/A

5.2.1.2 The Simulation Results with MHSERM Model

MHSERM was simulated to calculate rainfall excess for each grid by using the SCS CN method. Base CN's raster was created from non-storm condition of landcover and soil data, however, CNs' used in the simulation were further selected to reflect AMCs and landcover condition when the storm event started. MHSERM can simulate the hydrological response for nine conditions (three AMCs and three landcover conditions). From the water-data report for these stations (White *et al.*, 2003), it is much wetter for Rivanna river basin in 2003 than usual years. The annual runoff at the USGS gage station 02034000 is 26.09 inches, and the average value is about 14.85 inches for water years 1935 through 2003. The surface flow data of USGS gage stations before the 9.18 storm event also shows this condition. The stream flows before the event for three stations (Table 5.2) are much higher than their daily median values in September from 1935 to 2003. Thus, the AMC of the study site was normal to wetter conditions (AMC II or III) before the storm event.

For the storm event, the simulation period is from 12:30, 09/18/2003 to 7:00, 09/21/2003 with a time step of 15-minute increment. The rain related to this storm event in the research area started (with 0.1 in./hr intensity) at 12:30, 09/18/2003, and stopped at 7:00, 09/19/2001 based on NEXRAD radar data. 192 time steps (2 days) were added beyond the end of the storm event. Simulated hydrographs of the corresponding streams were extracted from the result database for six groups of AMC and Landcover conditions, i.e., AMC II and Poor Condition, AMC II and Fair Condition, AMC II and Good Condition, AMC III and Poor Condition, AMC III and Fair Condition, AMC III and Good Condition. These hydrographs were compared with the observed data from the USGS gauge stations 02031000, 02032640 and 02034000 (Figures 5.5, 5.6 and 5.7).

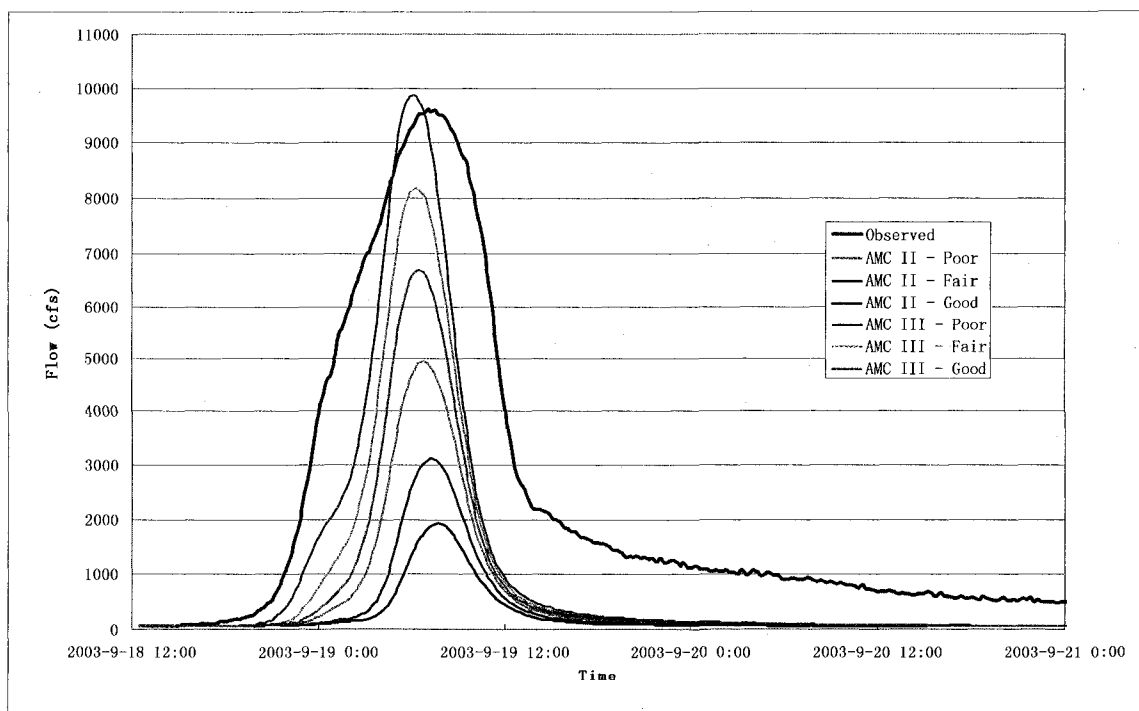


Figure 5.5 The comparison between the hydrograph observed at Station 02031000 and the calculated hydrographs of stream 102089 -

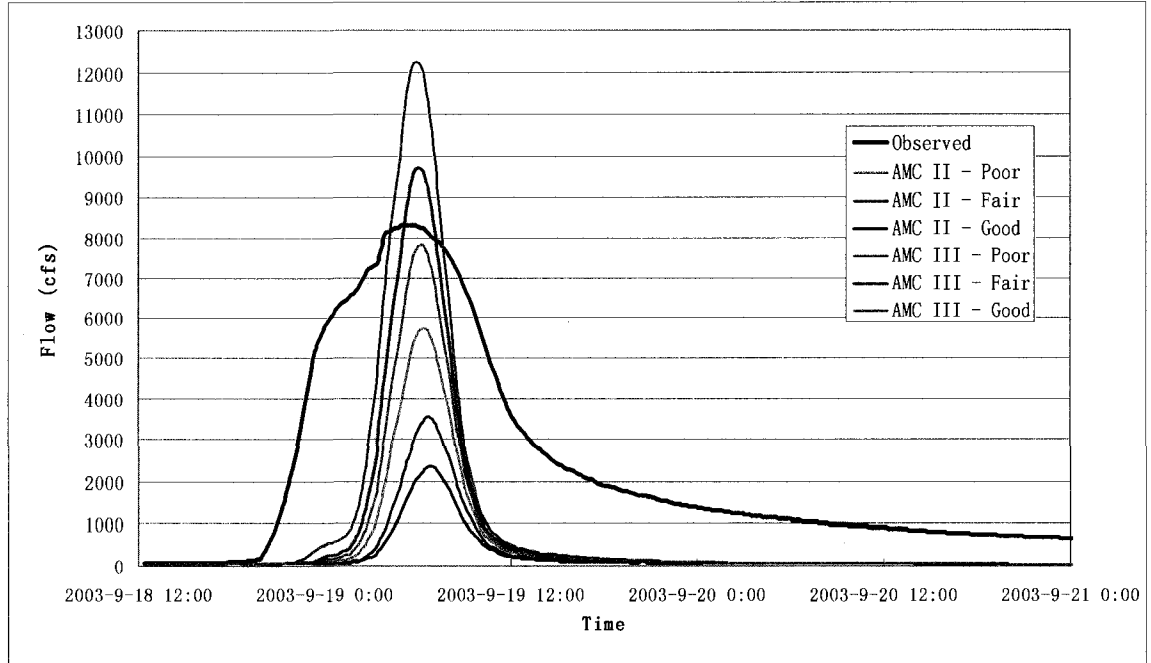


Figure 5.6 The comparison between the hydrograph observed at Station 02032640 and the calculated hydrographs of stream 86010

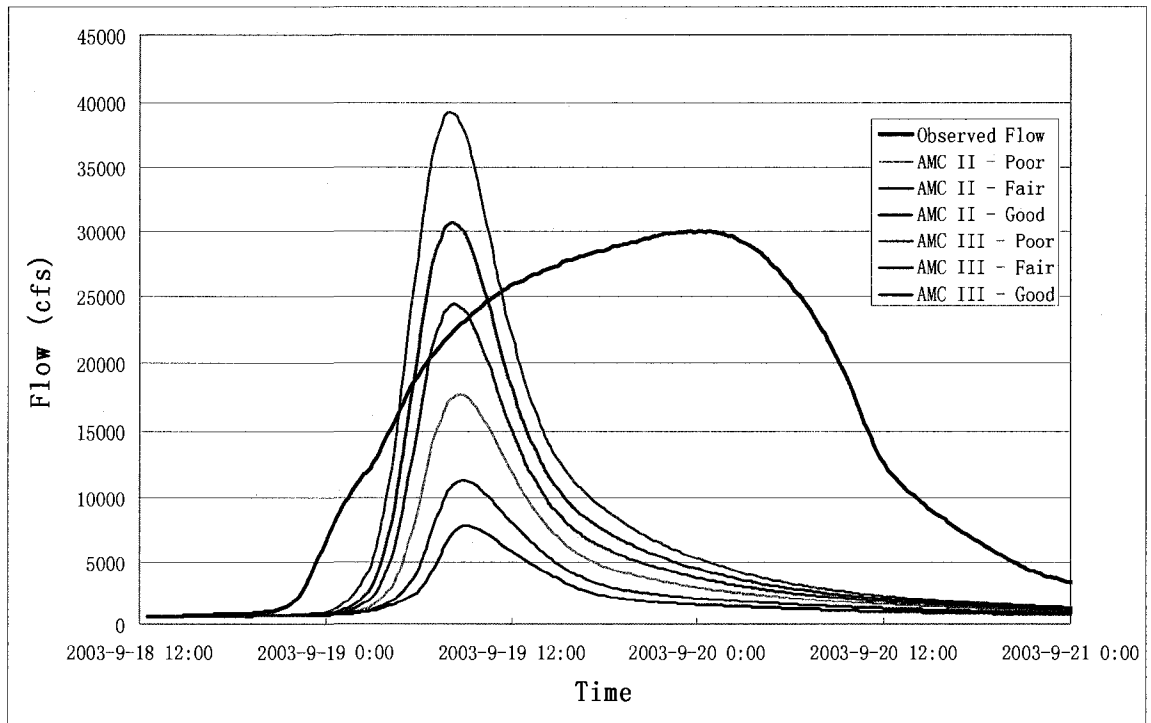


Figure 5.7 The comparison between the hydrograph observed at Station 02034000 and the calculated hydrographs of stream 86305

For the results of station 02031000 (Figure 5.5 and Table 5.3), the simulated peak flow with the AMC III-Poor condition was the closest to the observed peak flow with a deviation of 2.7%. Simulated peak time was in the range of ± 1.0 hours of the observed peak time of station 02031000.

Table 5.3 The observed and simulated peak flow and peak time at station 02031000

Condition Groups	Peak Flow (cfs)	Peak Time	Flow Deviation to Observed Peak Flow (%)	Difference in Time to Peak (hr)
Observed	9620	2003.9.19 7:00	0	0
AMC II-Poor	4941	2003.9.19 6:45	-48.6%	-0.25
AMC II-Fair	3108	2003.9.19 7:15	-67.7%	0.25
AMC II-Good	1933	2003.9.19 7:45	-79.9%	0.75
AMC III-Poor	9878	2003.9.19 6:00	2.7%	-1.0
AMC III-Fair	8179	2003.9.19 6:15	-15.0%	-0.75
AMC III-Good	6692	2003.9.19 6:30	-30.4%	-0.5

For the results of station 02032640 (Figure 5.6 and Table 5.4), the simulated peak flow with AMC III-Good condition was the closest to the observed peak flow with a deviation of -6.1%. Simulated peak time was a little bit late (0.25-1hour) compared to the observed peak time of station 02032640.

Table 5.4 The observed and simulated peak flow and peak time at station 02032640

Condition Groups	Peak Flow (cfs)	Peak Time	Flow Deviation to Observed Peak Flow (%)	Difference in Time to Peak (hr)
Observed	8340	2003.9.19 5:30	0	0
AMC II-Poor	5764	2003.9.19 6:15	-30.9%	0.75
AMC II-Fair	3547	2003.9.19 6:30	-57.5%	1.0
AMC II-Good	2354	2003.9.19 6:30	-71.8%	1.0
AMC III-Poor	12279	2003.9.19 5:45	47.2%	0.25
AMC III-Fair	9708	2003.9.19 6:00	16.4%	0.5
AMC III-Good	7834	2003.9.19 6:00	-6.1%	0.5

For the results of station 02034000 (Figure 5.7 and Table 5.5), The simulated peak flow with AMC III-Fair condition was the closest to the observed peak flow with a deviation of 2.2%, but there was a large time lag to the peak time of 16.5 hours compared to the observed peak time of station 02034000.

Table 5.5 The observed and simulated peak flow and peak time at station 02034000

Condition Groups	Peak Flow (cfs)	Peak Time	Flow Deviation to Observed Peak Flow (%)	Difference in Time to Peak (hr)
Observed	30000	2003.9.20 0:45	0	0
AMC II-Poor	17623	2003.9.19 8:45	-41.3%	-16
AMC II-Fair	11298	2003.9.19 9:00	-62.3%	-15.75
AMC II-Good	7823	2003.9.19 9:15	-73.9%	-15.5
AMC III-Poor	39260	2003.9.19 8:00	30.9%	-16.75
AMC III-Fair	30673	2003.9.19 8:15	2.2%	-16.5
AMC III-Good	24375	2003.9.19 8:15	-18.8%	-16.5

From the results, it is evident that the AMC conditions had a dominant influence on the resulting surface flow, especially for the estimation of the peak flow. For these three stations 02031000, 02032640 and 02034000, simulated peak flow estimates matched closely to the observed peak flows under AMC III condition and were generally underestimated under AMC II condition. For example, with the same storm event, the simulated peak flows under the AMC II-Good condition was only 1/5-1/4 of the corresponding observed peak flow. The results also show that the simulated hydrographs have a sharper curve than the observed hydrographs, i.e., the rising limbs were a little bit time-lagged and the falling limbs decreased much faster, especially in case of station 02034000 located in the downstream.

5.2.2 Hydrological Response of Multiple Storm Events on August 24, 2007

5.2.1.1 Introduction of Multiple Storm Events on 2007.08.24-2007.08.27

Multiple storm events simulated with MHSERM were composed of three events over a duration of 40 hours. The hydrological response of the sequential events can be influenced by the foregoing ones, and MHSERM was designed to simulate a cumulative hydrological response within a series of storm events. Three storm events occurred from 2007.8.24 20:00 to 2007.8.27 02:00 and registered in NEXRAD radar data. These events were cell storms that only covered part of the Rivanna River Basin at any one time step during the event and moved quickly over the area (Figures 5.8, 5.9 and 5.10). The first event started at 2007.8.24 20:00, moved quickly through the northern and western part of the area, and moved out after 23:00 as shown in Figure 5.8. The second storm event started at 2007.8.25 19:00, but it only intensified after 22:00 and moved from north to the

south, and exited the area completely after 2007.8.26 4:00 as shown in Figure 5.9. The third storm event started at 2007.8.26 21:00, moved through the area from the north to the south, and exited the area after 2007.8.27 01:30 as shown in Figure 5.10.

From the maps of cumulative rainfall depth for the three storm events illustrated in Figure 5.11, the second storm event was by far the major event, which covered most of the Rivanna River Basin. On the other hand, the first storm event only covered the western part of the area, i.e. the upstream area of station 02031000 with a total rainfall depth of about 2-3 inches. The second storm event covered most of the area, especially for the upstream area of station 02032640, where the total rainfall depth was about 3-5 inches. The third and last storm event was relatively moderate compared to two previous events. Its rainfall was received mainly at the southern part of the area, and the cumulative rainfall depth was about 1-2.5 inches.

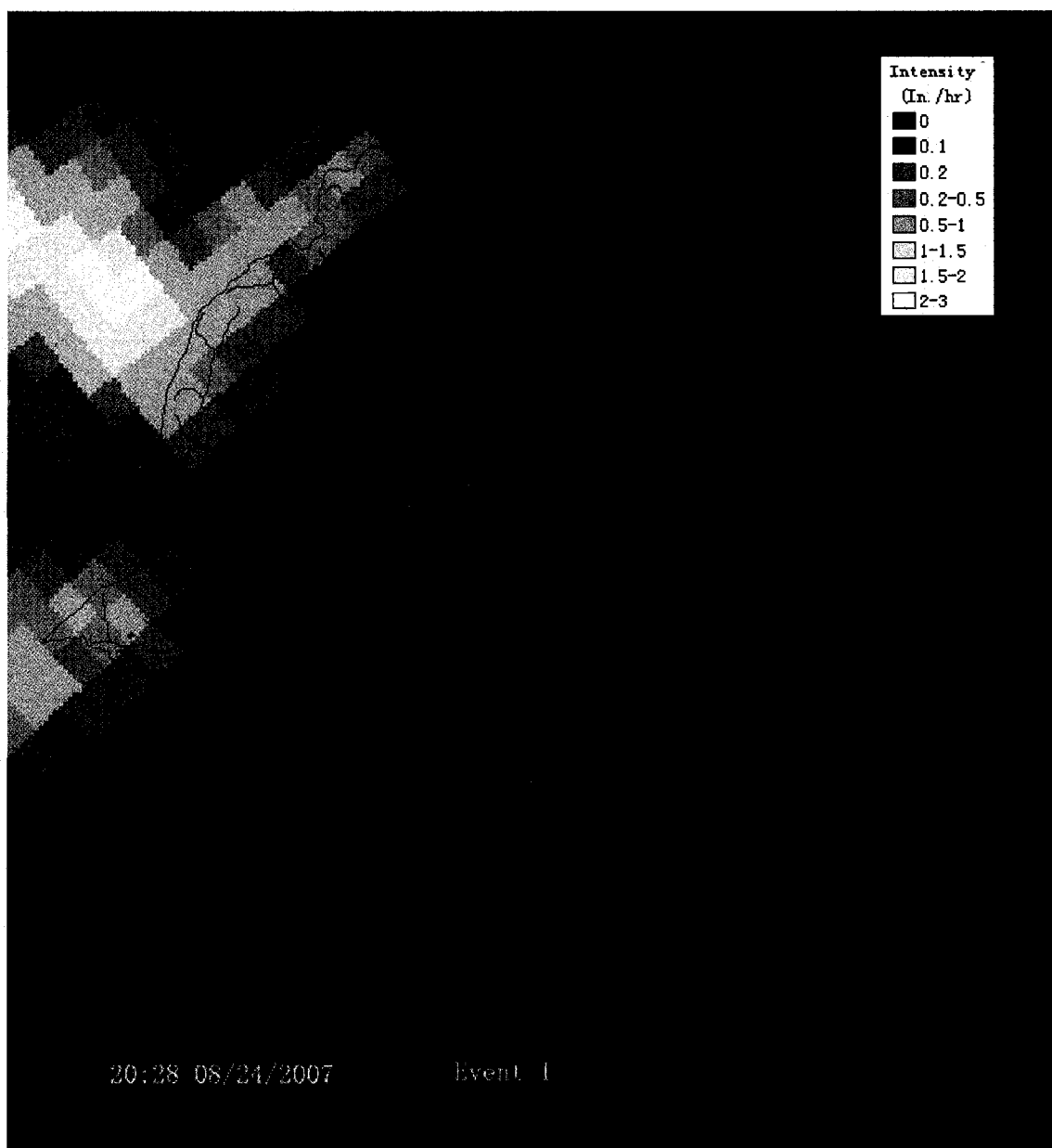


Fig. 5.8 (a) Temporal NEXRAD Radar Image of the First Storm Event on 2007.08.24-2007.08.27 at 2007.08.24 20:28.

There is a cell storm in the northwestern part of this area.

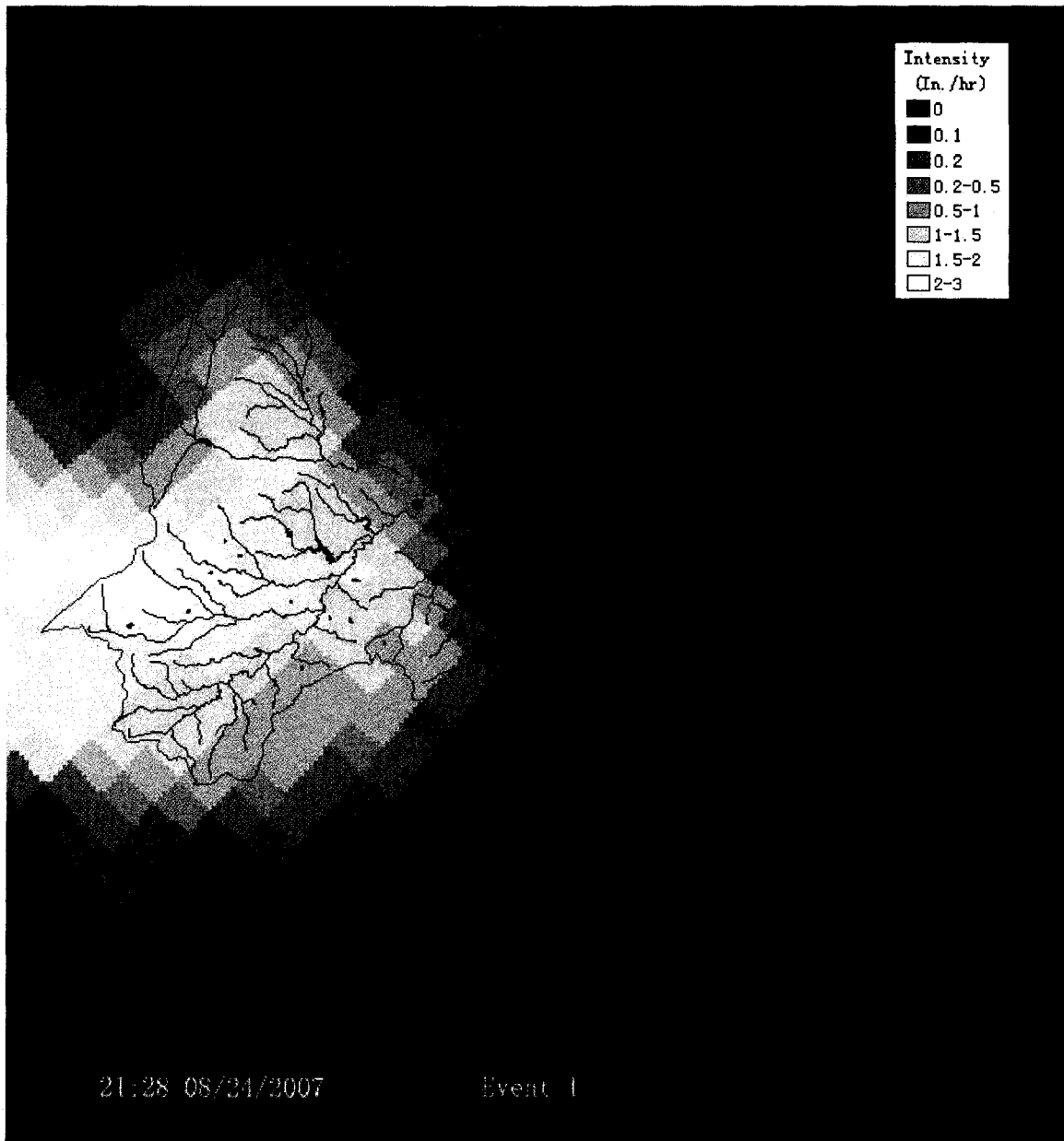


Fig. 5.8 (b) Temporal NEXRAD Radar Image of the First Storm Event on 2007.08.24-2007.08.27 at 2007.08.24 21:28.

The cell storm moved into the northwestern part of this area, upstream of station 02031000 and 02032250.

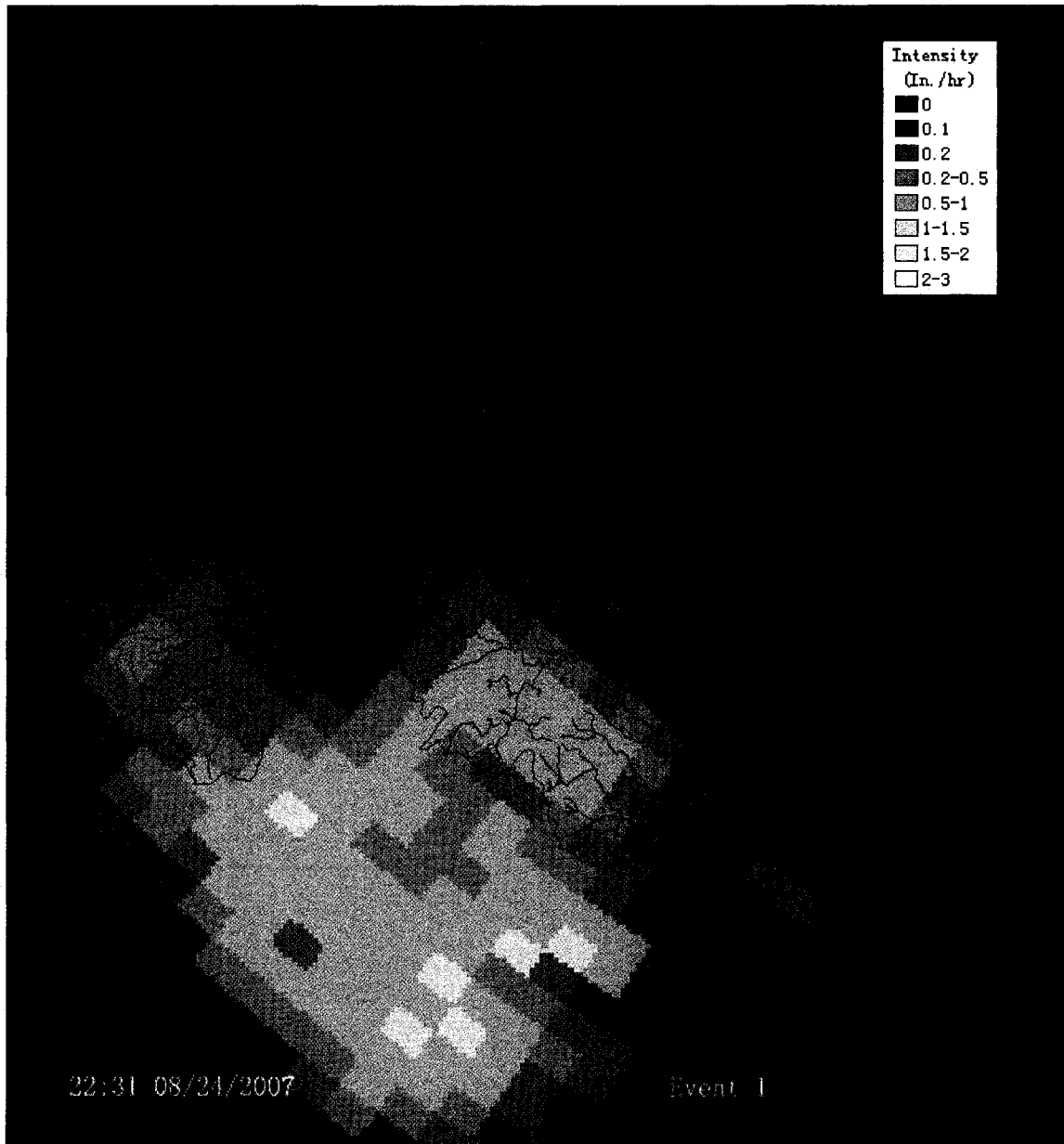


Fig. 5.8 (c) Temporal NEXRAD Radar Image of the First Storm Event on 2007.08.24-2007.08.27 at 2007.08.24 22:31.

The cell storm moved quickly along the western part of this area.



Fig. 5.8 (d) Temporal NEXRAD Radar Image of the First Storm Event on 2007.08.24-2007.08.27 at 2007.08.24 23:01.

The cell storm kept moving quickly along the western part of this area, and almost moved out the area.

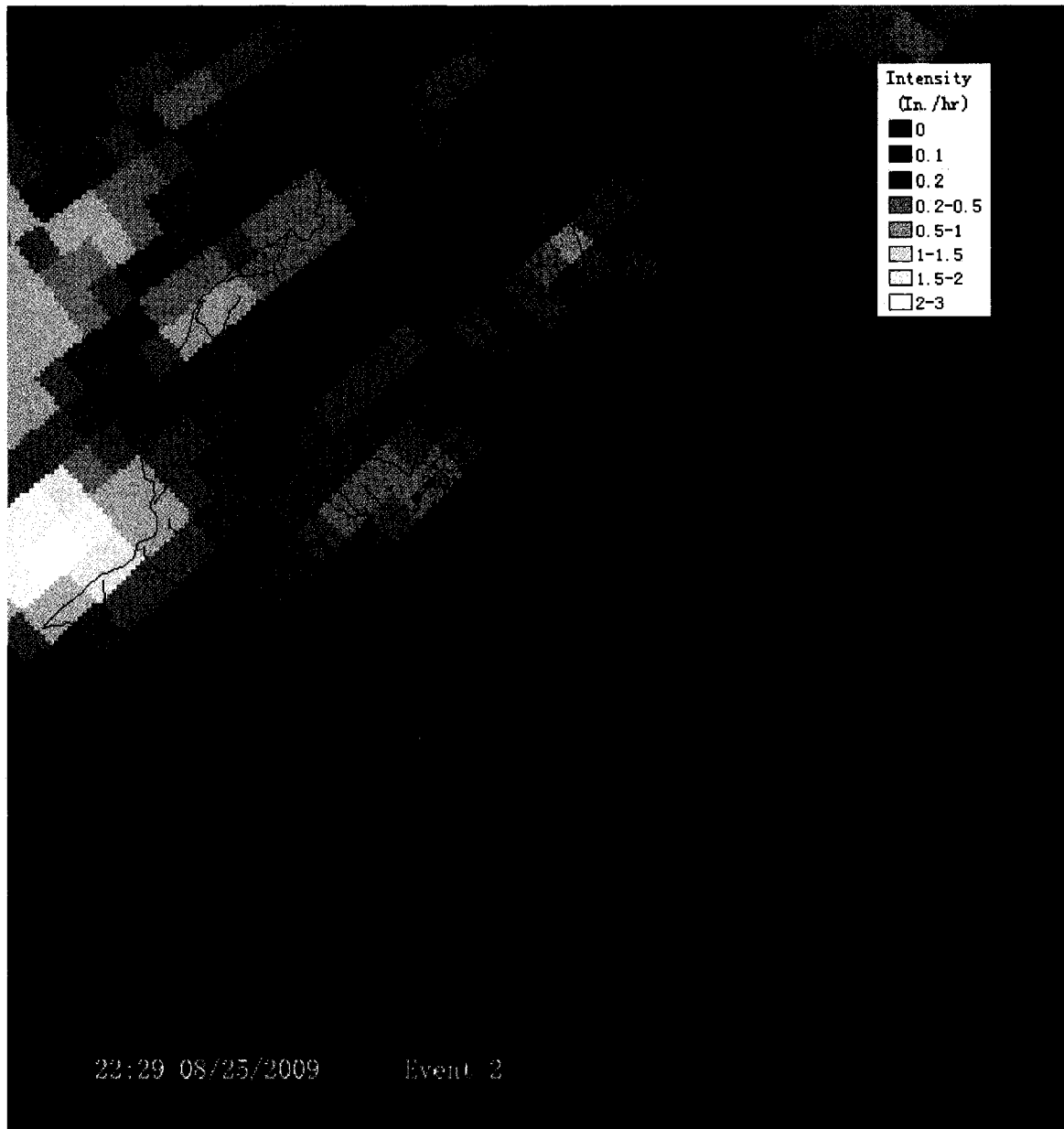


Fig. 5.9 (a) Temporal NEXRAD Radar Image of the Second Storm Event on 2007.08.24-2007.08.27 at 2007.08.25 22:29.

The cell storm was moving into the northern part of this area.

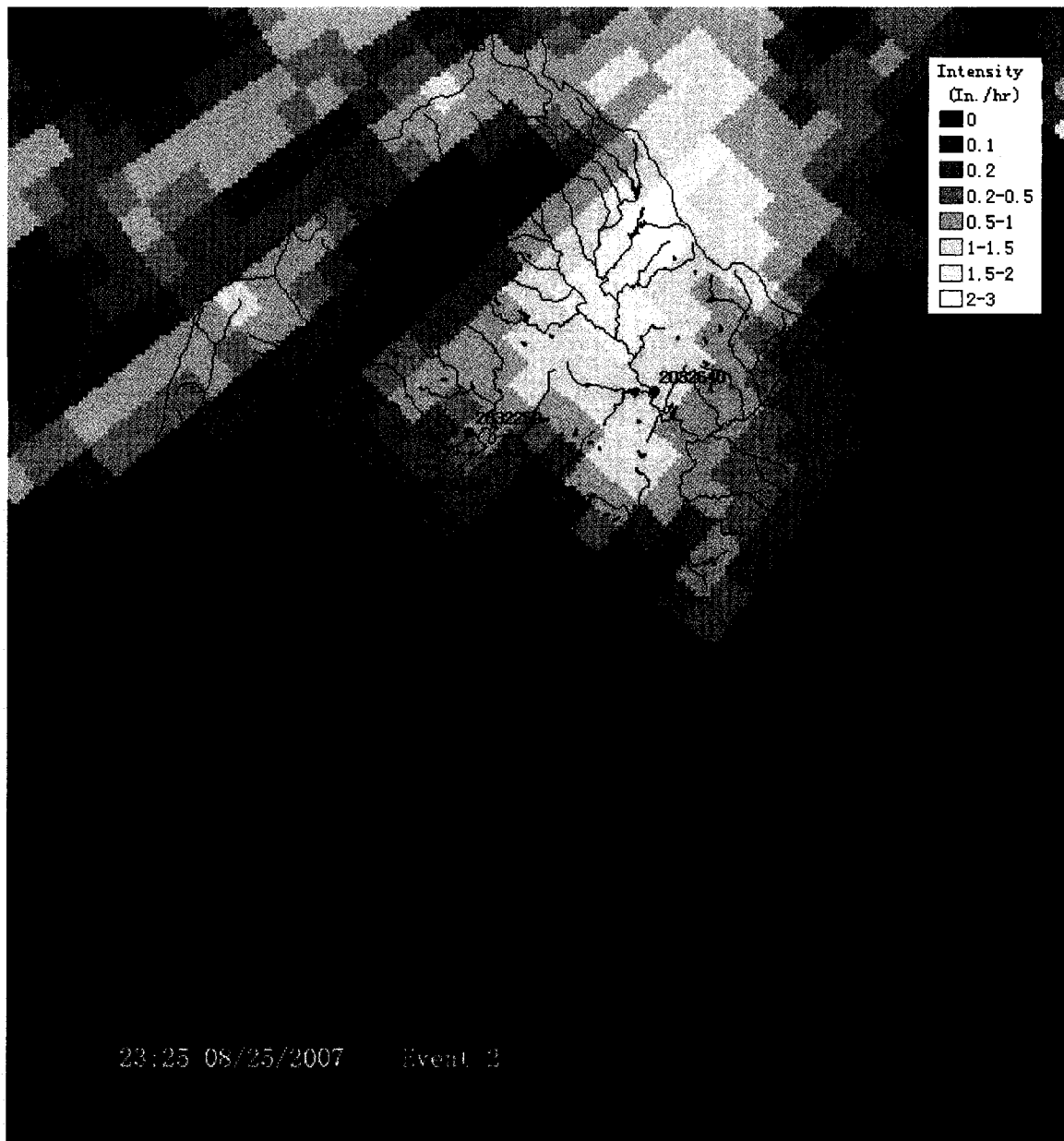


Fig. 5.9 (b) Temporal NEXRAD Radar Image of the Second Storm Event on 2007.08.24-2007.08.27 at 2007.08.25 23:25.

The cell storm was moving into the northern part of this area, especially the upstream area of station 02032640.

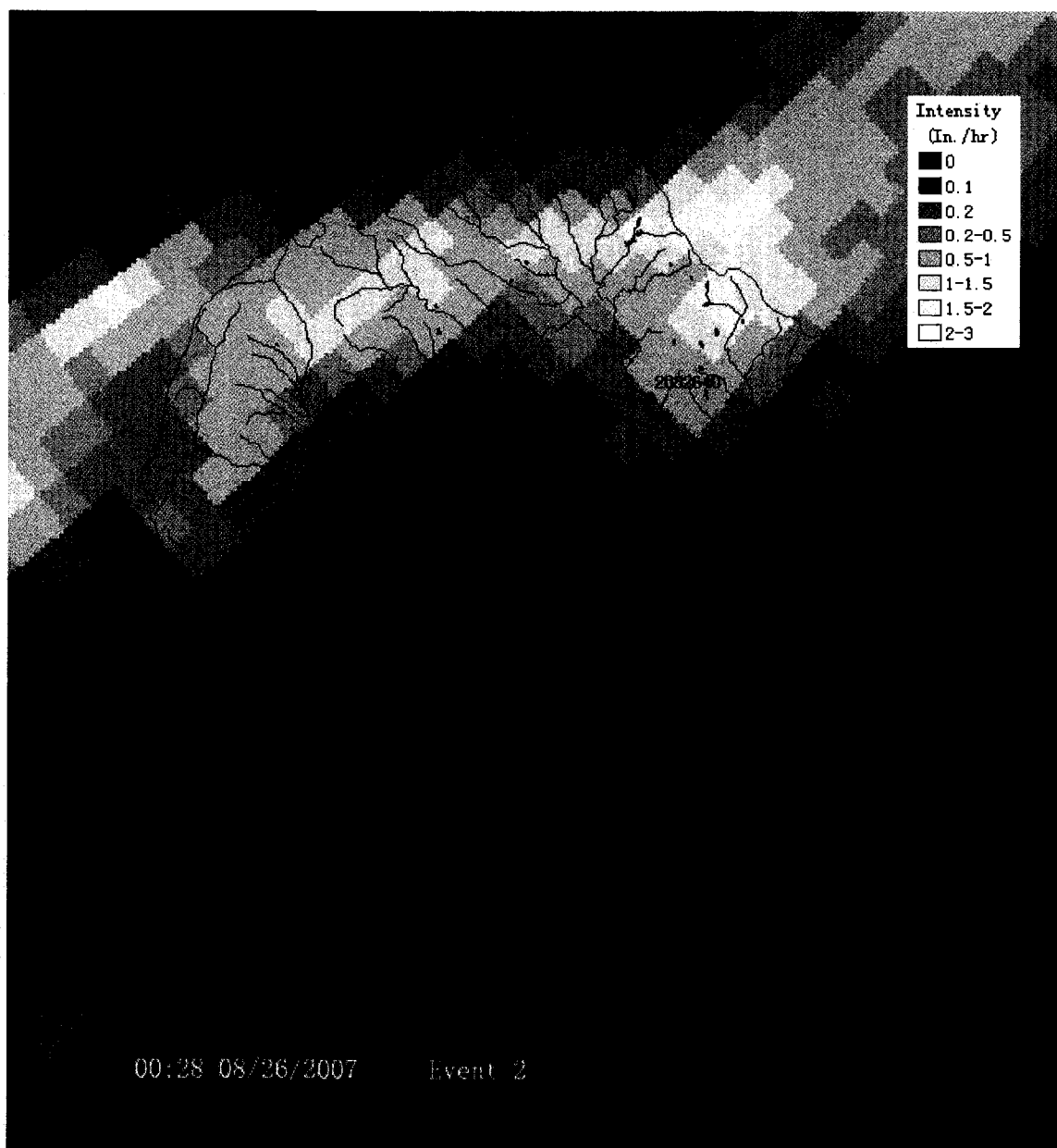


Fig. 5.9 (c) Temporal NEXRAD Radar Image of the Second Storm Event on 2007.08.24-2007.08.27 at 2007.08.26 00:28.

The cell storm was still within the northern part of this area.

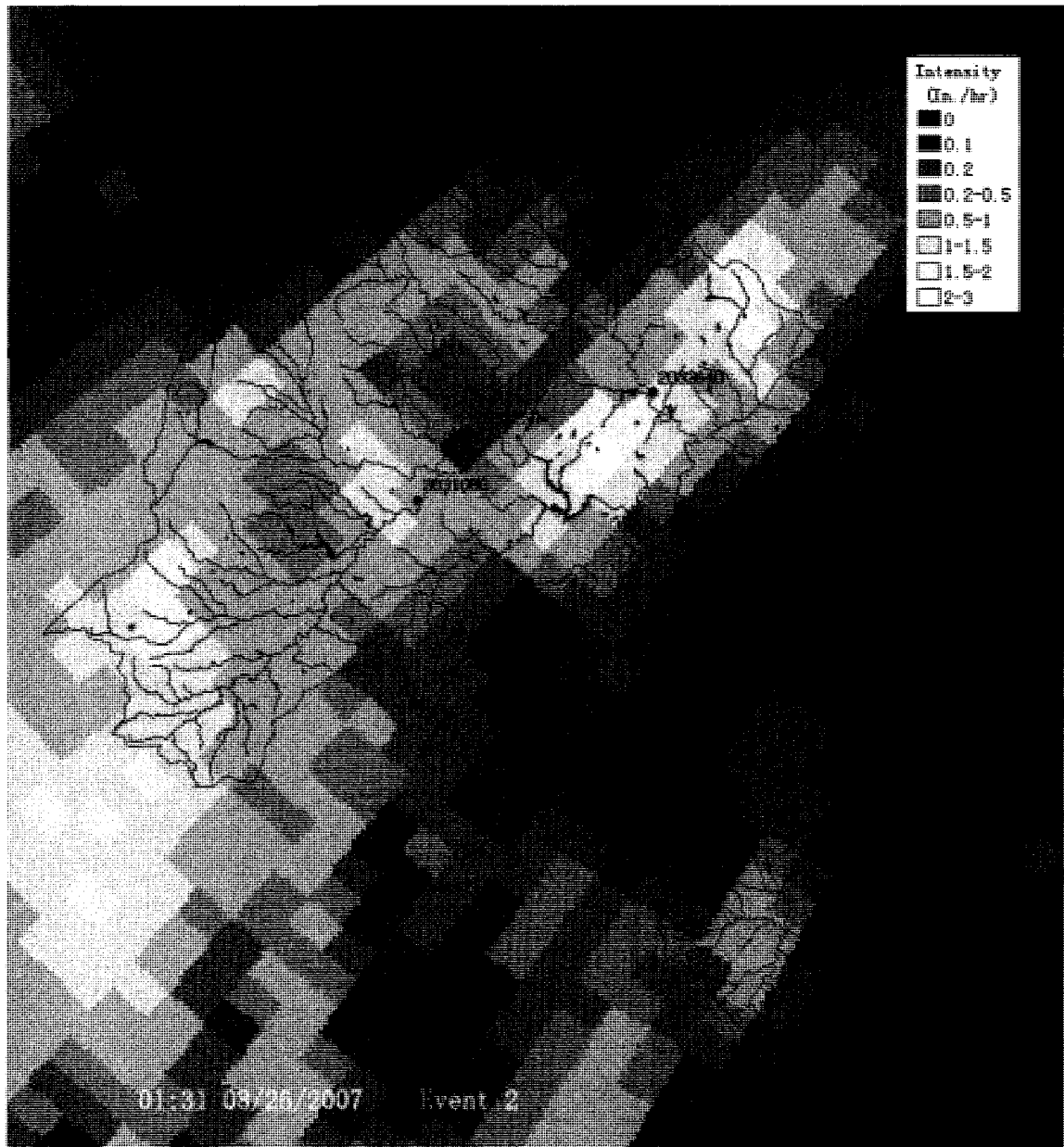


Fig. 5.9 (d) Temporal NEXRAD Radar Image of the Second Storm Event on 2007.08.24-2007.08.27 at 2007.08.26 01:31.

The cell storm almost covered the northern part of this area

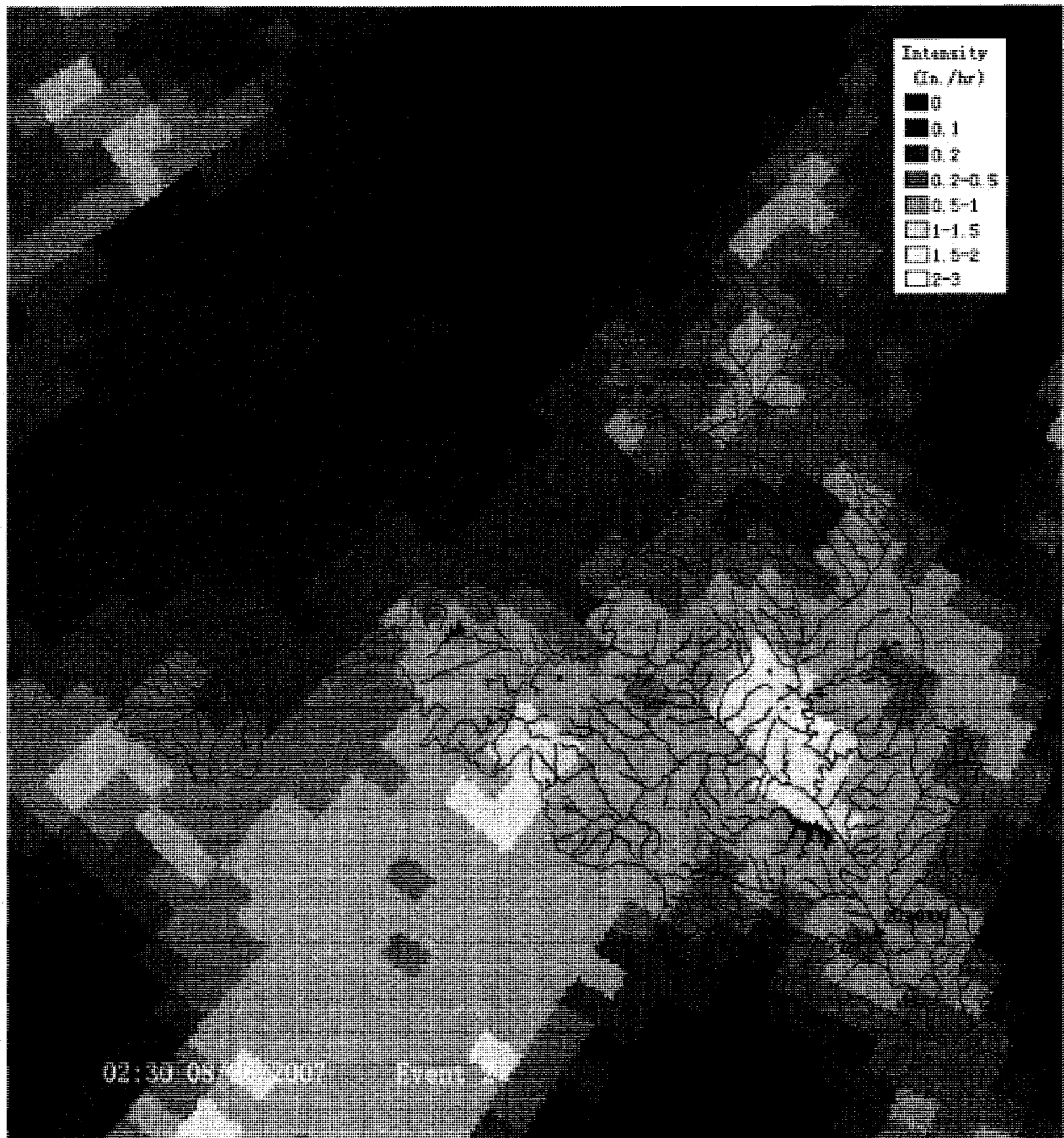


Fig. 5.9 (e) Temporal NEXRAD Radar Image of the Second Storm Event on 2007.08.24-2007.08.27 at 2007.08.26 02:30.

The cell storm moved to the southern part of this area, and almost covered all the southern part of this area

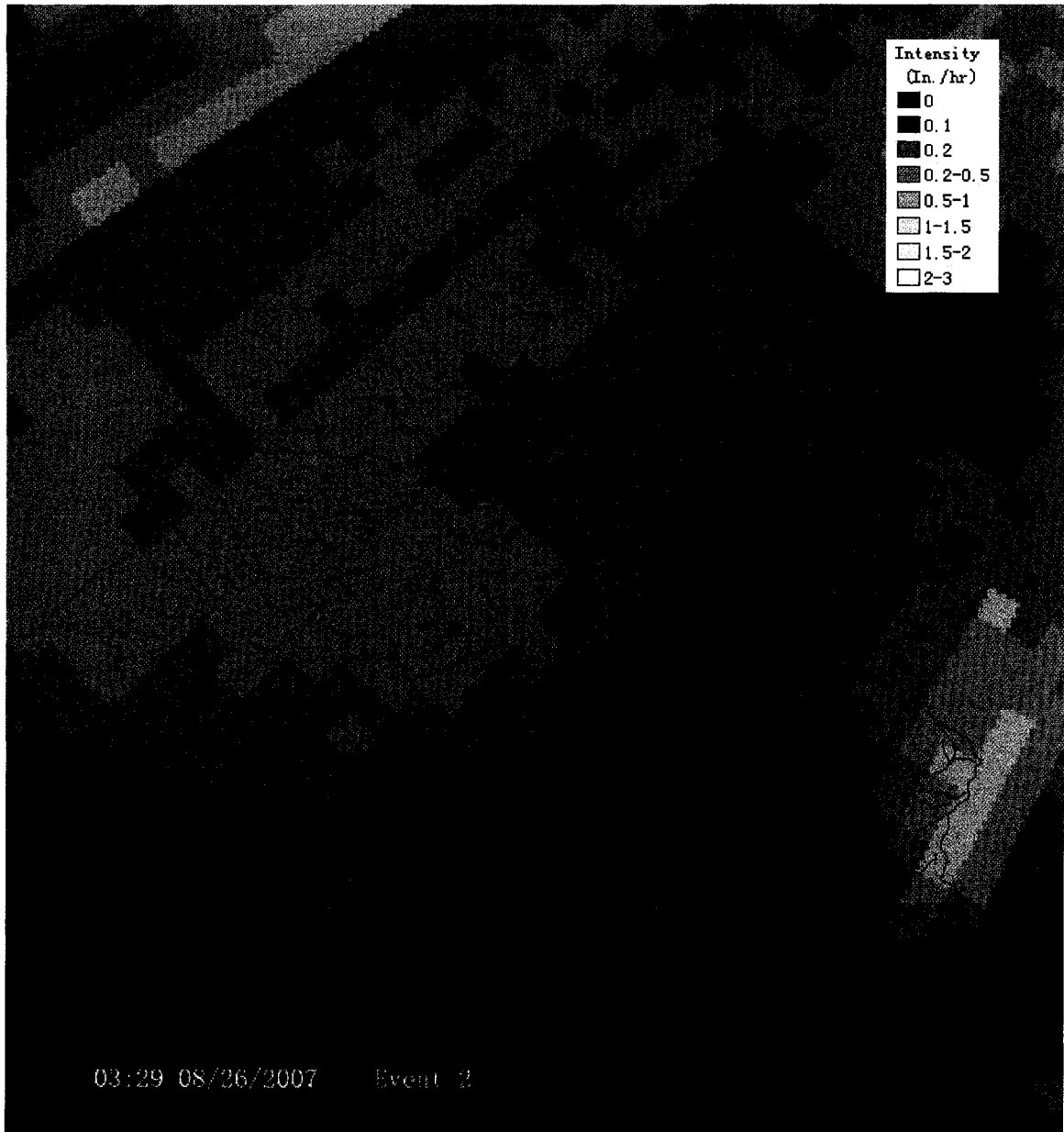


Fig. 5.9 (f) Temporal NEXRAD Radar Image of the Second Storm Event on 2007.08.24-2007.08.27 at 2007.08.26 03:29.

The cell storm center moved out of this area, there is only light rain in the northern part.

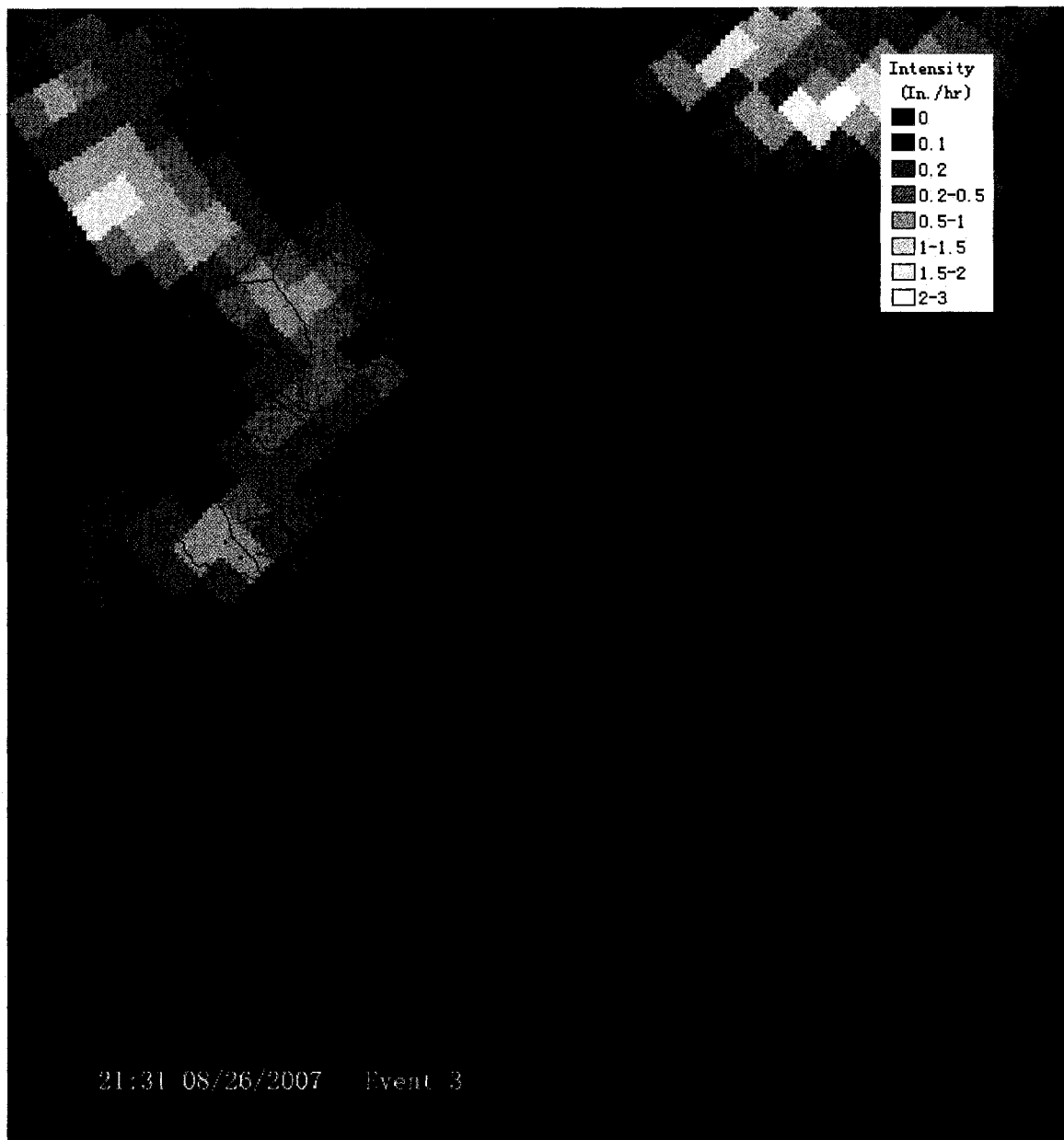


Fig. 5.10 (a) Temporal NEXRAD Radar Image of the Third Storm Event on 2007.08.24-2007.08.27 at 2007.08.26 21:31.

There were two cell storms in the north.

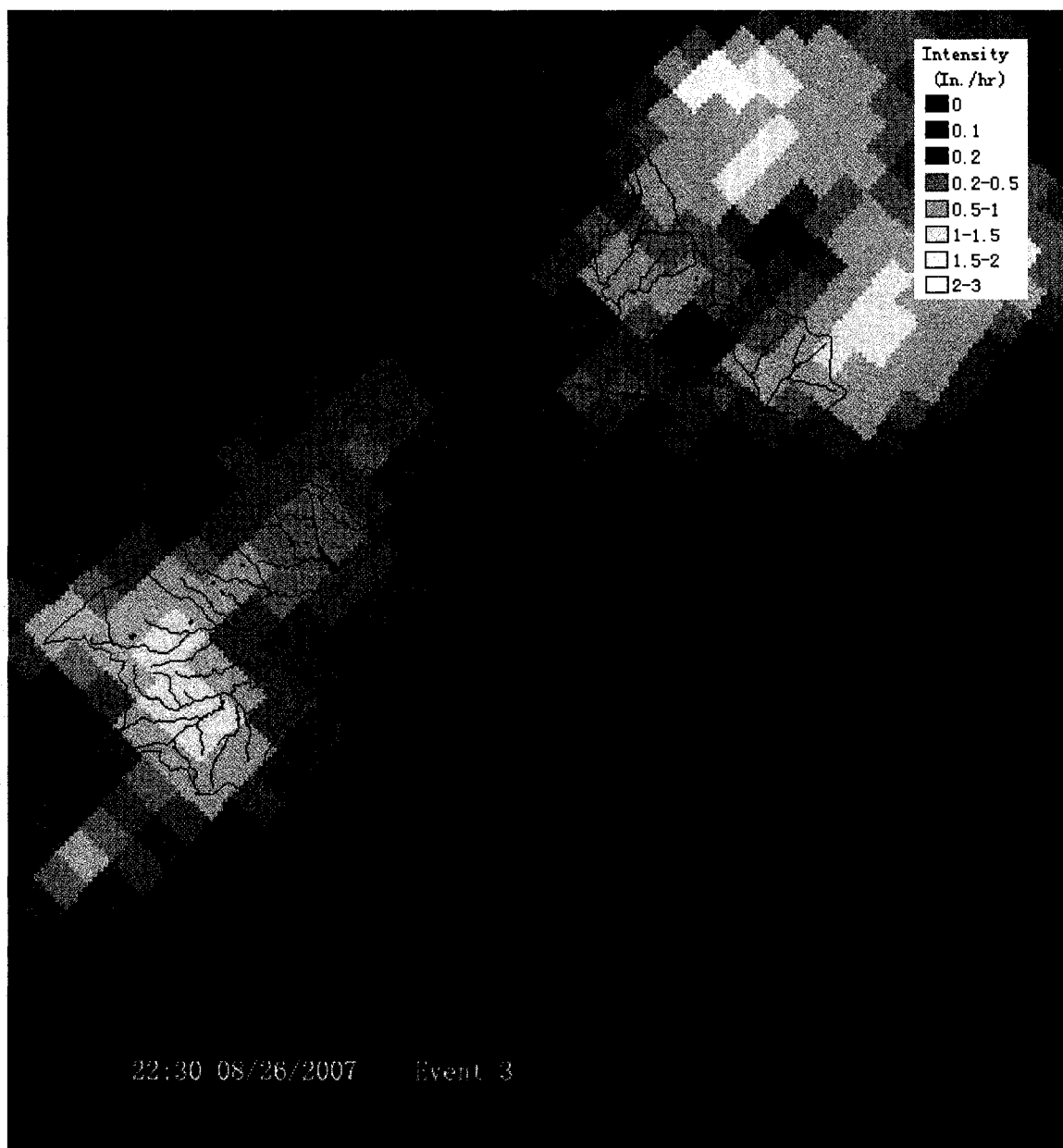


Fig. 5.10 (b) Temporal NEXRAD Radar Image of the Third Storm Event on 2007.08.24-2007.08.27 at 2007.08.26 22:30.

The two cell storms both moved into the northern part of the area.

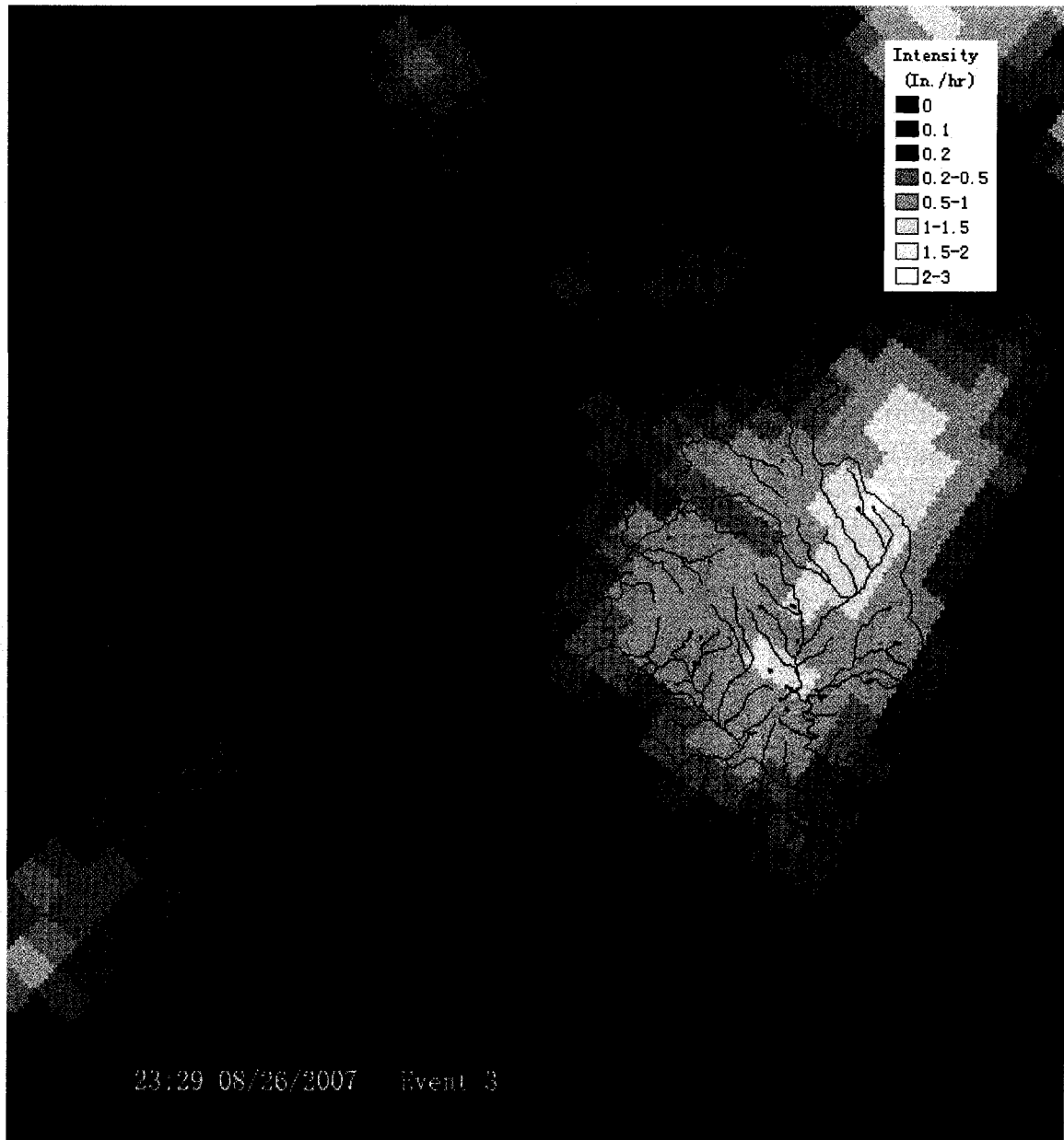


Fig. 5.10 (c) Temporal NEXRAD Radar Image of the Third Storm Event on 2007.08.24-2007.08.27 at 2007.08.26 23:29.

The eastern cell storm moved quickly to the south.

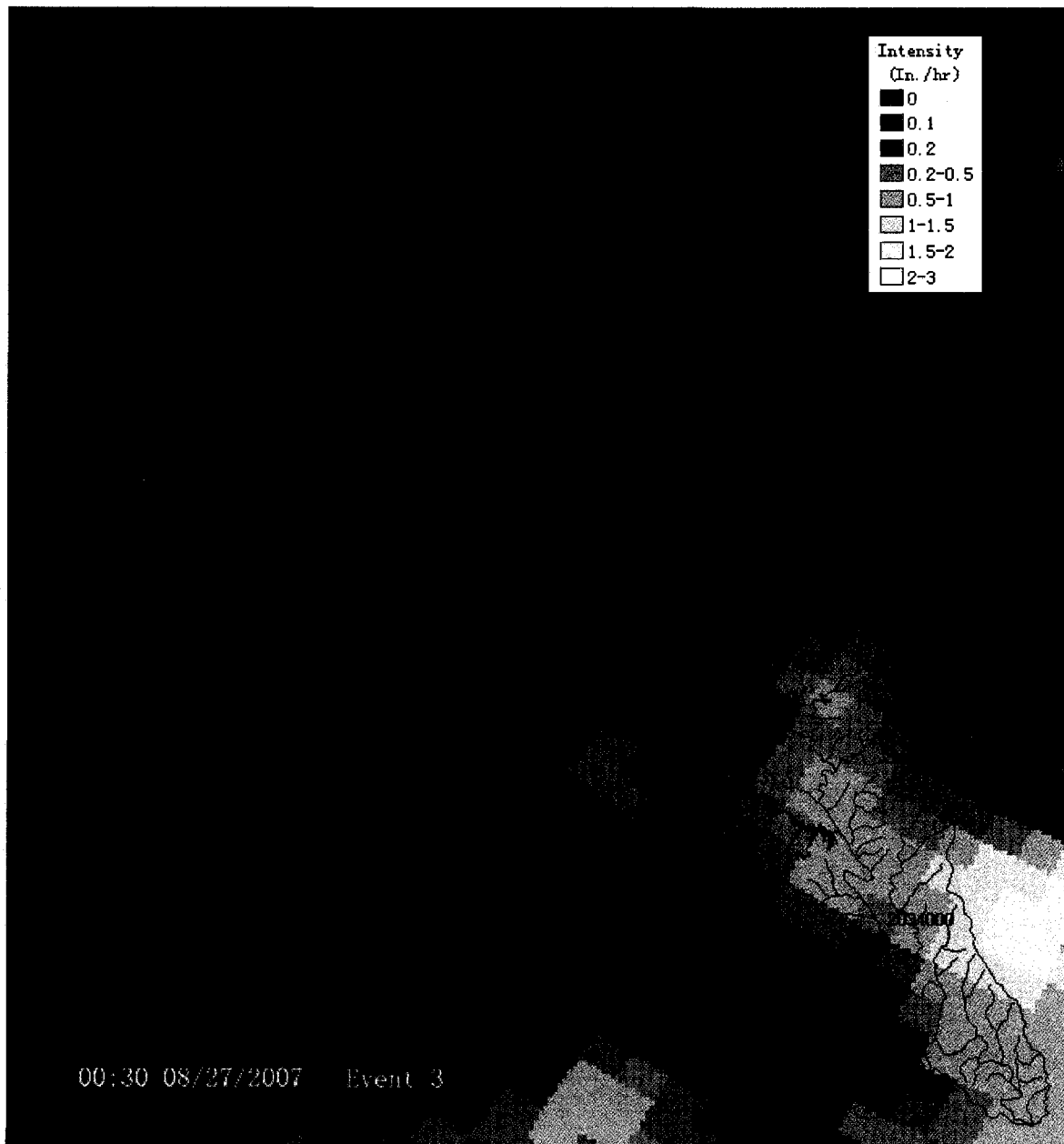
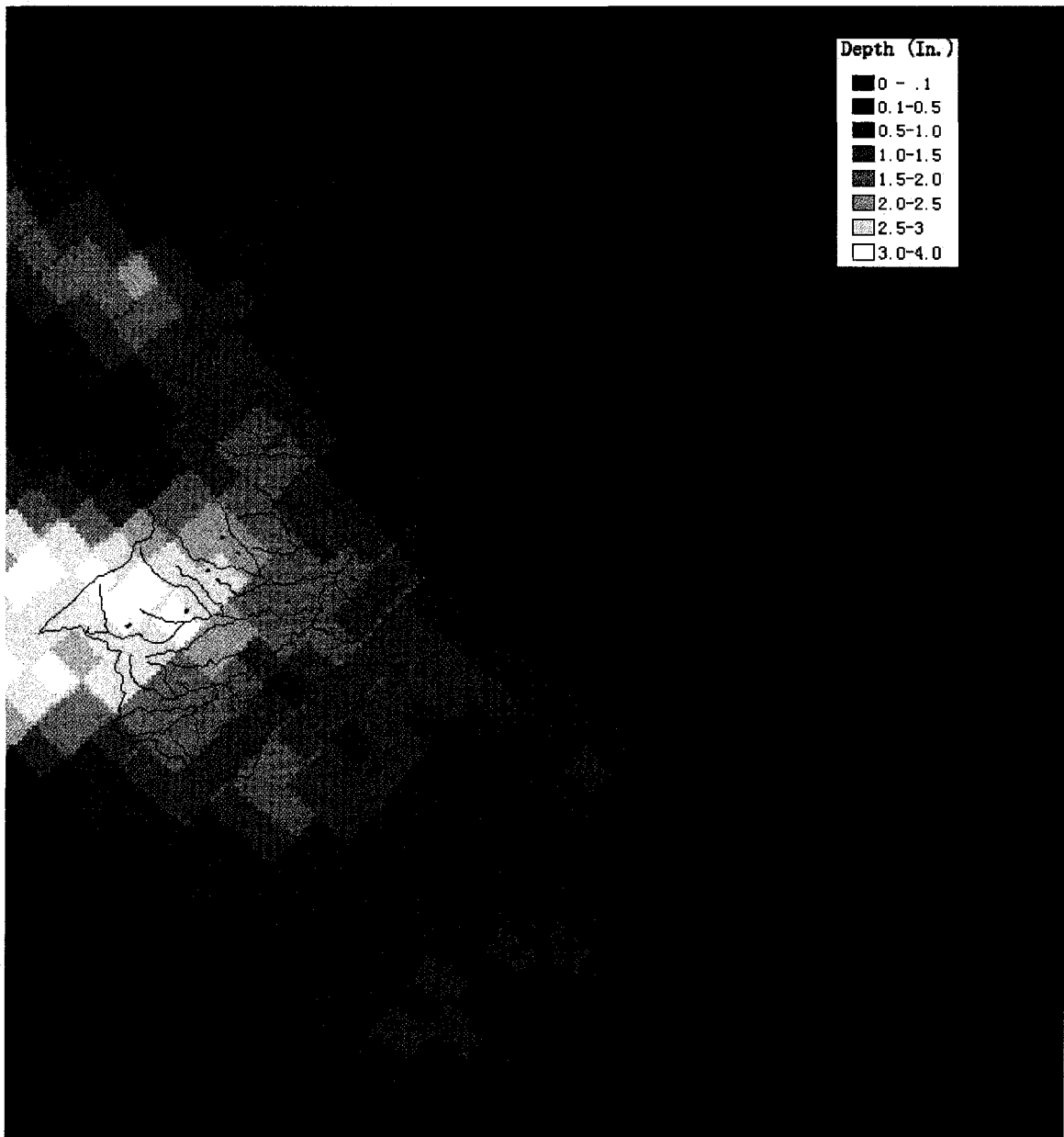


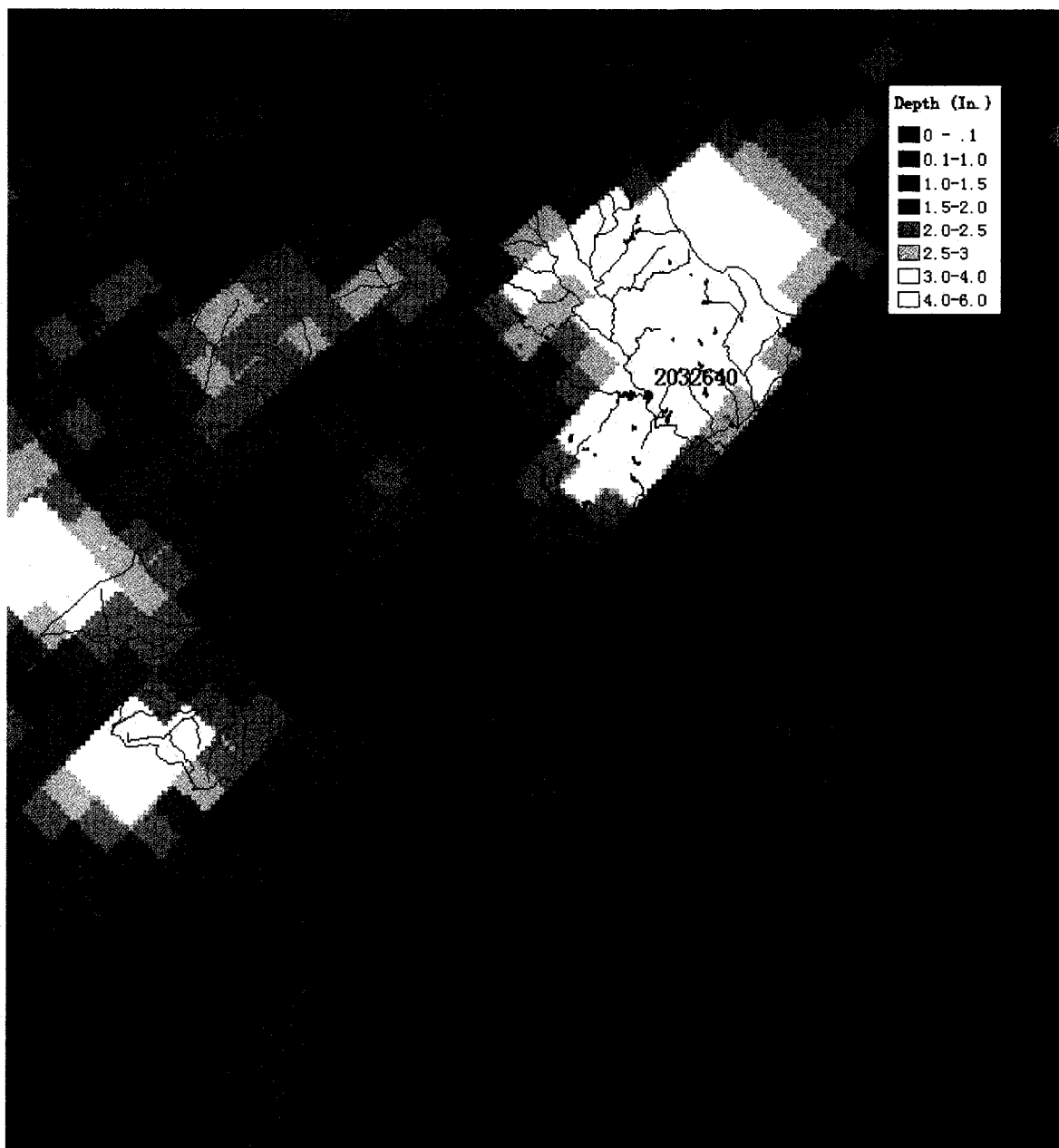
Fig. 5.10 (d) Temporal NEXRAD Radar Image of the Third Storm Event on 2007.08.24-2007.08.27 at 2007.08.27 00:30.

The eastern cell storm moved quickly to the south, and moved out of this area.



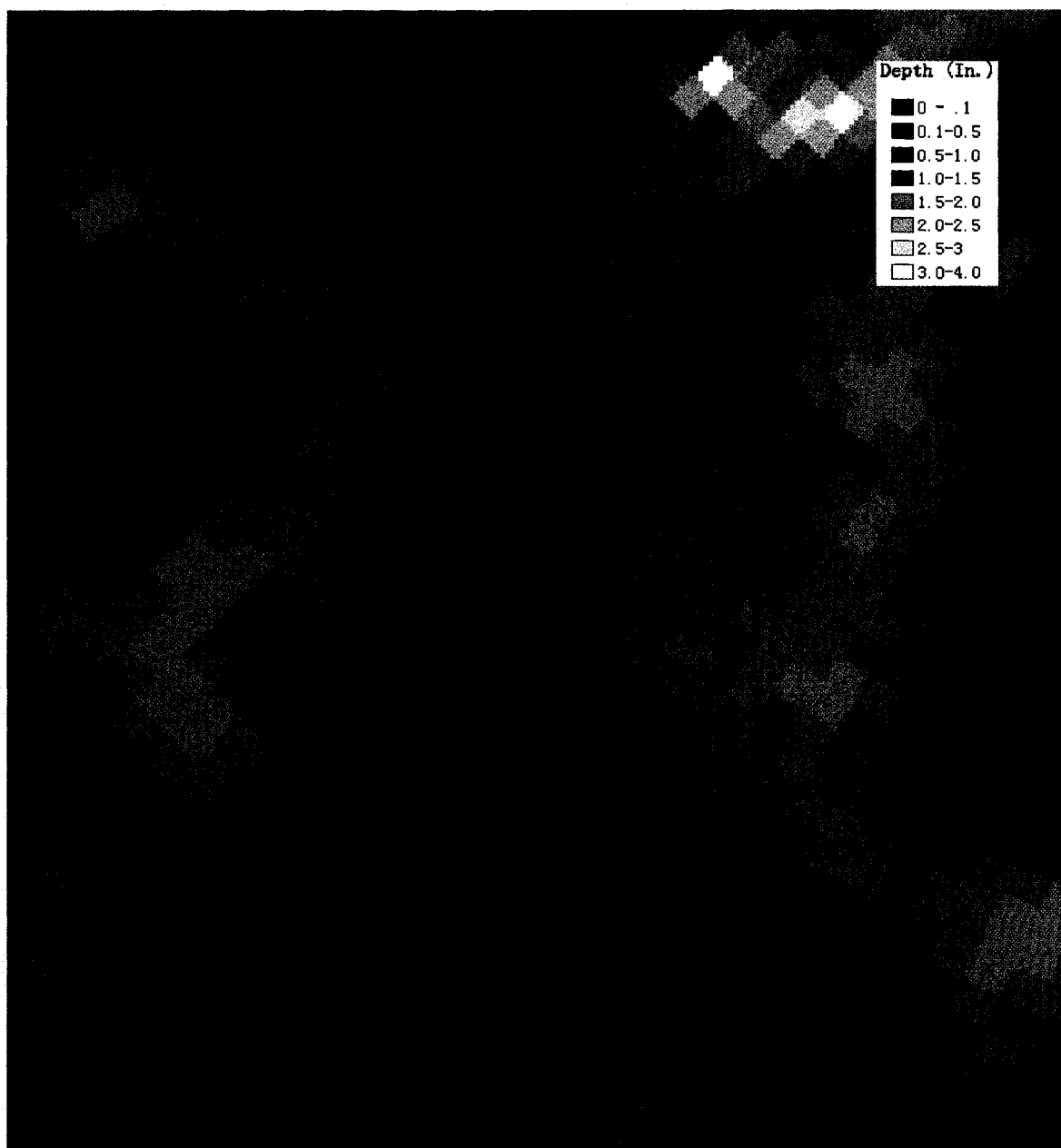
Event 1

Figure 5.11 (a) Cumulative Rainfall Depth Raster for the First Event of Multiple Storm Events, over 2007.08.24-2007.08.27, Rivanna River Basin, Central Virginia



Event 2

Figure 5.11(b) Cumulative Rainfall Depth Raster for the Second Event of Multiple Storm Events, over 2007.08.24-2007.08.27, Rivanna River Basin, Central Virginia



Event 3

Figure 5.11(c) Cumulative Rainfall Depth Raster for the Third Event of Multiple Storm Events, over 2007.08.24-2007.08.27, Rivanna River Basin, Central Virginia

With the three possible AMC conditions (AMC I, AMC II and AMC III), three landcover conditions (Poor, Fair and Good) and over three storm events, there are 81

possible combinations for MHSERM to simulate the hydrological response from the watershed. However, considering the actual surface flow data, we can make a reasonable assumption about the possible AMC conditions and reduce the number of combinations to be simulated. In this case, the AMC condition before these three storm events can be considered as 'Dry' on the basis of the flow data. From the surface flow data (Table 5.6) summarized from four USGS gauge station records and Water Data Report 2007 (U.S. Geological Survey, 2007), the flow was well below the mean values for August between 1943 and 2007. Moreover, the peak flows occurred after the second storm event, and these peak flows were also not significant compared to the rainfall depths registered in the watershed. For the second storm event, AMC condition was still considered as 'Dry' or 'Normal' because the first storm event was really small and only passed through a part of the study area, resulting almost no significant contribution of precipitation to the watershed. To simplify the process, only the results of two AMC combinations with three landcover conditions are compared with the observed flow data (Table 5.7).

Table 5.6 Flow Data Extracted from USGS Gauge Stations within Rivanna River Basin

Site No. and Name	Peak Time	Peak Flow (cfs)	Observed Flow before the storm event (cfs)	The August Mean Flow between 1943-2007 (cfs)
02034000 RIVANNA RIVER AT PALMYRA, VA	5:45pm, 8/26/2007	2640	103	440
02031000 MECHUMS RIVER NEAR WHITE HALL, VA	4:30am, 8/26/2007	691	15	52.3
02032640 N F RIVANNA RIVER NEAR EARLYSVILLE, VA	11:30pm, 8/25/2007	1740	17	41.8
02032250 MOORMANS RIVER NEAR FREE UNION	4:30am, 8/26/2007	185	4.5	29.4

5.2.1.2 Simulation Results for the Multiple Storm Events with MHSERM

MHSERM simulated hydrological responses of the watershed for the three storm events with two AMC combinations and three landcover conditions, i.e. in total six groups of hydrographs for all the streams in the Rivanna River Basin. The hydrographs of these six groups at four streams where the four USGS gauge stations are located were estimated by MHSERM and compared with the observed gauge station records. Results are shown in Figures 5.12, 5.13, 5.14 and 5.15 for four USGS gauge stations.

Combinations of AMC and landcover condition used in the simulation are listed and described in Table 5.7.

Table 5.7 Combinations of AMC and landcover condition used in the Simulation for the 2007.8.24-2007.8.27 Storm Events

Combination Name	Description
AMC I-I-III-P	The AMC conditions for the 1 st event, 2 nd event and 3 rd event are dry, dry and wet, respectively; the landcover condition is Poor.
AMC I-I-III-F	The AMC conditions for the 1 st event, 2 nd event and 3 rd event are dry, dry and wet, respectively; the landcover condition is Fair.
AMC I-I-III-G	The AMC conditions for the 1 st event, 2 nd event and 3 rd event are dry, dry and wet, respectively; the landcover condition is Good.
AMC I-II-III-P	The AMC conditions for the 1 st event, 2 nd event and 3 rd event are dry, normal and wet, respectively; the landcover condition is Poor.
AMC I-II-III-F	The AMC conditions for the 1 st event, 2 nd event and 3 rd event are dry, normal and wet, respectively; the landcover condition is Fair.
AMC I-II-III-G	The AMC conditions for the 1 st event, 2 nd event and 3 rd event are dry, normal and wet, respectively; the landcover condition is Good.

The simulation period was from 8:00 PM, 08/24/2007 to 0:00 AM, 8/28/2007 (a total of 78 hours) with a 15-minute time step increment. Results indicate that a combination of AMC and landcover condition of AMC I-II-III-G simulated peak flows most closely to the observed peak flows (Fig. 5.12, 5.13, 5.14 and 5.15).

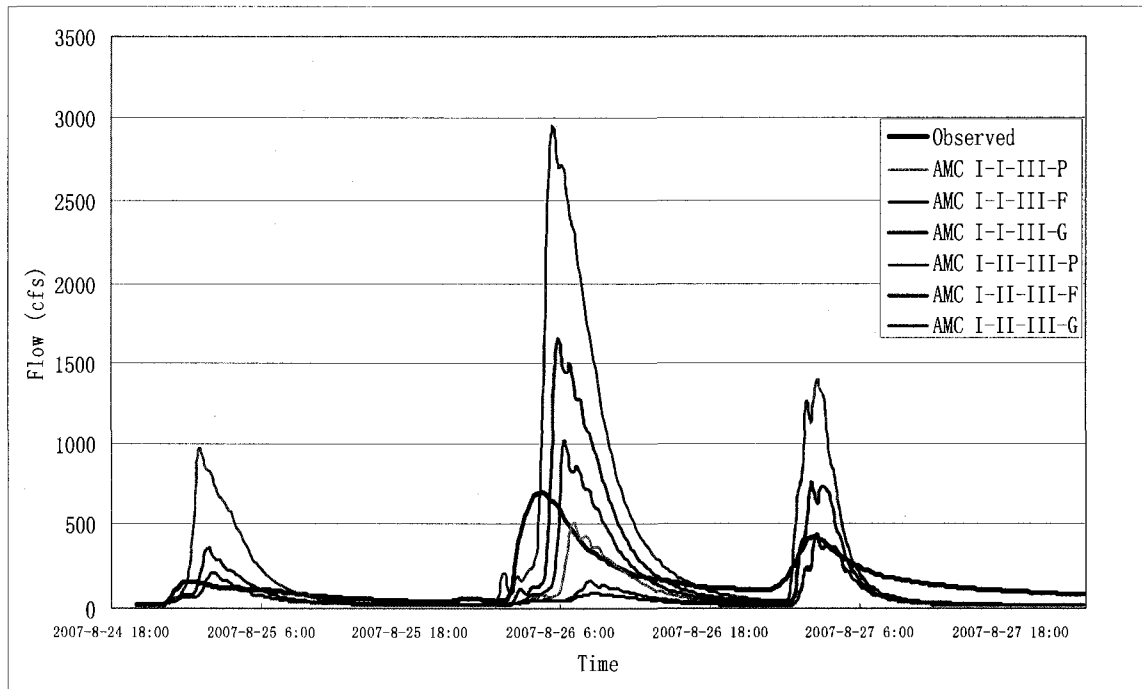


Figure 5.12 MHSERM Outflow Hydrograph Estimates vs. Observed USGS Gauge Station 02031000, under six AMC-Landcover combinations

Figure 5.12 shows the comparison of the hydrographs simulated for stream 102089 vs. observed from USGS gauge station 02031000. The station is located on the northwestern corridor of the basin, through which all three storm events had passed. From the hydrographs in Figure 5.9, the observed peak flow registered at about 156cfs, 691cfs and 422cfs, respectively. Among the estimated hydrographs from six different combinations, the closest hydrograph was estimated with a combination of AMC I-II-III-

G (Table 5.8). Moreover, as MHSERM's results show, the peak flows estimates could be much higher if AMC and landcover condition were changed for this area (Table 5.8).

Table 5.8 The observed and simulated peak flows for 2007.8.24-2007.8.27 events at station 02031000

Condition Groups	Peak Flow (cfs) For Event 1	Peak Flow (cfs) For Event 2	Peak Flow (cfs) For Event 3	Flow Deviation to Observed Peak Flow (%) for Event 1	Flow Deviation to Observed Peak Flow (%) for Event 2	Flow Deviation to Observed Peak Flow (%) for Event 3
Observed	156	691	422	0	0	0
AMC I-I-III-P	974	502	1399	524%	-27.3%	232%
AMC I-I-III-F	358	160	742	129%	-76.8%	75.8%
AMC I-I-III-G	209	91	436	34.0%	-86.8%	3.32%
AMC I-II-III-P	974	2939	1270	524%	325%	201%
AMC I-II-III-F	358	1656	746	129%	140%	76.8%
AMC I-II-III-G	209	1007	374	34.0%	45.7%	-11.4%

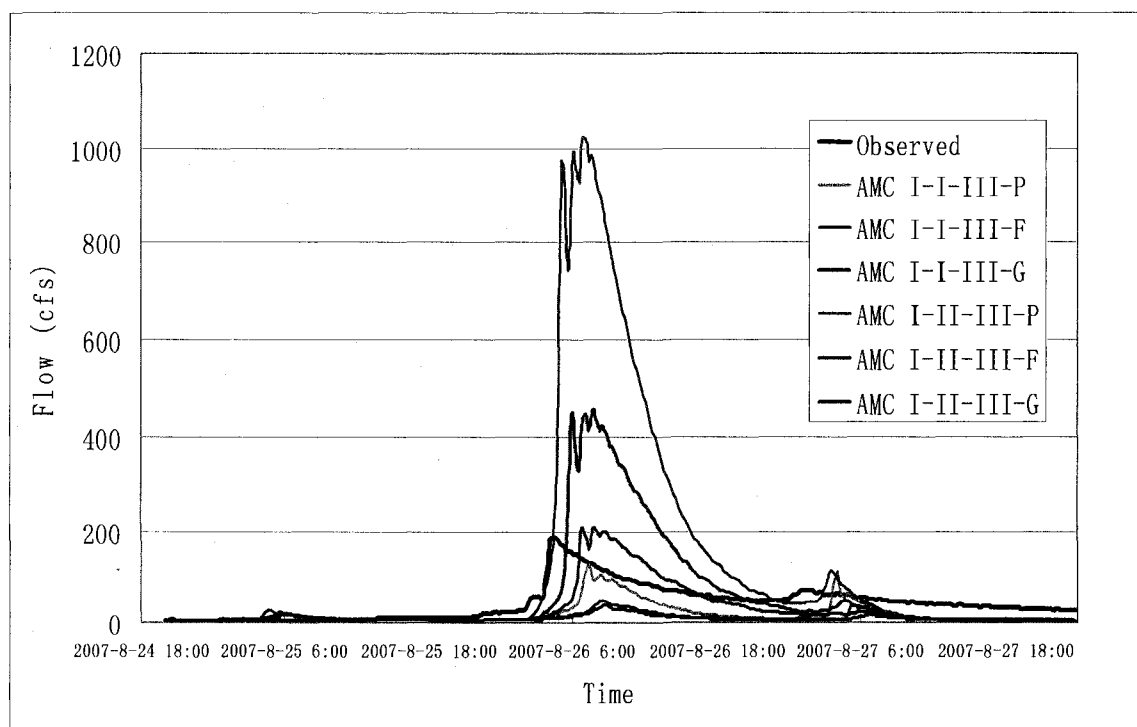


Figure 5.13 MHSERM Outflow Hydrograph Estimates vs. Observed USGS Gauge Station 02032250, under six AMC-Landcover combinations

Figure 5.13 shows the comparison of the hydrographs simulated for stream 93605 and hydrograph observed on USGS gauge station 02032250. The first and third storm events had little influence on the surface flow in this location, and the second storm event alone resulted in an observed peak flow of 185cfs USGS gauge station 02032250. Simulated peak flow with AMC I-II-III-Good was about 209cfs, which is very close to the observed peak flow (Table 5.9).

Table 5.9 The observed and simulated peak flows for Event 2 at station 02032250

Condition Groups	Peak Flow (cfs) For Event 2	Flow Deviation to Observed Peak Flow (%) for Event 2
Observed	185	0
AMC I-I-III-P	127	-31.4%
AMC I-I-III-F	47	-74.6%
AMC I-I-III-G	37	-80%
AMC I-II-III-P	1021	452%
AMC I-II-III-F	459	148%
AMC I-II-III-G	209	13.0%

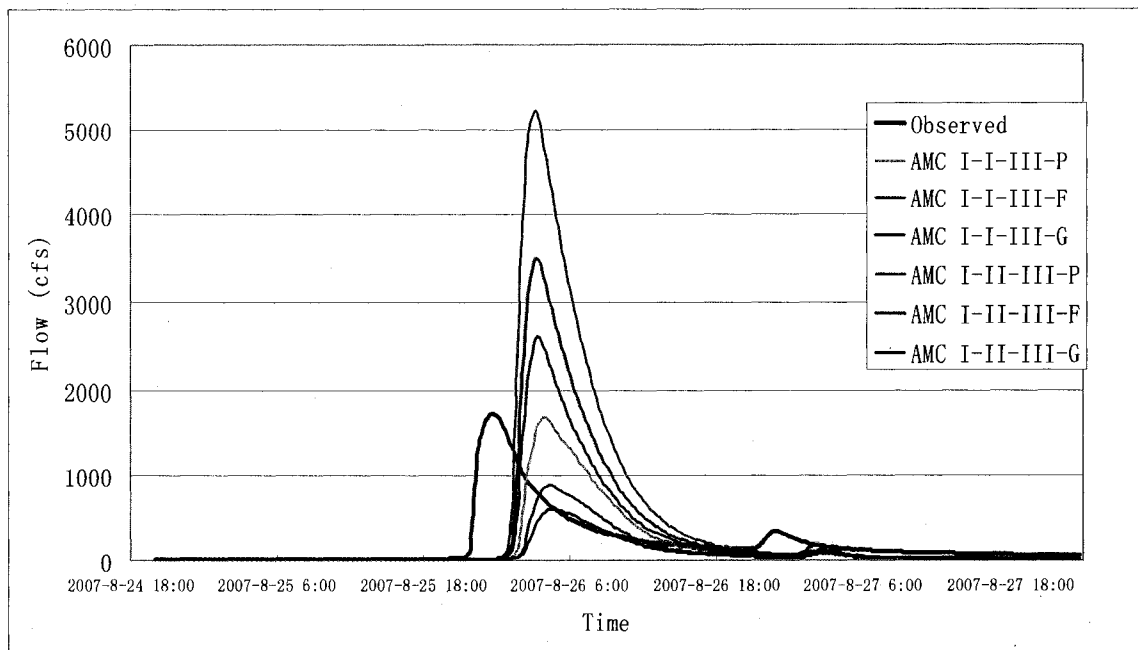


Figure 5.14 MHSERM Outflow Hydrograph Estimates vs. Observed USGS Gauge Station 02032640, under six AMC-Landcover combinations

Figure 5.14 shows a comparison of the hydrographs simulated for stream 86010 and the hydrograph observed on USGS gauge station 02032640. The first storm event contributed little to the surface flow of this stream/station, and the second storm event resulted in a peak flow at 1740cfs, which is close to the simulated peak flow with condition AMC I-I-III-P; the deviation is about -2.87% (Table 5.10). However, there was about a 3.5-hour time lag in the time-to-peak simulated hydrographs compared to the observed time-to-peak of USGS gauge station 02032640. The rising limb of the observed flow is started at 22:00, and the peak time is about 23:30 August 25. In comparison, the simulated peak flow time was at 03:00 August 26 with a time lag of 3.5 hours. The cause for this time lag in hydrographs can be explained by NEXRAD radar data series where NEXRAD data registered almost no rainfall on the upstream area of station 02032640 before 22:30 August 25. Thus, in a reverse manner, MHSERM actually responded to and

reflected well the spatiotemporal rainfall distribution registered in NEXRAD radar data, so that it can be stated that the more accurate NEXRAD radar data quality in spatiotemporal rainfall distribution, the better MHSERM simulation results can be.

Table 5.10 The observed and simulated peak flows for Event 2 at Station 02032640

Condition Groups	Peak Flow (cfs) For Event 2	Flow Deviation to Observed Peak Flow (%) for Event 2
Observed	1740	0
AMC I-I-III-P	1690	-2.87%
AMC I-I-III-F	792	-54.5%
AMC I-I-III-G	597	-65.9%
AMC I-II-III-P	5222	200%
AMC I-II-III-F	3492	101%
AMC I-II-III-G	2600	49.4%

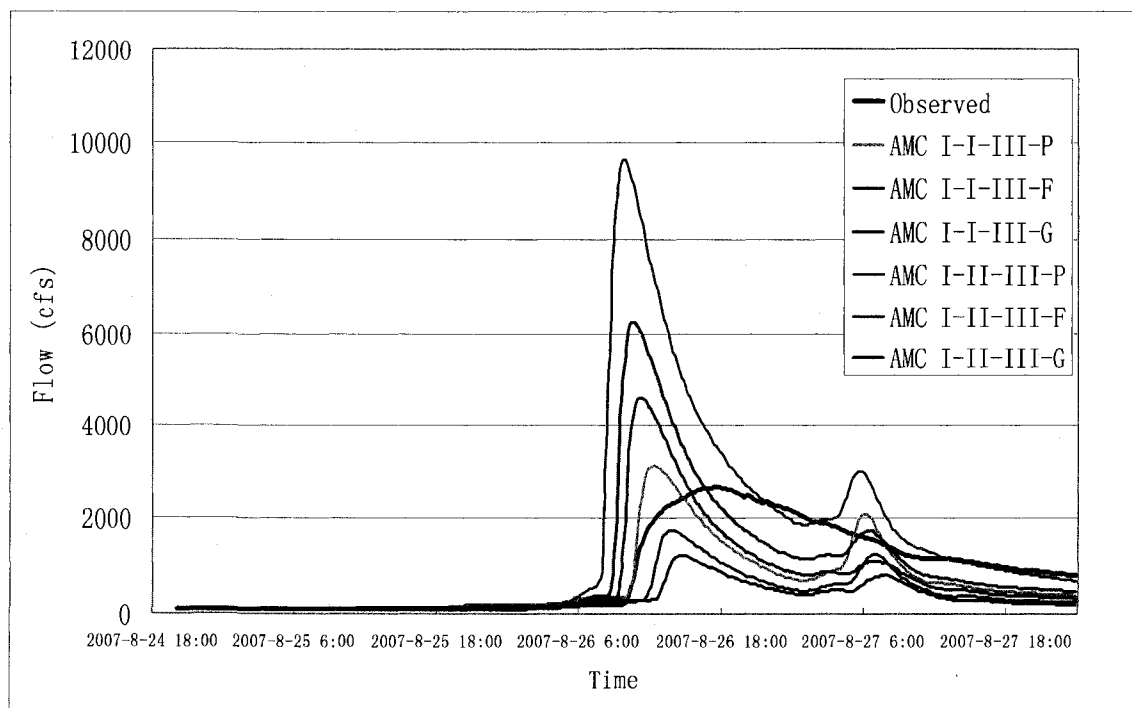


Figure 5.15 MHSERM Outflow Hydrograph Estimates vs. Observed USGS Gauge Station 02034000, under six AMC-Landcover combinations

USGS gauge station 02034000 is located the most downstream in the Rivanna River Basin compared to other three gauge stations used in this comparison. Since the location is fed by a much bigger contributing upstream area and therefore has more numbers of upstream streams and a larger cumulative flow, the gauge station was most difficult to estimate its hydrograph and peak flow. This can be possibly explained by the cumulative variability amplified in flow routing estimates of 886 catchments (as previously shown in Figure 4.6) at this USGS gauge station 02034000 location. From the observed data, the peak flow was 2640 cfs, at 5:45 PM, 8/26/2007. The simulated peak flow with AMC I-I-III-P was about 3110 cfs, but the falling limb of simulated hydrographs had a steeper gradient than that of the observed.

Table 5.11 The observed and simulated peak flows for Event 2 at Station 02034000

Condition Groups	Peak Flow (cfs) For Event 2	Flow Deviation to Observed Peak Flow (%) for Event 2
Observed	2640	0
AMC I-I-III-P	3110	17.8%
AMC I-I-III-F	1723	-34.7%
AMC I-I-III-G	1198	54.6%
AMC I-II-III-P	9619	264%
AMC I-II-III-F	6258	137%
AMC I-II-III-G	4599	74.2%

5.2.3 The Summary of the Above Studying Cases

From two case studies consisting of single storm event and a series of storm events, massive watershed scale storm event hydrological response model (MHSERM) showed its strength and its weakness. Simulated hydrographs were in better fits with

observed flow in upstream stations, i.e., USGS gauge stations 02031000, 02032250 and 02032640, but in a moderate fit in the downstream station, i.e. 02034000 based on the results in section 5.2.2.

The AMC and landcover conditions have the dominant influence on the estimated peak flow for these two storm events. From Tables 5.3, 5.4 and 5.5, the same storm with the condition AMC III-Poor can generate as five times of flow volume than the flow generated with a condition AMC II-Good. For example, the simulated peak flow was 1933 cfs with AMC II-Good, and it was 9878 cfs with AMC III-Poor at station 02031000 for the 2003.9.18-2003.9.19 storm event. With the same landcover condition, the peak flow simulated with AMC III condition could be still 2-3 times higher than the peak flow simulated with AMC II condition. For example, the peak flow was 3108 cfs with AMC II-Fair, and was 8179 cfs with AMC III-Fair condition at station 02031000 for the 2003.9.18-2003.9.19 event (Table 5.3).

Thus, it is very important to carefully choose the AMC-Landcover combinations that will best represent the characteristics of hydrologic features and vegetation of the studying area. In two case studies, the AMC condition was estimated by comparing the observed flows before the storm event with the historical mean monthly flows at the USGS gauge stations. If the observed flow is below the mean monthly flow, the AMC condition can be considered as I or II (i.e., dry or normal), or as II or III (i.e., normal or wet). There is no simple way to determine landcover conditions, so MHSERM can simulate the hydrological response for all three conditions (Poor, Fair and Good), which can give the users the ranges of results representative of best and worst scenarios.

5.3 Conclusion and Discussion

5.3.1 Benefits of the MHSERM Model

MHSERM provides a framework to quickly simulate the hydrological response to storm events by utilizing the new, high precision spatial dataset as well as the time-lapsed NEXRAD precipitation radar data feed. The high precision spatial dataset include the USGS Digital Elevation Model (DEM) and Landcover data, NRCS Soil Survey Geographic Database (SSURGO) and soil spatial dataset, State Soil Geographic Database (STATSGO) soil data and National Hydrology Dataset (NHD). Based on these datasets, MHSERM calculates rainfall runoff at a spatiotemporal grid/cell resolution, instead of conventional lumped-sum catchment or subcatchment scale; that can simulate detailed variations in terrain, vegetation, land cover and use, and soil far accurately since a spatiotemporal grid/cell resolution can be as small as the resolution of the USGS DEM data, which is typically 30 by 30 meters.

MHSERM can produce several useful interim datasets including the grid discretization of rainfall runoff catchments contributing to the streams, SCS CN number, Manning roughness, the distance to the streams and corresponding time of concentration, the slope to the streams, etc. that describe overland and in-stream flows resulting from storm events. Unlike other conventional delineation methods, MHSERM delineates the contributing area by reverse-tracing upstream from the known streams or outlets, thus ensuring correct detection of gradient-based flow directions and subsequently ensuring correct delineation of runoff contributing areas. This backward method based on known NHD flowline data is far more efficient and much faster than other existing methods,

especially for delineating a watershed composed of tens of millions of grids. The grid datasets of SCS CN number, Manning roughness, the distance and slope to the streams are then used to calculate the rainfall excess, time of concentration, etc. required for calculating overland runoff and resulting inflow and outflow hydrograph in the streams.

The stream network is constructed automatically in the MHSERM. MHSERM can establish the stream network consisting of thousands of streams and impounded waterbodies by utilizing NHD hydrograph dataset. With this ability, MHSERM can simulate the flow routing in a complete actual stream network, not a schematic or simplified stream network. Some of the stream parameters such as length and longitudinal slope are also extracted and estimated based on the DEM and NHD dataset.

With the time-lapsed NEXRAD precipitation radar data feed, MHSERM can capture the spatial variations in the catchments over incremental time steps during storm events. From two case study runs conducted for the Rivanna River Basin, the storm events can move very quickly and varied spatially-temporally over the watershed. MHSERM was conceptualized and designed to use a grid-based representation of the watershed to capture such spatiotemporal variations with great flexibility. Once the watershed grids are prepared, MHSERM can calculate the rainfall excess for each grid, and estimate the time of concentration only for those specific grids with rainfall excess at each time step.

MHSERM is highly portable to any watershed by rapidly prepare and estimate physical parameters of the watershed from high precision spatial dataset as well as the time-lapsed NEXRAD precipitation radar data feed, which takes weeks and months

depending on the size of the watershed in interest. Among the physical parameters of the watershed, Antecedent Moisture Condition (AMC) and landcover conditions are two of the most dominant influences on rainfall excess calculation, and users can set different combinations of the conditions to further refine the simulation of the hydrological response based on their experience and judgment. Other than parameters extracted from the existing datasets, MHSERM also uses a Microsoft Access database to store all input parameters for the flow routing and output estimates from the simulation, so that users can efficiently modify the parameters of stream/waterbody if more accurate data are available.

5.3.2 Advantages of the MHSERM over Conventional SERM

Applied on Complicated Natural Hydrological System

Compared to a conventional hydrological modeling system like HEC-HMS, MHSERM has some obvious advantages, especially for handling a complicated, large natural system. The main advantages are summarized below:

1. MHSERM can be quickly applied to a complicated and large watershed, but a conventional SERM usually requires tremendous amount of time and workload to prepare the data and simulate. A complicated and large watershed can comprise of hundreds of streams and impounded waterbodies, and be over 1000 square miles with innumerable spatial variations on terrain, land cover, soil and vegetation. It is almost not possible for a user to obtain all of the data in a conventional manner for a SERM to run for this watershed. However, MHSERM can finish the processing of required data in a couple of days by accessing on-line and extracting parameters from the

publically available, high precision dataset and with standard assumptions such as the shape of waterbodies and streams.

2. MHSERM is a grid-based system, which provides the capability utilizing the high precision spatial data in a raster format, thus ensure spatial variability of the watershed is correctly represented, and subsequently, system responses from the watershed such as runoff are correctly simulated. A conventional SERM is usually based on a lumped-sum catchment/subcatchment scheme, simplified assumption of the hydrological homogeneity. The less detail of physical variability of the watershed a model has, the more obtuse the simulated responses from the watershed.

The grid-based system gives MHSERM great flexibility in capturing small spatial variations of the terrain, soil and vegetation. The grid size used in the system is the same with the DEM data, e.g. 30 m by 30 m. But for a conventional SERM, the variations in a catchment are usually omitted.

3. Stream network for flow routing is automatically established in the MHSERM on the basis of NHD data. For a conventional SERM, the users usually need to set up the network manually. This is a huge time and effort saving component of MHSERM compared to other SERMs.

Hundreds of streams and waterbodies in a stream network make it very time consuming to set up the network manually for a conventional SERM; moreover, the MHSERM provides better visualization for the stream network since MHSERM is fully integrated with ArcGIS platform.

4. MHSERM uses time-lapse NEXRAD precipitation radar data in increment of 5-6 minutes updates, and it can capture the spatial variations at any time steps during storm events by overlaying watershed grids over NEXRAD grids. Few conventional

SERM can utilize NEXRAD precipitation data as an input, however these conventional SERM usually cannot capture the variations inside a catchment over time.

5. MHSERM does not require repeated preprocessing or adjustment for new applications of simulating different storm events. Furthermore, MHSERM facilitates simulation under different combinations of AMC and landcover conditions for sensitivity analysis, and most of all, evaluation of various what-if scenarios. A conventional SERM requires a lot of adjustments for a new application of storm events even for the same watershed because AMC and landcover conditions can change and vary with the time. With MHSERM, users can choose the different combination of AMC and landcover conditions for simulations as needed.
6. MHSERM can be potentially used for pseudo-real-time flood prediction with time-lapsed NEXRAD radar data feed. Because the NEXRAD radar data series is updated on-line in a near real time manner with a 5-6 minutes increment, MHSERM can take advantage of predicting the flood in a timely fashion.
7. MHSERM can handle tens of millions grids, thousands of streams for the watershed in great detail. There is currently no conventional SERM that can match such capability and expandability.

5.3.3 Existing Issues and Future Recommendations

Although the results of two MHSERM case studies showed reasonable fits between the simulated and the observed peak flows with specific combinations of AMC and landcover conditions, there are still several issues that need to be further addressed.

1. The rising limb of the simulated hydrographs sometimes has a time lag compared to the observed hydrographs. MHSERM is using the SCS CN method to calculate the rainfall excess for each grid. With the SCS CN method, no rainfall excess exists before the rainfall depth reaches the grid's initial abstraction (I_a parameter, see Equation 4.4), which is 0.2 times soil moisture storage deficit. However, 0.2 can be too big for some cases; some studies found that an I_a value of 0.05 was generally a better fit than a value of 0.2 (Hawkins *et al.*, 2002; Jiang, 2001). MHSERM is still using 0.2 for I_a value however. In the future, MHSERM may utilize the physical rainfall loss formulas to correct this problem.
2. The falling limb of the simulated hydrographs decreased faster than the observed hydrographs, especially for the downstream station 02034000 (even though the rising limb characteristic is a more important design variable for flood mitigation in general than falling limb characteristic). The main cause of this issue could be the subsurface flow, which is not currently accounted for in MHSERM. MHSERM only estimates the base flow on the basis of its contributing area, and the estimated base flow is used during the simulation period without accounting any further loss. For particular locations that have strong subsurface flow

component or a big watershed, the subsurface flow may not be neglected, and MHSERM may need integrating the subsurface flow in the future.

3. The peak time occurred earlier on the simulated hydrographs than the observed hydrograph at the downstream station 02034000. This issue is observed only on station 02034000. For the first study case, the peak time of the simulated hydrographs was at about 8:30 PM September 19, but the observed peak flow happened at 0:45 AM September 20. It looks like a big delay at first, however, the observed flow increased very slowly after 8:30 PM September 19, from about 23000 cfs to the peak flow at 30000 cfs. Thus, this delay may result from two possible causes: upstream reservoir routing adjustment, and the subsurface flow. MHSERM currently does not have the ability to simulate these issues and may need to further enhance reservoir routing as well as address subsurface flow in the future.

REFERENCE

Abbott, M. B., J.C. Bathurst, J.A. Cunge, P.E. O'Connell, and J. Rasmussen, (1986a), An introduction to the European Hydrological System – Systeme Hydrologique Europeen, SHE. 1 History and philosophy of a physically-based distributed modelling system. *Journal of Hydrology*, Vol(87): 45-59.

Abbott, M. B., J.C. Bathurst, J.A. Cunge, P.E. O'Connell, and J. Rasmussen, (1986b), An introduction to the European Hydrological System – Systeme Hydrologique Europeen, SHE. 2 Structure of a physically-based distributed modelling system. *Journal of Hydrology*, Vol(87): 61-77.

Akan, A.O., (1992), "Horton Infiltration Formula Revisited," *Journal of Irrigation and Drainage Engineering*, ASCE, Vol.(118), No. 5: 828-830.

Akan, A. O., (1993), *Urban Stormwater Hydrology - A Guide to Engineering Calculations*, Technomic Publishing Co., Lancaster, Pennsylvania, 1993, ISBN: 0-87762-966-6.

Akan, A.O. and R.J. Houghtalen, (2003), *Urban Hydrology, Hydraulics and Stormwater Quality*. Wiley, Hoboken, NJ, 373 pp. ISBN: 0-471-43158-3.

Anderson, J.F., E.E. Hardy, J.T. Roach, and R.E. Witmer, (1976), A landuse and land cover classification system for use with remote sensor data, U.S. Geological Survey Professional Paper 964, 28 pp.

Association of State Floodplain Managers, Inc., (1996), *Addressing Your Community's Flood Problems: A Guide for Elected Officials*. Joint project with the Federal Interagency Floodplain Management Task Force.

Band, L. E., (1986), "Topographic Partition of Watersheds with Digital Elevation models," *Water Resources Research*, 22(1): 15-24.

Bedient, P.B., A. Holder, J.A. Benavides and B.E. Vieux, (2003), Radar-based flood warning system applied to tropical storm allison, *Journal of Hydrologic Engineering*. Vol. (8): 308–318.

Bernhardsen, T. (1999), *Geographic information systems: An introduction*. p. 85–89. John Wiley & Sons, New York.

Beven, J. and H. Cobb, (2003), "Hurricane Isabel Tropical Cyclone Report". National Hurricane Center. At <http://www.nhc.noaa.gov/2003isabel.shtml>, Retrieved on 2008-09-20.

Beven, K. J. and M. J. Kirkby, (1979), A physically based variable contributing area model of basin hydrology. *Hydrologic Science Bulletin*. 24(1):43-69.

- Beven, K.J., M.J. Kirkby, N. Schofield, and A.F. Tagg, (1984), Testing a physically-based flood forecasting model (TOPMODEL) for three U.K. Catchments. *Journal of Hydrology*, Vol.(69):119- 143.
- Beven, K. J., R. Lamb, P.F. Quinn, R. Romanowicz and J. Freer, (1995), TOPMODEL, in V P Singh (Ed). *Computer Models of Watershed Hydrology*, Water Resources Publications, 1995, 627-668.
- Borah, D. K., and M. Bera, (2003), Watershed-scale hydrologic and nonpoint-source pollution models: Review of mathematical bases. *Transactions of the ASAE*. v46 I6: 1553-1566.
- Borah, D. K., and M. Bera, (2004), Watershed-scale hydrologic and nonpoint-source pollution models: Review of applications. *Transactions of the ASAE*. v47 i3. 789-803.
- Burke, R., (2003), *Getting to Know ArcObjects*. Redlands, CA: ESRI Press
- Chow, V.T., D.R. Maidment, and L.W. Mays, (1988), *Applied Hydrology*, McGraw-Hill Book Co, New York, NY, USA.
- Crawford, N.H. and R.K. Linsley, (1966), *Digital Simulation in Hydrology—Stanford Watershed Model IV* Technical Report No. 39, Department of Civil Engineering, Stanford University, Stanford, CA (1966).
- Cunge, J. A., (1969), On the Subject of a Flood Propagation Computation Method (Muskingum Method), *Journal of Hydraulic Research*, Vol.(7), No. 2:205-230.
- Di Luzio, M., R. Srinivasan and J.G. Arnold, (2004) A GIS-Coupled Hydrological Model System for the Watershed Assessment of Agricultural Nonpoint and Point Sources of Pollution *Transactions in GIS* 8 (1):113–136.
- Di Luzio, M., R. Srinivasan and J.G. Arnold, (2002) Integration of watershed tools and SWAT model into BASINS. *Journal of American Water Resources Association*. 38(4): 1127-1141.
- Donigian, A.S. Jr. and W.C. Huber, (1991), Modeling of nonpoint source water quality in urban and non-urban areas. EPA 68-03-3513(#29). U.S. Environmental Protection Agency, Athens, GA.
- Donigian, A.S. Jr. and J.C. Imhoff. (2002), From the Stanford Model to BASINS: 40 Years of Watershed Modeling. ASCE Task Committee on Evolution of Hydrologic Methods Through Computers. ASCE 150th Anniversary Celebration. November 3-7, 2002. Washington, DC.
- Duda, P.B., Jr. J.L. Kittle, P.R. Hummel, M. H. Gray, and R. S. Kinerson, (2005), The BASINS Watershed Analysis System - Evolving to Embrace New Data and Techniques. In: *Managing Watersheds for Human and Natural Impacts: Engineering, Ecological, and Economic Challenges*. Proceedings of the 2005 Watershed Management Conference, July

19-22, 2005, Williamsburg, VA; Sponsored by Environmental and Water Resources Institute (EWRI) of the American Society of Civil Engineers, July 19–22, 2005, Williamsburg, Virginia, USA

Fairfield, J. and P. Leymarie, (1991), "Drainage Networks from Grid Digital Elevation Models," *Water Resources Research*, 27(5): 709-717.

Fang, Z., E. Safiolea and P.B. Bedient, (2006), "Enhanced Flood Alert and Control Systems for Houston", in Chapter 16, *Coastal Hydrology and Processes*, Ed. By V.P Singh, and Y.J. Xu, Water Resource publications, LLC, (2006): 199-210.

Freeze R.A. and R.L. Harlan, (1969), Blueprint for a physically-based digitally simulated, hydrologic response model. *Journal of Hydrology*, Vol.(9): 237–258.

Giannoni, F., J.A. Smith, Y. Zhang and G. Roth, (2003), Hydrological modeling of extreme floods using radar rainfall estimates, *Advances in Water Resources* 26 (2003) (2): 195–203.

Green W.H., and G.A. Ampt, (1911), Studies on soil physics, part I, the flow of air and water through soils. *J. Agric. Sci.*, 4(1): 1-24.

Habib, E., W.F. Krajewski and A. Kruger, (2001), Sampling Errors of Tipping-Bucket Rain Gauge Measurements. *Journal of Hydrologic Engineering*, Vol.(6):159-166.

Henderson, F. M., (1966), *Open Channel Flow*. Published by Prentice-Hall, Inc. Upper Saddle River, NJ. ISBN 0-02-353510-5.

Homer, C., C. Huang, L. Yang, B. Wylie and M. Coan. (2004), Development of a 2001 National Landcover Database for the United States. *Photogrammetric Engineering and Remote Sensing*, Vol.(70), No. 7:829-840.

Horton R. E. (1940), An approach towards physical interpretation of infiltration capacity. *Proceedings of the Soil Science Society of America*. Vol.(5):399–417.

Hydrologic Engineering Center, (1990), HEC-1 Flood hydrograph package user's manual: U.S. Army Corps of Engineers, Davis, CA, 410 p.

Ivanov, V. Y., E.R. Vivoni, R.L. Bras and D. Entekhabi, (2004a), Preserving High-Resolution Surface and Rainfall Data in Operational-scale Basin Hydrology: A Fully-distributed Physically-based Approach. *Journal of Hydrology*, Vol.(298): 80-111.

Ivanov, V. Y., E.R. Vivoni, R.L. Bras and D. Entekhabi, (2004b), Catchment Hydrologic Response with a Fully-distributed Triangulated Irregular Network Model. *Water Resources Research*, Vol.(40), I(11): 2101-2122.

Jayakrishnan, R. (2001), Effect of rainfall variability on hydrologic simulation using WSR-88D (NEXRAD) data. PhD Dissertation, Biological and Agricultural Engineering Department, Texas A&M University. 159pp.

Jayakrishnan, R., R. Srinivasan and J.G. Arnold, (2004), "Comparison of raingage and WSR-88D Stage III precipitation data over the Texas-Gulf basin." *Journal of Hydrology*, Vol.(292), 135-152.

Jayakrishnan, R., R. Srinivasan, C. Santhi, and J.G. Arnold, (2005), Advances in the application of the SWAT model for water resources management. *Hydrological Processes*, Vol.(19):749–762.

Jenson, S. K., (1991), "Applications of Hydrologic Information Automatically Extracted From Digital Elevation Models," *Hydrological Processes*, 5(1): 31-44.

Jenson, S. K. and J. O. Domingue, (1988), "Extracting Topographic Structure from Digital Elevation Data for Geographic Information System Analysis," *Photogrammetric Engineering and Remote Sensing*, 54(11): 1593-1600.

Johnson, D., M. Smith, V. Koren and B. Finnerty, (1999), "Comparing mean areal precipitation estimates from NEXRAD and rain gauge networks." *Journal of Hydrology Engineering*, ASCE, 4(2):117-124.

Johnson, N. W., D.R. Maidment, and L.E. Katz, (2005) CRWR Online Report 05-9: ArcGIS and HSPF Model Development, August 2005. Extracted at <http://www.crwr.utexas.edu/reports/2005/rpt05-9.shtml>.

Judi, D., A. Kalyanapu, S. Burian, S. Linger, A. Berscheid, and T. McPherson, (2007), GIS-Based Prediction of Hurricane Flood Inundation. *Proceedings of the World Environmental and Water Resources Congress 2007*, May 15–19, 2007, Tampa, Florida, USA.

Klazura, G.E., and D.A. Imy, (1993), A Description of the Initial Set of Analysis Products Available from the NEXRAD WSR-88D System. *Bulletin of the American Meteorological Society*, Vol.(74):1293–1311.

Knebl, M.R., Z. L. Yang, K. Hutchison and D.R. Maidment, (2005), Regional scale flood modeling using NEXRAD rainfall, GIS, and HEC-HMS/RAS: a case study for the San Antonio River Basin Summer 2002 storm event. *Journal of Environmental Management*, Vol.(75), Issue 4:325-336.

Kouwen, N., E.D. Soulis, A. Pietroniro, J. Donald and R.A. Harrington, (1993), Grouping Response Units for Distributed Hydrologic Modelling, *ASCE Journal of Water Resources Management and Planning*, 119(3):289-305.

Kouwen, N., (2007), WATFLOOD / WATROUTE Hydrological Model Routing & Flow Forecasting System. Department of Civil Engineering, University of Waterloo, Waterloo, Ontario, Canada. First Edition: March 1986, Last Revision: Nov. 2007.

Kull, D., and A. Feldman, (1998), Evolution of Clark's unit graph method to spatially distributed runoff. *Journal of Hydrologic Engineering*, ASCE, 3(1):9-19.

- Laurenson, E.M., R.G. Mein and R.J. Nathan, (2006), RORB Version 5 Runoff Routing Program User Manual. Monash University, Department of Civil Engineering.
- Maidment, D.R., (1993), GIS and Hydrologic Modeling. In: Environmental Modeling With GIS, M.F. Goodchild, B.O. Parks, and L.T. Steyaert (Editors). Oxford University Press, New York, New York, pp. 147-167.
- Maidment, D.R., (2002), Arc Hydro: GIS for Water Resources. Environmental Systems Research Institute, Inc., Redlands, California.
- Martin, P. H., E.J. LeBoeuf, J. P. Dobbins, E. B. Daniel and M. D. Abkowitz (2005), INTERFACING GIS WITH WATER RESOURCE MODELS: A STATE-OF-THE-ART REVIEW. Journal of the American Water Resources Association, 41(6):1471-1487.
- Martz, L. W. and J. Garbrecht, (1992), "Numerical Definition of Drainage Network and Subcatchment Areas From Digital Elevation Models." Computers and Geosciences, 18(6): 747-761.
- Miles, S.B. and C.L. Ho, (1999), Applications and issues of GIS as Tool for Civil Engineering Modeling. Journal of Computing in Civil Engineering, 13(3): 144-152.
- Moon, J., R. Srinivasan and J. H. Jacobs, (2004), Stream Flow Estimation Using Spatially Distributed Rainfall in the Trinity River Basin, Texas. Transactions of the ASAE. 47(5): 1445-1451.
- Morgali, J.R., and R.K. Linsley (1965). "Computer Simulation of Overland Flow", Journal of Hydraulic Division, ASCE, Vol.(90): 81-100.
- National Research Council, (1996), Toward a New National Weather Service: Assessment of Hydrologic and Hydrometeorological Operations and Services. National Academy Press. Washington, DC.
- Natural Resources Conservation Service (NRCS), (1995), Soil Survey Geographic (SSURGO) Data Base Data Use Information. United States Department of Agriculture, Natural Resources Conservation Service, National Soil Survey Center Miscellaneous Publication Number 1527. Jan, 1995. Available at http://tahoe.usgs.gov/files/ssurgo_database.pdf. Accessed in Jan. 2008.
- NWS (National Weather Service), (2002), Distributed Model Intercomparison Project: About the Stage III Data. Available at http://www.nws.noaa.gov/oh/hrl/dmip/stageiii_info.htm. Accessed in Jan. 2008.
- O'Callaghan, J. F. and D. M. Mark, (1984), "The Extraction of Drainage Networks From Digital Elevation Data," Computer Vision, Graphics and Image Processing, Vol.(28): 328-344.

- Ogden, F.L., J. Garbrecht, P.A. DeBarry and L.E. Johnson, (2001), GIS and Distributed Watershed Models. II: Modules, Interfaces and Models. *Journal of Hydrologic Engineering* 6(6):515-523.
- Olivera, F. and D.R. Maidment, (1999), Geographic Information Systems (GIS)-Based Spatially Distributed Model for Runoff Routing. *Water Resources Research* 35(4):1155-1164.
- Olivera, F., R. Raina, (2003) Development Of Large Scale Gridded River Networks From Vector Stream Data. *Journal of the American Water Resources Association*, 39(5), 1235–1248.
- Over, T. M., E.A. Murphy, T. W. Ortel and A.L. Ishii, (2007), Comparisons between NEXRAD Radar and Tipping-Bucket Gage Rainfall Data: A Case Study for DuPage County, Illinois. In: *Proceedings of the World Environmental and Water Resources Congress 2007*. Karen C. Kabbes - Editor, May 15–19, 2007, Tampa, Florida, USA
- Pereira Fo, A.J., K.G. Crawford and C.L. Hartzell, (1998), “Improving WSR-88D hourly rainfall estimates.” *Weather and Forecasting*, 13(12), 1016-1028.
- Pielke, Jr. R.A., M.W. Downton and J.Z. Barnard Miller, (2002), *Flood Damage in the United States, 1926-2000: A Reanalysis of National Weather Service Estimates*. Boulder, CO: UCAR.
- Ponce, V. M. and F. D. Theurer, (1982), Accuracy criteria in diffusion routing. *Journal of the Hydraulics Division, ASCE*, 108(HY6), 747-757.
- Rawls, W. J., D. L. Brakensiek and B. Soni, (1983), Agricultural management effects of soil water processes: Part I - Soil water retention and Green ampt infiltration parameters. *Trans., Amer. Soc. of Agric. Engin.* 26(6): 1747-1752.
- Rawls, W.J. and D.L. Brakensiek, (1985), Prediction of soil water properties for hydrologic modeling. *Watershed Management in the Eighties*. ASCE. 293-299.
- Rawls, W. J., D. L. Brakensiek and M. R. Savabi, (1989), Infiltration parameter for rangeland soils. *J. Rangeland Management*. 42(2): 139-142.
- Robayo, O., T. Whiteaker, D. Maidment, (2004), Converting a NEXRAD map to a floodplain map. Paper presented at the meeting of the American Water Resources Association, Nashville, TN.
- Rossman, L. A., (2007), *Storm Water Management Model User’s Manual, Version 5.0*. EPA/600/R-05/040, National Risk Management Research Laboratory, U.S. Environmental Protection Agency, OFFICE OF RESEARCH AND DEVELOPMENT, Cincinnati, OH.

Samuels, W.B., R. Bahadur and J. Pickus, (2003), Integrating the National Hydrography Dataset Into RiverSpill. Proceedings of the Twenty-Third Annual ESRI User Conference. San Diego, CA, July 7-11, 2003.

Seo, D.J. and J.P. Breidenbach, (2002), Real-Time Correction of Spatially Nonuniform Bias in Radar Rainfall Data Using Rain Gauge Measurements. *Journal of Hydrometeorology* Vol.(3):93-111.

Soil Conservation Service (SCS), (1986), Urban hydrology for small watersheds: Technical Release No. 55, 210-VI-TR-55, 156 p

Soil Conservation Service (SCS), (1983), TR-20 Project formulation-hydrology (1982 version), Technical Release No. 20, 296 p.

Singh, V.P. (Ed.), (1995), Computer models of watershed hydrology. Water Resources Publications, Highlands Ranch, CO.

Singh V. P., and D.K. Frevert, (2002a), Mathematical models of small watershed hydrology and applications. Water resources publications, 2002.

Singh V P and D.K. Frevert, (2002b), Mathematical models of small watershed hydrology and applications. Water resources publications, 2002.

Singh, V. P. and D.K. Frevert, editions. (2006). Watershed Models, CRC Taylor and Francis, Boca Raton, Fla. p.3-20.

Smith M.B., D-J Seo, V.I. Koren, S.M. Reed, Z. Zhang, Q. Duan, F. Moreda and S. Cong, (2004), The distributed model intercomparison project (DMIP): motivation and experiment design, *Journal of Hydrology*, Vol.(298):4-26.

Soil Survey Staff, Natural Resources Conservation Service, United States Department of Agriculture. U.S. General Soil Map (STATSGO) for State [Online WWW] Available URL: <http://soildatamart.nrcs.usda.gov>, Accessed 14/01/2007.

Stanislawski, L.V., M.P. Finn, M.J. Starbuck, E.L. Usery and P. Turley, (2006), Estimation of Accumulated Upstream Drainage Values in Braided Streams Using Augmented Directed Graphs—Paper from the Auto-Carto 2006, A Cartography and Geographic Information Society Research Symposium, Vancouver, Washington. June 25-28, 2006.

Stellman, K.M., H.E. Fuelberg, R. Garza and M. Mullusky (2001). "An examination of radar and rain gauge-derived mean area precipitation over Georgia watersheds." *Weather Forecasting*, 16(2):133-144.

Tarboton, D. G., (2003), "Terrain Analysis Using Digital Elevation Models in Hydrology," 23rd ESRI International Users Conference, San Diego, California, July 7-11.

- Tarboton, D. G. and D. P. Ames, (2001), "Advances in the mapping of flow networks from digital elevation data," in World Water and Environmental Resources Congress, Orlando, Florida, May 20-24, ASCE.
- Tarboton, D. G., R. L. Bras and I. Rodriguez-Iturbe, (1991), "On the Extraction of Channel Networks from Digital Elevation Data," *Hydrologic Processes*, 5(1): 81-100.
- Tarboton, D. G., R. L. Bras and I. Rodriguez-Iturbe, (1988), "The Fractal Nature of River Networks," *Water Resources Research*, 24(8): 1317-1322.
- Terstriep, M.L. and J.B. Stall, (1974), *The Illinois Urban Drainage Area Simulator, ILLUDAS, Bulletin 58*, Illinois State Water Survey, Urbana.
- The Rivanna River Basin Roundtable, (1998), RIVANNA RIVER BASIN PROJECT The STATE OF THE BASIN: 1998. May 20, 1998. Virginia. 109 pages.
- U.S. Army Corps Of Engineers (USACE), (2003a), Annual Flood Damage Reduction Report To Congress For Fiscal Year 2003 Includes Statistical Data 1994-2003.
- U.S. Army Corps Of Engineers (USACE), (2003b), Geospatial Hydrologic Modeling Extension – HEC-GeoHMS User’s Manual Version 1.1. Hydrologic Engineering Center, Davis, CA.
- U.S. Army Corps of Engineers (USACE), (2000a), Hydrologic Modeling System, HEC-HMS: Technical Reference Manual. CPD-74B. U.S. Army Corps of Engineers, Hydrologic Engineering Center, Davis, CA.
- U.S. Army Corps of Engineers (USACE), (2000b), HEC-HMS hydrologic modeling system user’s manual. Hydrologic Engineering Center, Davis, CA.
- U.S. Geological Survey (USGS), (2007), Water-Data Report 2007. Accessed Oct. 14, 2007 at <http://wdr.water.usgs.gov/>.
- U.S. Geological Survey (USGS), (2000), The National Hydrography Dataset: Concepts and Contents. Accessed Jan. 14, 2007, at http://nhd.usgs.gov/chapter1/chp1_data_users_guide.pdf.
- U.S. Geological Survey (USGS), (1999), The National Hydrography Dataset Fact Sheet 106-99 (April 1999). Accessed Jan. 14, 2007, at <http://erg.usgs.gov/isb/pubs/factsheets/fs10699.html>
- Vieux, B.E., P.B. Bedient and E. Mazroi, (2005), Real-time urban runoff simulation using radar rainfall and physics-based distributed modeling for site-specific forecasts. 10th International Conference on Urban Drainage. Copenhagen/Denmark.
- Vivoni, E.R., V.Y. Ivanov, R.L. Bras and D. Entekhabi, (2004), Generation of triangulated irregular networks based on hydrological Similarity. *Journal of Hydrologic Engineering* 9(4):288–303.

Vivoni, E.R. and D.D. Sheehan, (2000), Using NEXRAD Rainfall Data in an ArcView-Based Hydrology Model as an Educational Tool. In: Proceedings of the 2004 ESRI International User Conference, San Diego, California, ESRI, Redlands, California, USA.

Vivoni, E.R., D. Entekhabi and R.N. Hoffman, (2007), Error propagation of Radar Rainfall Nowcasting Fields through a Fully-Distributed Flood Forecasting Model. *Journal of Applied Meteorology and Climatology*, 46(6): 932-940.

Vogelmann, J.E., S.M. Howard, L. Yang, C.R. Larson, B.K. Wylie and J.N. Van Driel, (2001), Completion of the 1990's National Land Cover Data Set for the conterminous United States, *Photogrammetric Engineering & Remote Sensing*, Vol.(67):650-662.

Nathan, W., (2004), State Soil Geographic Data Base (STATSGO) Soil Survey Geographic Data Base (SSURGO). On-line publication of Agriculture and Natural Resources and Ohio Geospatial Extension Program, the Ohio State University. August, 2004. <http://geospatial.osu.edu/resources/ssurgo.pdf>

Wang, D., M.B. Smith, Z. Zhang, S. Reed and V.I. Koren, (2000), "Statistical comparison of mean areal precipitation estimates from WSR-88D, operational and historical gage networks." Paper 2.17, 15th Conference on Hydrology, American Meteorological Society, Jan. 9-14, 2000, Long Beach, CA.

Westcott, N. E., and H.V. Knapp, (2006), Evaluation of the Accuracy of Radar-based Precipitation for Use in Flow Forecasting for the Fox Chain of Lakes, Illinois State Water Survey, Champaign, Illinois.

White, R.K., D.C. Hayes, J.R. Guyer and E.D. Powell, (2003), Water Resources Data, Virginia, Water Year 2003 Volume 1. Surface-Water Discharge and Surface-Water Quality Records. Water-Data Report VA-03-1. Prepared in cooperation with the Virginia Department of Environmental Quality and with other agencies.

Whiteaker, T. L. and D. R. Maidment, (2004), Geographically Integrated Hydrologic Modeling Systems. Dissertation. The University of Texas at Austin, 2004. CRWR Online Report 04-04. Available at <http://www.crwr.utexas.edu/reports/2004/rpt04-4.shtml>.

Whiteaker, T.L., O. Robayo, D.R. Maidment and D. Obenour, (2006), From a NEXRAD rainfall map to a flood inundation map. *Journal of Hydrologic Engineering*, Vol.(11), Issue 1:37-45 (January/February 2006).

Whittemore, R.C. and J. Beebe, (2000), EPA's BASINS Model: Good Science or Serendipitous Modeling?, *Journal of the American Water Resources Association*, 36(3):493-499.

Wilson, J. P. and J. C. Gallant, (2000), *Terrain Analysis: Principles and Applications*, John Wiley and Sons, New York, 479 p.

WMO (World Meteorological Organization), (1992), Simulated Real Time Intercomparison of Hydrological Models, Operational Hydrology Report No. 38, Geneva, 1992.

Wurbs, R. A., (1994), "National Study of Water Management During Drought: Computer Models for Water Resources Planning and Management." U.S. Army Corps of Engineers Institute for Water Resources, Alexandria, VA; IWR Report 94-NDS-7.

Xie, H., X. Zhou, J.M.H. Hendrickx, E.R. Vivoni, H. Guan, Y.Q. Tian and E.E. Small, (2006), "Evaluation of NEXRAD Stage III precipitation data over a semiarid region." Journal of American Water Resource Association, 42(1), 237-256.

Ye, Z., D.R. Maidment and D.C. McKinney, (1996), Map-based surface and subsurface flow simulation models: an object-oriented and GIS approach; CRWR Online Report 96-5, Austin, Texas, 1996.

Young, C.B., A.A. Bradley, W.F. Krajewski, A. Kruger and Morrissey, M.L. (2000), "Evaluating NEXRAD multisensor precipitation estimates for operational hydrologic forecasting." Journal of Hydrometeorology, 1(3): 241-254.

Zarriello, P.J., (1998), Comparison of nine uncalibrated runoff models to observed flows in two small urban watersheds, in Proceedings of the First Federal Interagency Hydrologic Modeling Conference, April 19-23, 1998, Las Vegas, NV: Subcommittee on Hydrology of the Interagency Advisory Committee on Water Data, p. 7-163 to 7-170.

Zeiler, M. (Editor), (2001), Exploring ArcObjects, 1. Environmental System Research Institute, Redlands.

Zhang Z, V. Koren, M. Smith, S. Reed and D. Wang, (2004), Use of Next Generation Weather Radar Data and Basin Disaggregation to Improve Continuous Hydrograph Simulations. Journal of Hydrologic Engineering 9(2): 103-115.

VITA

Changqing Song was born in Weifang, China, on November 9th, 1972. He entered the Department of Geology, Beijing University in 1990, where he earned a B.S. degree in 1995. He went to the graduate school of Chinese Academy of Sciences that same year, and then entered the Institute of Geology, China Earthquake Administration in 1996. He earned the M.S. in Geology there in August, 1998. After the graduation, he worked in the same institution as research scientist for three years. In August 2001, he entered the department of Civil and Environmental Engineering for PhD study. He also worked as a part time research assistant in the Lab for Earth Observing and Spatial Data Processing of CET (August, 2001 to May, 2003) and CEE computer lab (June, 2003 to July, 2007). Since November 2007, He joined the Haestad Methods Solution Center, Bentley Systems, Inc.

Permanent Address: 42 Pleasant Street, New Haven, CT 06511.